TROLL 4.0: representing water and carbon fluxes, leaf phenology and intraspecific trait variation in a mixed-species individual-based forest dynamics model – Part 1: Model description

Isabelle Maréchaux[1], Fabian Jörg Fischer[2,3], Sylvain Schmitt[1,4,5], Jérôme Chave[2]

1. AMAP, Univ Montpellier, CIRAD, CNRS, INRAE, IRD, 34000 Montpellier, France
2. CRBE, Université de Toulouse, CNRS, IRD, Toulouse INP, 118 route de Narbonne 31062 Toulouse, France
3. School of Biological Sciences, University of Bristol, Bristol, BS8 1TQ United Kingdom
4. CIRAD, UPR Forêts et Sociétés, F-34398, Montpellier, France
5. Forêts et Sociétés, Univ Montpellier, CIRAD, Montpellier, France

Correspondence to: Isabelle Maréchaux (isabelle.marechaux@inrae.fr)

Short summary: We describe TROLL 4.0, a simulator of forest dynamics that represents individual trees in a virtual space at metric resolution. Tree birth, growth, death and the underlying physiological processes such as carbon assimilation, water transpiration and leaf phenology depend on plant traits measurable in the field for many individuals and species. The model is thus capable of jointly simulating forest structure, diversity and ecosystem functioning, a major challenge in modelling vegetation dynamics.

Abstract. TROLL 4.0 is an individual-based forest dynamics model that is capable of jointly simulating forest structure, diversity and ecosystem functioning, including the ecosystem water balance and productivity, leaf area dynamics and the tree community functional and taxonomic composition. Specifically, trees are modeled as three-dimensional individuals with a metric-scale spatial representation, providing a detailed description of ecological processes such as competition for resources and tree demography. Carbon assimilation and plant water loss are explicitly represented at tree level using coupled photosynthesis and stomatal conductance models, depending on the micro-environmental conditions experienced by trees. Soil water uptake by trees is also modelled. Physiological and demographic processes are parameterized using plant functional traits measured in the field. TROLL 4.0 now represents ecosystem flux processes in a manner similar to dynamic global vegetation models, while adopting a representation of plant community structure and diversity at a resolution consistent with that used by field ecologists. Here we provide a detailed description and discussion of the model implementation. An evaluation of the model at two tropical forest sites is provided in a companion paper (Schmitt et al., submitted companion paper). TROLL 4.0's representation of processes reflects the state of the art, and we discuss possible developments to improve its predictive capability and its capacity to address challenges in forest monitoring, forest dynamics and carbon cycle research.

1 Introduction

Modelling vegetation dynamics remains a major challenge (Prentice et al., 2015; Song et al., 2021; Mahnken et al., 2022), and the wide variety of modelling concepts that coexist depend on models' initial objectives. Early versions of global vegetation models were developed to provide boundary conditions for energy, carbon and water budgets in global atmospheric models (Sellers et al., 1986, 1997). With the refinement of modeling concepts and computer power, feedback loops between the atmosphere and vegetation have gradually been taken into account (Charney, 1975; Cox et al., 2000; Meir et al., 2006), leading to an improved representation of fluxes of energy, carbon and water across the vegetation layer (Fisher et al., 2015; Moorcroft, 2003; Pitman, 2003). However, dynamic global vegetation models (DGVMs) typically adopt a simplified representation of floristic composition and vegetation structure (Fisher et al., 2014; Prentice et al., 2007). In many of these models, fluxes between vegetation and the atmosphere are still calculated in an average environment per grid cell (e.g. 1°*1°), for an average leaf of an individual drawn from a dozen of plant functional types (PFTs). The diversity of plant strategies is therefore typically represented by a small number of PFTs even in highly diverse tropical forests (Fisher et al., 2014; Poulter et al., 2011).

In parallel, stand-scale process-based models have been developed to better understand the exchanges between vegetation and the atmosphere through an up-scaling of fine-scale ecophysiological processes, and to account for within-stand micro-environmental heterogeneity (Wang and Jarvis, 1990; Gu et al., 1999; Williams et al., 1996; Ogée et al., 2003; Duursma and Medlyn, 2012; Fyllas et al., 2014). These process-based models are conceptually close to DGVMs, but they implement a more detailed representation of plant structure at the stand scale, and they have nurtured some important advances in DGVM-development over the past decades (e.g., Chen et al., 2016). Typically used to assimilate eddy-flux data, they do not include demographic processes however.

Forest growth models have a different history as they were initially developed to predict successional dynamics and inform forest management (Watt, 1947; Botkin et al., 1972; Vanclay, 1994; Porté and Bartelink, 2002; Liang and Picard, 2013). A key innovation have been forest gap models that represent recruitment, growth, mortality and competition between individual trees within forest patches. Forest patches are typically the size of a canopy opening created by the fall of a dominant tree (gap, or chablis, Bugmann 2001) and modelled as horizontally homogeneous, with a spatially implicit representation of tree positions. Through the simulation of a large number of patches, gap models can represent spatial heterogeneity due to gap dynamics within stands. Overall, these models adopt a finer representation of vegetation structure than classic DGVMs, but biogeochemical processes are generally modeled more coarsely, using ideal yield curves for tree growth rates combined with limiting factors imposed by the patch environment. Since these empirical relationships can only be parameterized on the basis of a large amount of data – readily available in plantations, but difficult to obtain elsewhere – , gap models typically also use plant functional types to simulate diverse forest stands. The number and definition of these groups has been much discussed in the literature, with no clear consensus (Botkin, 1975; Swaine and Whitmore, 1988; Vanclay, 1991; Köhler and Huth, 1998;

Köhler et al., 2000; Gourlet-Fleury et al., 2005; Kazmierczak et al., 2014), and these plant functional types are difficult to transfer from one site to another (Picard and Franc, 2003; Picard et al., 2012).

Modelling vegetation from a completely different perspective and building upon flora distribution maps and biogeographic concepts (Humboldt, 1849; Grisebach, 1872), plant species distribution models have been developed for long (SDMs; Guisan et al., 2017). Generally, SDMs first estimate the envelope of environmental conditions for a species based on species occurrence data (Guisan and Thuiller, 2005; Hutchinson, 1957; Soberón, 2007), which is used to infer a probability distribution in space (Elith and Leathwick, 2009). These models require little knowledge on the processes underlying species distribution, which explains their widespread use. However, because these models are statistical in nature, their ability to project future states is unclear, and a great deal of research has been devoted to implementing process-based versions of these SDMs (Chuine and Beaubien, 2001; Ferrier and Guisan, 2006; Morin and Lechowicz, 2008; Morin and Thuiller, 2009; Kearney and Porter, 2009; Dormann et al., 2012; Journé et al., 2020).

From this brief and non exhaustive overview it emerges that each research community in vegetation modeling emphasizes one representation of vegetation dimension –functioning, structure or diversity -- to the detriment of the others (Maréchaux et al., 2021). Data availability and computing power partly explain such tradeoffs, and increasing model complexity does not necessarily translate into an increase in reliability and robustness (Mahnken et al., 2022; Prentice et al., 2015). However, a consensus has emerged in the literature that a better integration of plant species diversity, structure and functioning should improve the predictive power of vegetation models (Purves and Pacala, 2008; Thuiller et al., 2008; McMahon et al., 2011; Evans, 2012; Dormann et al., 2012; ; Mokany et al., 2016; Fisher et al., 2018). For example, tree species diversity influences the productivity and resilience of forest ecosystems (Schnabel et al., 2019), and these biodiversity-ecosystem functioning relationships result from local interactions where competition for resources is a key process (Fichtner et al., 2018; Guillemot et al., 2020; Jourdan et al., 2020; Yu et al., 2024; Nemetscheck *et al.* 2024). Similarly, the fine details of stand structure control the uptake of resources by vegetation (Braghiere et al., 2019, 2021; Brum et al., 2019; Ivanov et al., 2012; De Deurwaerder et al., 2018), and they also determine the response to environmental stresses and disturbances (Blanchard et al., 2023; Jucker et al., 2018; Seidl et al., 2014; De Frenne et al., 2019). More generally, the contribution of vegetation in biogeochemical cycles, although typically comprehended and quantified from stand to global scales (e.g. biomass, productivity), ultimately depends on individual processes (e.g. mortality, Johnson et al., 2016) controlled by fine-scale heterogeneity and the various ecological strategies of species (Poorter et al., 2015).

Therefore, recent developments in DGVMs have sought to better represent plant community structure and diversity. Several cohort-based DGVMs have been developed to refine the representation of vegetation heterogeneity (Moorcroft et al., 2001; Fisher et al., 2015; Longo et al., 2019; Smith et al., 2001). Continuous representations of functional diversity have also been proposed using the distribution and co-variation of traits at the individual level or trait-climate relationships (Sakschewski et al., 2015; Verheijen et al., 2015; Scheiter et al., 2013; Pavlick et al., 2013; Berzaghi et al., 2020; Van Bodegom et al., 2014). These developments represent major advances in vegetation modelling, but scale mismatches between field data and model representations limit the ability to assimilate data of various nature and resolution. While inverse modelling approaches can

partially alleviate these constraints (Hartig et al., 2012; Dietze et al., 2013; LeBauer et al., 2013; Fer et al., 2018; Lagarrigues et al., 2015), they rely heavily on confidence in the model structure, can therefore raise equifinality issues (Medlyn et al., 2005), and increase rapidly in computational complexity in high-dimensional parameter sets.

Finally, most of these challenges are exacerbated for tropical forests, as they are structurally complex (Doughty et al., 2023), support a large number of tree species per hectare (up to several hundred, Wilson et al., 2012), and are more difficult to access for evaluation in the field (Schimel et al., 2015). Given that they provide a range of ecosystem services and play a major role in regional and global biogeochemical cycles (Beer et al., 2010; Bonan, 2008; Pan et al., 2011; Harper et al., 2013), tropical forests and their responses to changing environmental factors have been identified as one of the greatest sources of uncertainty in Earth system models (Koch et al., 2021; Powell et al., 2013; Restrepo-Coupe et al., 2017; Huntingford et al., 2013). Thus, many advances in vegetation modelling have been, and still are, motivated by the challenge of tropical forests.

Here we describe a major upgrade of the TROLL forest dynamics model (Chave, 1999; Maréchaux and Chave, 2017; Fischer, 2019), referred to here as TROLL 4.0. TROLL 4.0 brings together various modelling traditions, including elements of DGVMs, stand-scale process-based models and forest gap models while adopting a species-level representation of plant diversity, to jointly simulate the functioning, structure and diversity of forest ecosystems, and in particular tropical forests. TROLL is a spatially explicit forest dynamics model, with an individual- and trait-based representation (Fig. 1). Individual trees from 1cm diameter at breast height (*dbh*) are explicitly represented in a three-dimensional space discretized at a resolution of one meter, allowing a fine representation of stand structure and local interactions via explicit competition for resources. Each tree belongs to a species, with a list of mean traits per species provided as input. These traits control the physiological and demographic processes of the tree's functioning and life cycle, from recruitment to growth, to seed dispersal and death. This type of trait-based parameterization is based on recent advances in plant physiology and functional ecology, has been facilitated by the expansion of large databases of functional traits (Díaz et al., 2016, 2022; Kattge et al., 2011, 2020), in particular for tropical trees (Baraloto et al., 2010a; Vleminckx et al., 2021).

In TROLL 4.0, carbon assimilation and water loss by transpiration are represented explicitly using a photosynthesis model coupled with a stomatal conductance model. Both take into account variation in micro-environmental conditions between and within tree crowns, as well as the tree's access to soil water. A water cycle is now simulated, with the state and dynamics of soil water explicitly represented and coupled with the vegetation dynamics. The influence of water availability on leaf-level gas exchanges, leaf phenology, tree recruitment and death is parameterized through the leaf water potential at turgor loss point (Bartlett et al., 2012) and mechanistic-based coordination with other hydraulic traits (Bartlett et al., 2016). Carbon that is not consumed by the respiration of living tissues is then allocated to leaf production, carbon storage and tree growth through allometric relationships. Compared to TROLL version 2.3.2 (Maréchaux and Chave, 2017), TROLL 4.0 includes other improvements: plant functional traits can vary among trees of the same species; tree crown shapes can be more realistic than cylinders; and leaf density can vary within the tree crowns.

In this contribution, we provide a detailed description of the structure and objectives of the TROLL 4.0 model, discussing how new modeling representations are an outcome of the state of knowledge and the availability of data. Finally,

we discuss the limitations of the model and future developments. An evaluation of the model's ability to simulate forest structure, diversity and functioning for two Amazonian forest sites is reported in a companion paper (Schmitt et al., submitted companion paper). The model is written in C++ and wrapped in the R environment through a dedicated package named *rcontroll* (Schmitt et al. 2023).

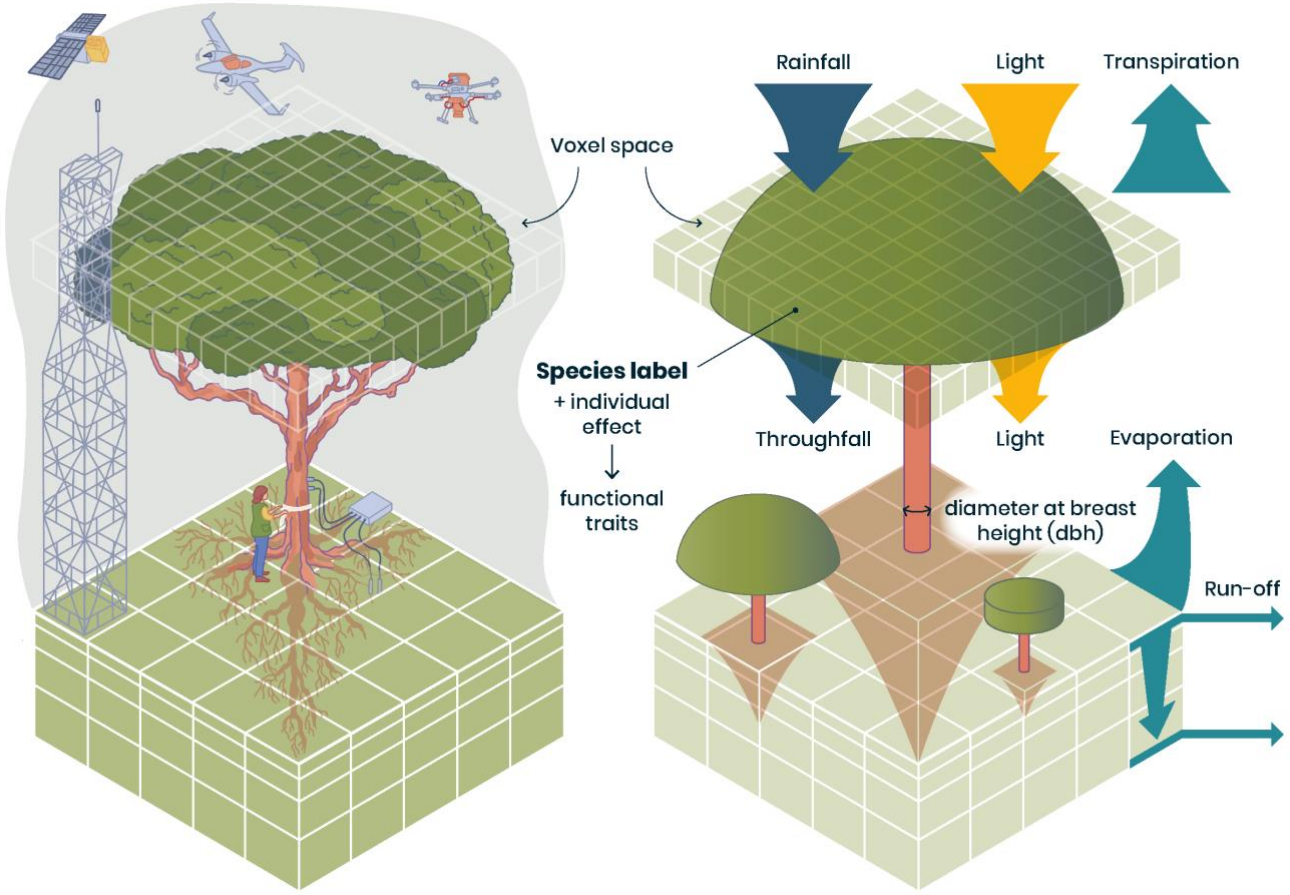

Figure 1: Representation of individual trees in a spatially explicit environment in TROLL 4.0 (right) allowing direct comparison with data of various nature (left). In TROLL 4.0, each tree is composed of a trunk, a crown, whose shape evolves from a cylinder to an umbrella as tree grows, and root biomass that decreases exponentially with soil depth. Tree dimensions are updated at each timestep, depending on the net assimilated carbon that is allocated to growth, and following allometric relationships depending on tree diameter at breast height (*dbh*). Each tree has a species label associated with plant functional traits provided as input, which, together with an individual effect randomly attributed at tree birth, determines the tree functional traits. These traits are used to parameterize physiological and demographic processes that govern tree functioning and life cycle. Light diffusion is computed explicitly at each time step and within each voxel from the canopy top to the ground. Water balance is also computed at each timestep, and the resulting water availability across soil voxels influence tree functioning. With this representation of forest structure, composition and functioning, model outputs can be directly compared with a range of data, including carbon and water fluxes provided by eddy-flux towers and field inventories. In TROLL 4.0, aboveground voxels typically have a finer horizontal resolution than belowground voxels, but the latter can be vertically finer and of increasing thickness with depth, and this resolution matches the one of fine-scale remote-sensing products or soil water content monitoring.

2 Model description

2.1 Environmental conditions

TROLL 4.0 simulates an idealized forest stand with a typical size of 1 to 100 ha. Parallel computing may be used to simulate several times the same stand, or to simulate several forest stands with different environmental conditions. Climatic drivers are similar to those represented in many DGVMs (air temperature, vapor pressure deficit, wind speed, and light intensity above the canopy, as well as precipitation). The forest ecosystem is divided into an above-ground and below-ground part. Soil is explicitly represented as a water reservoir, but soil nutrients are not modeled. The topography within a stand is assumed to be flat.

2.2 Light availability and aboveground variation in micro-climate

Above ground, the simulated forest stand is represented as a discrete grid of $1m^3$ cubic voxels. Light diffuses through the forest's leaf layers from the top of the canopy to the ground, with one recalculation each day. In a given voxel, light availability is the photosynthetic photon flux density in μmol photons m^{-2} s^{-1} and is computed as a function of the incident light intensity at top canopy ($PPFD_{top}$, see Table A1 for a list of symbols), the cumulated leaf density of voxels above and the (constant) leaf density within the voxel itself. The Beer-Lambert extinction of light within the canopy allows to calculate the incident PPFD (per unit ground area) above any layer at vertical extent v as:

$$PPFD(v) = PPFD_{top} \times \exp[-k \times LAI(v)] \quad (1)$$

where $LAI(v)$ is the cumulated leaf area above height v, and k is the extinction coefficient. We here define $k = k_{geom} \times \text{absorptance}_{\text{leaves}}$, where k_{geom} reflects the geometric arrangement of leaves in the voxel (a value of 0.5 reflecting spherical leaf distribution; Ross, 1981) and $\text{absorptance}_{\text{leaves}}$, the fraction of absorbed light within a single leaf (Long et al., 1993; Poorter et al., 1995). The absorbed light in a layer a of thickness Δa is then

$$PPFD_{abs}(a) = PPFD_{top} \times \exp[-k \times LAI(a)] - PPFD_{top} \times \exp[-k \times LAI(a + \Delta a)] \quad (2)$$

Assuming that leaf area per unit ground area (m^2 m^{-2}), or *dens(a)*, is constant within the layer, this simplifies to:

$$PPFD_{abs}(a) = PPFD_{top} \times \exp[-k \times LAI(a)] \times (1 - \exp[-k \times dens(a)]) \quad (3)$$

For photosynthesis calculations, absorbed PPFD per unit ground area is converted into absorbed PPFD per unit leaf area by dividing $PPFD_{abs}(a)$ by $dens(a)$.

Air microenvironmental variation within the canopy is represented as follows. Nighttime temperature (T_{night}) is assumed constant throughout the night and within the canopy, while temperature (T) and vapor pressure deficit (VPD) vary across voxels depending on the variable $\lambda(v) = \frac{LAI(v)}{LAI_{sat}}$ with LAI_{sat} a threshold LAI and LAI(v) the LAI above voxel v. At height v above ground, we calculate temperature and VPD as follows:

$$T(v) = T_{top} - \Delta T \times \lambda(v) \quad (4)$$

$$VPD(v) = VPD_{top} \times \left[C_{VPD0} + (1 - C_{VPD0}) \sqrt{(1 - \lambda(v))}\right] \quad (5)$$

where ΔT and C_{VPD0} are set parameters and T_{top} and VPD_{top} are values at the top of canopy. For any given layer a of depth Δa, temperatures and VPDs are then calculated by averaging both functions from a to $a + \Delta a$:

$$T_{mean}(a) = \frac{1}{\Delta a} \int_a^{a+\Delta a} (T_{top} - \frac{\Delta T}{LAI_{sat}} \times LAI(v)) \mathrm{d}v \quad (6)$$

$$VPD_{mean}(a) = \frac{1}{\Delta a} \int_a^{a+\Delta a} VPD_{top} \times \left[C_{VPD0} + \frac{(1-C_{VPD0})}{\sqrt{LAI_{sat}}} \sqrt{(LAI_{sat} - LAI(v))}\right] \mathrm{d}v \quad (7)$$

Equations 6 and 7 can then be simplified using the assumption of constant leaf density within a layer and redefining v with respect to the current layer a, so that $LAI(v) = LAI(a) + dens(a) \times v$.

This representation of variation of T and VPD within the canopy is in qualitative agreement with empirical observations of microclimate gradients within tropical forest canopies (Camargo and Kapos, 1995; Shuttleworth, 1985; Shuttleworth et al., 1989, Tymen et al. 2017), with a consistent buffering effect of forest canopies on understory micro-environment (De Frenne et al., 2019), and a strong control by forest structure (Gril et al., 2023b, a; Tymen et al., 2017; Zellweger et al., 2019).

Wind speed attenuation inside the canopy is simulated as described in Rau et al. (2022), who explored the effect of wind speed on forest structure in a forest exposed to cyclones using TROLL. Wind speed is usually measured above the canopy and decreases as one approaches the canopy top layer, so wind speed at the top of the canopy is (Monteith & Unsworth 2008):

$$u(z) = \frac{u_*}{\kappa} \ln\left(\frac{z-d}{z_0}\right), \ if \ z \geq H \quad (8)$$

where $u(z)$ is the horizontal wind speed in m s^{-1} at a height z (in m) above ground, H the height of the top of the canopy (in m), u_* is the friction velocity, κ the von Karman constant (κ=0.40), d the zero-plane displacement height, here assumed to be equal to 0.8H, and z_0 the aerodynamic roughness, here assumed to be equal to 0.06H (Rau et al., 2022). Within the canopy, wind speed decreases as (Inoue 1963):

$$u(z) = u(H) \exp\left(-\alpha\left(1 - \frac{z}{H}\right)\right), \ if \ z < H \quad (9)$$

with $\alpha \approx 3$ (Raupach et al., 1996). Wind speed was not computed at the voxel scale, but using the coarser horizontal resolution of the belowground field (see section 2.3 below, e.g. 25x25 m), and a mean top canopy height H was computed as input to Eqs (8) and (9).

2.3 Soil water availability

In TROLL 4.0, the belowground part of the ecosystem is explicitly represented, and its discretization is specified by the user, including the number and depth of layers, and horizontal dimensions of the cells. Belowground voxels are typically coarser horizontally (e.g. 25m x 25m, as commonly implemented in gap models Bugmann, 2001), but finer vertically, than aboveground 1-m^3 voxels. Metric-scale lateral water fluxes are difficult to parameterize and evaluate, and neglecting them

here limits the computational burden. Soil layers typically increase in thickness with depth, as in most DGVMs or forest physiological models (Prentice et al., 2015) and in standard soil assessments (e.g. Hengl et al., 2017). In this representation, contrasting root depth and access to water can be represented across individual trees together with potential variation in soil properties and hydraulic state. This approach contrasts with some forest dynamics models that use a single-layer belowground representation (e.g. Gutiérrez et al., 2014; Christoffersen et al., 2016; Fyllas et al., 2014).

The water content in each belowground voxel is simulated using a bucket model, which relies on the vertical water balance for each voxel. Neglecting horizontal lateral fluxes, the water balance for a given soil column amounts to:

$$\Delta SWC = P - I - Q - E - T - L \quad (10)$$

where SWC is the soil water content, P the incident rainfall, I the canopy interception, Q the run-off, E the evaporation from the soil, T the transpiration, i.e. the plant water uptake, and L the leakage. This water balance is established for each soil layer, with inputs from upwards and outputs downwards starting from the top layer (l=1): outputs of layer l are inputs for layer $l+1$, with L corresponding to the output of the deepest layer, and P-I-Q to the input of the top layer. Note that this downward iteration neglects: (i) potential hydraulic lift (upward water redistribution, see e.g. Dawson, 1993; Burgess et al., 1998; Oliveira et al., 2005); and (ii) potential interaction with the water table (Costa et al., 2023; Sousa et al., 2022). Further developments could account for these two mechanisms where they are expected to play a significant role. In particular, flooded areas could be easily represented, with a shallower soil depth and a prescribed boundary condition, i.e. a shallower water table. We now describe and discuss each term of the water balance and the corresponding modeling choices.

Rainfall. Rainfall (P, in mm) is a model input. It is assumed that the total daily rainfall corresponds to a single event of rain per day (one storm, as in, e.g., Rodriguez-Iturbe et al., 1999; Laio et al., 2001; Fischer et al., 2014; Gutiérrez et al., 2014).

Interception. Rainfall interception by the canopy is simulated using a model where interception depends on LAI, as proposed by Liang et al. (1994):

$$I = \min(P, K \times LAI) \quad (11)$$

where K=0.2mm and LAI corresponds to the leaf area index at ground level, averaged across the ground-level aboveground voxels that contribute to a single belowground voxel (typically $625=25^2$ aboveground voxels contribute to one belowground voxel). Similar simple formulations of canopy interception have been used elsewhere (e.g. Liu et al., 2017), and this choice is justificed by the lack of relevant data to properly parameterize more complex formulations at most field sites. More complex models of rainfall interception also exist however (Rutter and Morton, 1977; Gash, 1979; Gash et al., 1995).

Run-off and infiltration. As in most bucket models coupled with a forest dynamics model, the temporal propagation of the wetting front into the soil is not explicitly simulated here, because of the daily timestep and the vertically lumped representation of soil moisture dynamics (e.g., Laio et al., 2001, Guimberteau et al., 2014). When the soil top layer has enough available storage to absorb the totality of the throughfall (*i.e.* when throughfall is smaller than the layer water content at field capacity minus the current soil water content), it is assumed that the increment in soil water content of that top layer is equal to the throughfall. Otherwise, the excess water percolates to the next layer below. In the absence of an explicit wetting front,

runoff occurs only when the superficial layer is already saturated, which is similar to Dunne run-off (Dunne and Black, 1970). More complex formulations of run-off exist (d'Orgeval et al., 2008; Guimberteau et al., 2014; Horton, 1933), but because of the high porosity of many tropical forest soils (Hodnett and Tomasella, 2002; Sander 2002) and the lack of explicit topography in this version, our choice is parsimonious.

Soil evaporation. We assumed that water evaporates from the top soil layer only, a reasonable assumption if the top soil layer is not too thin. We followed Sellers et al. (1992) under which evaporation from the soil is expressed as (see Merlin et al., 2016 for a review of alternatives):

$$E = \frac{M_w}{RT_s} \times \frac{e_s - e_a}{r_{soil} + r_{aero}} \quad (12)$$

where E is in kg m^{-2} s^{-1}, M_w is the molar mass of water vapor (M_w=18 kg mol^{-1}), R is the ideal gas constant (R=8.31 J mol^{-1} K^{-1}), T_s is the temperature at soil surface in K, e_s is the vapor pressure of the soil surface in Pa, e_a is the vapor pressure of air above the soil surface in Pa, r_{soil} is the soil surface resistance in s m^{-1}, and r_{aero} is the aerodynamic resistance to heat transfer in s m^{-1}. Soil water pressure e_s is a function of the water potential of the top soil belowground voxel ($\psi_{soil,top}$, in MPa; Jones, 2013, Eq. (5.14) therein):

$$e_s = e_{sat}(T_s) \times \exp\left(\frac{V_w}{RT_s} \times \psi_{soil,top}\right) = e_{sat}(T_s) \times \exp\left(2.17 \times \frac{\psi_{soil,top}}{T_s}\right) \quad (13)$$

Where V_w is the partial molal volume of water ($V_w = 18 \times 10^{-6}$ m^3 mol^{-1}), and $e_{sat}(T_s)$ is the saturated vapor pressure at T_s computed following the Buck equation (Jones, 2013, Appendix 4 therein). e_a is by definition equal to $e_{sat}(T_s) - VPD_{ground}$, where the latter is the VPD at ground level in Pa. r_{soil} is computed following Sellers et al. (1992, Eq. (19) therein, see also Merlin et al., 2016, Eq. (12)):

$$r_{soil} = \exp\left(8.206 - 4.255 \times \frac{\theta_{top}}{\theta_{fc,top}}\right) \quad (14)$$

where θ_{top} is the water content of the top soil belowground voxel and $\theta_{fc,top}$ is its water content at field capacity (in m^3). Aerodynamic resistance r_{aero} is computed as follows (Merlin et al., 2016, Eq. (B10) therein):

$$r_{aero} = \frac{1}{\kappa^2 \times u(Z)} \ln\left(\frac{Z}{Z_m}\right)^2 \quad (15)$$

with κ again the von Karman constant (κ=0.40), $u(Z)$ is the wind seed (in m s^{-1}) at reference height Z, here taken at 1m above ground, and Z_m is the momentum soil roughness in m, set to 0.001m.

Transpiration. Trees transpire soil water from the belowground voxel they are rooted in (see section 2.4.3). For a given tree, the total daily soil water uptake is the sum of the water transpired by leaves across its crown and across day-time half hours (see section 2.5.2). Soil layers contribute to water uptake as a function of tree-dependent weights, w_l (see Eq. (21), section 2.4.3), which depend on root biomass and on the soil hydraulic state in each layer.

For each belowground voxel in layer l, the soil water potential (ψ_l) and the soil hydraulic conductivity (K_l) are computed at each time step from the soil water content in the focal voxel using the van Genuchten-Mualem soil characteristic and hydraulic conductivity curves (Mualem, 1976; van Genuchten, 1980; see Table 1 in Marthews et al., 2014). Parameters of

these curves are estimated using regression models (pedotransfer functions) for tropical soils (Hodnett and Tomasella, 2002), except the saturated hydraulic conductivity, which is computed following Cosby et al. (1984; see Table 2 in Marthews et al., 2014). In practice, when only soil texture data is available, TROLL 4.0 contains a default option to apply the texture-based only pedotransfer function provided by Tomasella and Hodnett (1998), coupled to the soil characteristic and hydraulic conductivity curves of Brooks and Corey (1964) (see Tables 1 and 2 in Marthews et al., 2014).

2.4 Representation of trees in the model

2.4.1 Species affiliation and intra-specific trait variability

In TROLL 4.0, each tree (and seed) is attributed a botanical species defined by a taxonomic binomial. It is assumed that the user has sufficiently good knowledge of the tree species growing in the study area so that a list of species-specific mean plant functional trait values can be provided as input. These are the leaf mass per area (LMA, in g m^{-2}), the leaf area (LA, cm^2), the leaf nitrogen content per dry mass (N, in mg g^{-1}), the leaf phosphorous content per dry mass (P, in mg g^{-1}), the wood specific gravity (wsg, in g cm^{-3}), the leaf water potential at turgor loss point (ψ_{tlp}, in MPa), and three allometric parameters (dbh_{thres}, h_{lim}, a_h, all in m; see section 2.4.2). The number of species provided in input is not limited. In addition to mean plant functional trait values, it is possible to input individual trait values from which a trait variance-covariance matrix is computed (alternatively the trait variance-covariance matrix can be prescribed). With this option, for each recruited tree, the trait values are drawn from a distribution rather than attributed the species-specific mean value (hence implementing an intraspecific variation that is not structured in space or time, Girard-Tercieux et al., 2023). For each trait i and tree j, the species-specific mean value is multiplied by a factor $e^{\varepsilon_{i,j}}$ where $\varepsilon_{i,j} \sim N(0, \sigma_i)$ where σ_i the trait-specific standard deviation on a logarithmic scale (lognormal variation). The sole exception is wood specific gravity, which we assume to be normally distributed around the mean with $\varepsilon_{wsg,j} \sim N(0, \sigma_{wsg})$. Trait covariance is only considered for leaf N, leaf P and LMA, and other traits are assumed to be decoupled (Baraloto et al., 2010b).

2.4.2 Aboveground structure

Above ground, the tree geometry is represented as a three-dimensional object within the voxelized space and consists of a trunk and a crown filled with leaves. The trunk is assumed to be a cylinder characterized by its total height and its diameter (*dbh*, for diameter at breast height, by analogy with forest inventories). The aboveground dimensions of trees are predicted from their *dbh* via scaling rules. For tree j with dbh_j, we calculate its height h_j, its crown radius cr_j, and its crown depth cd_j as follows:

$$h_j = \frac{h_{lim} \times dbh_j}{(a_h + dbh_j)} \times e^{\varepsilon_{h,j}} \quad (16)$$

$$cr_j = e^{a_{cr}} \times dbh^{b_{cr}} \times e^{\varepsilon_{cr,j}} \quad (17)$$

$$cd_j = \min\left(\frac{h_j}{2}, (a_{cd} + b_{cd} \times h_j) \times e^{\varepsilon_{cd,j}}\right) \quad (18)$$

where h_{lim} and a_h are species-specific coefficients of the Michaelis-Menten function, and a_{cr}, b_{cr}, a_{cd}, and b_{cd} allometric coefficients that are species independent. $\varepsilon_{h,j}$, $\varepsilon_{cr,j}$ and $\varepsilon_{cd,j}$ are variance terms to simulate intraspecific variation with $\varepsilon_{h,j} \sim N(0, \sigma_h)$, $\varepsilon_{cr,j} \sim N(0, \sigma_{cr})$, and $\varepsilon_{cd,j} \sim N(0, \sigma_{cd})$. Tree crown architecture is known to depend on species ecological strategies (Bohlman and O'Brien, 2006; Iida et al., 2012; Poorter et al., 2006; Laurans et al., 2024), but given that crown extents are difficult to measure reliably in the dense canopies of tropical forests, we used a single set of parameters for all the species.

In the previous published version (Maréchaux and Chave, 2017), tree crowns were represented as cylinders with homogeneous leaf densities. Since v.3.0, TROLL can also model tree crowns as flexible, umbrella-like shapes with heterogeneous leaf density distributions. Small tree crowns are simulated as cylinders, but consist of up to three separate 1-m layers of leaves (top, intermediate and bottom layer). Each layer can be assigned a percentage of the total leaf area (e.g., 50%, 30%, 20%) to reflect gradients in leaf densities from the upmost to lower crown layers (Kitajima et al., 2005), but the default is an equal distribution (33%, 33%, 33%) across all layers. Once a tree surpasses 3 m in crown depth, no new layers are added. Instead, the treetop grows quicker in height than the outer crown parts. As a result, the three 1-m layers are folded around the tree trunk like an umbrella at various stages of opening (see Fig. 1b in Schmitt et al., 2023, and similar tree representations in Strigul et al., 2008). The exact slope of height variation from tree top to crown edge can be parameterized by a linear ("conifer-like") or a spherical ("broadleaf-like") function, with, *shape_crown*, the ratio between the radius of the crown at the top of the tree to the radius at the bottom of the crown being a global parameter.

We also relax the assumption that tree crowns are homogeneously filled across their horizontal extent. In TROLL 4.0, crowns have small 1-m^2 openings (or gaps) in their crowns, parameterized as percentage of total crown area that is not filled with leaves, f_{gap}. This allows for the modelling of a spatially heterogeneous light environment in the understory (Tymen et al., 2017), with a theoretical range from f_{gap} = 0% (full crown cover, no openings) to f_{gap} = 100% (a hypothetical crown with no leaf area). When calibrating TROLL for tropical forests with airborne laser scanning (Fischer et al., 2019), we found a value of f_{gap} = 15% to be a good approximation for this within-crown gap fraction. If intraspecific variation in crown extent is explicitly modelled, the fraction of crown gaps is rescaled so that the absolute crown cover stays constant (i.e., the fraction of crown gaps is divided by $e^{2\varepsilon_{cr,j}}$). Within species, variation in crown extent is thus assumed as decoupled from variation in leaf area, i.e., reflecting variation in branch angles and directions, but not branch number or biomass.

2.4.3 Belowground structure

TROLL 4.0 makes the common assumption that total fine root biomass is equal to leaf biomass. Future developments should endeavor to represent a more explicit belowground allocation scheme (Merganičová et al., 2019; Huaraca Huasco et al., 2021). Direct estimates of individual tree root depth and root distribution are rare in moist tropical forests (Canadell et al., 1996; Jackson et al., 1996, 1999; Nepstad et al., 1994; Cusack et al., 2024; Guerrero-Ramírez et al., 2021). Some studies have quantified the depth of tree water uptake using indirect methods, such as predawn leaf water potential, or isotope labeling

(Brum et al., 2019; Stahl et al., 2013), but this does not give access to the actual rooting depth. Tree root depth was here assumed to increase with tree size, and was computed as a function of tree *dbh* as follows (Kenzo et al., 2009, Fig. 4 therein):

$$RD = 0.35 \times dbh^{0.54} \quad (19)$$

with root depth, RD, in m, and diameter at breast height, dbh, in cm. As in Xu et al. (2016), the exponent was based on Kenzo et al. (2009), who reported on data from excavated trees in secondary forests in Malaysia. The first parameter (0.35, root depth at dbh=1cm) was adjusted to avoid unrealistic water depletion of the top soil layer. In the absence of relevant species-specific data, this allometric equation was assumed to hold for all species, even if root depth is known to be highly plastic (e.g. Rowland et al., 2023). Correlations between rooting depth and leaf phenological habit have been reported, but in drier or more seasonal sites than Amazonian rainforests (Brum et al., 2019; Hasselquist et al., 2010; Smith-Martin et al., 2020), and trait coordination are known to be typically stronger under harsher environmental conditions (Dwyer and Laughlin, 2017; Delhaye et al., 2020).

We assumed that vertical tree root distribution follows an exponential profile, as observed empirically at the stand scale (Fisher et al., 2007; Humbel, 1978; Jackson et al., 1996). The fine root biomass in layer l, at depths ranging from z_l to $z_{l+1} (> z_l)$ is computed as:

$$RB_l = RB_t \times \left(\exp\left(-3\frac{z_l}{RD}\right) - \exp\left(-3\frac{z_{l+1}}{RD}\right)\right) \quad (20)$$

where RB_t is the total tree fine root biomass (in g), RB_l the fine root biomass in layer l (in g), RD the tree rooting depth (in m). The factor 3 was determined so that about 95% of the tree biomass is contained between soil surface and RD (note that -log(0.05)≈3) (Arora and Boer, 2003). Tree roots are distributed across vertical layers, but do not spread across belowground voxels horizontally. As a result, trees only deplete the water content of the belowground voxels located below their trunk position (see section 2.3).

The soil water potential in the root zone, ψ_{root} (in MPa), captures how the plant equilibrates with the soil water state across its root profile. It is computed as the weighted mean of the belowground voxel water potentials across layers. We used the weighting scheme proposed by Williams et al. (2001; see also Bonan et al., 2014; Duursma and Medlyn, 2012), which accounts for the variation of soil water availability and conductance across layers as follows:

$$\psi_{root} = \sum_l w_l \times \psi_l \text{ with } w_l = \frac{(\psi_l - \psi_{R,min}) \times G_l}{\sum_{ll}(\psi_{ll} - \psi_{R,min}) \times G_{ll}} \quad (21)$$

where ψ_l is the soil water potential in layer l, and $\psi_{R,min}$ is the root water potential below which there is no water uptake within the layer (minimal root water potential, assumed to be -3 MPa as in Duursma and Medlyn, 2012). G_l, the soil-to-root water conductance in layer l, in mmol H_20 m^{-2} s^{-1} MPa^{-1}, computed as follows (Gardner, 1964):

$$G_l = \frac{2\pi L_{a,l} K_l}{\log\left(\frac{r_s}{r_r}\right)} \quad (22)$$

In Eq (22), $L_{a,l}$ is the total root length per unit area in the layer (in m m^{-2}), with the total root length in the layer computed as $RB_l \times SRL$ where SRL is the specific root length, here assumed to be constant (10 m g^{-1}, Bonan et al., 2014; Metcalfe et al., 2008; Weemstra et al., 2016). K_l is the soil hydraulic conductivity of layer l (in mmol H_20 m^{-1} s^{-1} MPa^{-1}, see section 2.3), r_r is

the mean fine root radius, here set at 1mm, and r_s is half the mean distance between roots, calculated with the assumption of uniform root spacing in a given layer (Newman, 1969):

$$r_s = \frac{1}{\sqrt{\pi L_{v,l}}} \quad (23)$$

where $L_{v,l}$ is the total root length per unit soil volume in the layer (in m m^{-3}), computed in the same way as $L_{a,l}$, but also divided by layer depth.

A range of other models have been used to infer ψ_{root} using the relative tree root biomass in each layer directly as weights (De Kauwe et al., 2015; Naudts et al., 2015; Powell et al., 2013; Schaphoff et al., 2018; Sakschewski et al., 2021; Verbeeck et al., 2011). However, tree do not uptake water simply as a proportion of root density, but can equilibrate with the wettest soil layers (Schmidhalter, 1997; Duursma and Medlyn, 2012): the contrasting temporal variations in water availability across layers result in seasonal changes in the depth of active water withdrawal (Bruno et al., 2006; Joetzjer et al., 2022). For instance, cavitation in the driest part of the soil disconnects roots from the soil (Sperry et al., 2002; see also Fisher et al., 2006). This is likely why deeper roots, although rare, contribute to explain the sustained forest productivity during the dry season.

2.5 Leaf physiology

The carbon assimilated and the water transpired by a tree within a day are the sum of the leaf-level carbon and water fluxes across day-time half hours. Leaf-level carbon assimilation is computed per crown layer of each tree, using the Farquhar-von Caemmerer-Berry model of C_3 photosynthesis (Farquhar et al., 1980, see section 2.5.1), coupled to the model of stomatal conductance of Medlyn et al. (2011; see section 2.5.2) as in Maréchaux and Chave (2017). In TROLL 4.0 the dependences on leaf temperature (T_l), vapor pressure deficit at the leaf surface (VPD_s), and CO_2 concentration at the leaf surface (c_s) are now determined iteratively at the leaf surface, starting from air temperature (T), air vapor pressure deficit (VPD_a) and air CO_2 concentration (c_a) averaged across the tree crown layer (see sections 2.2 and 2.4.2) and with transpiration computed using the Penman-Monteith equation (see section 2.5.4).

2.5.1 Photosynthesis

In Farquhar et al. (1980), leaf-level net carbon assimilation rate (A_n, µmol CO_2 m^{-2} s^{-1}) is limited by either Rubisco activity (A_v, µmol CO_2 m^{-2} s^{-1}), or RuBP regeneration (A_j, µmol CO_2 m^{-2} s^{-1}):

$$A_n = min\{A_v, A_j\} - R_p(T_l) \;\; ; \quad A_v = V_{cmax}(T_l, \psi_{pd}) \times \frac{c_i - \Gamma^*}{c_i + K_m(T_l)} \quad ; \quad A_j = \frac{J}{4} \frac{c_i - \Gamma^*(T_l)}{c_i + 2\Gamma^*(T_l)} \quad (24)$$

where R_p is the photorespiration rate (µmol C m^{-2} s^{-1}), V_{cmax} is the maximum rate of carboxylation (µmol CO_2 $m^{-2}s^{-1}$), c_i the CO_2 partial pressure at carboxylation sites, Γ^* the CO_2 compensation point in the absence of dark respiration, K_m the apparent kinetic constant of the Rubisco (von Caemmerer, 2000), and J the electron transport rate (µmol e^- m^{-2} s^{-1}), which depends on PPFD through:

$$J = \frac{1}{2\theta}\left[\alpha \times PPFD + J_{max}(T_l, \psi_{pd}) - \sqrt{\left(\alpha \times PPFD + J_{max}(T_l, \psi_{pd})\right)^2 - 4\theta \times \alpha \times PPFD \times J_{max}(T_l, \psi_{pd})}\right] \quad (25)$$

J_{max} is the maximal electron transport capacity (μmol e^- m^{-2} s^{-1}), θ the curvature factor (unitless), and α the apparent quantum yield to electron transport (mol e^- mol *photons*$^{-1}$), computed following von Caemmerer (2000) as $\alpha = (1 - LSQ) \times 0.5$, with LSQ the effective spectral quality of light, fixed at 0.15, and the factor 0.5 accounts for the fact that each photosystem absorbs half of the photons.

The V_{cmax} and J_{max} parameters depend on leaf properties, leaf temperature (T_l) and water state (through the leaf predawn water potential, ψ_{pd}, see Eq. (37)) and represent a large source of uncertainty in vegetation models (Zaehle et al., 2005; Mercado et al., 2009; Rogers et al., 2017). In tropical forest environments, Domingues et al. (2010) suggested that V_{cmax} and J_{max} are co-limited by the leaf concentration of nitrogen and phosphorus as follows (see also Walker et al., 2014):

$$V_{cmax-M}\ (25°C) = min\{-1.56 + 0.43 \times N\ - 0.37 \times LMA\ ;\ -0.80 + 0.45 \times P - 0.25 \times LMA\ \} \quad (26)$$

$$J_{max-M}\ (25°C) = min\{-1.50 + 0.41 \times N\ - 0.45 \times LMA\ ;\ -0.74 + 0.44 \times P\ - 0.32 \times LMA\ \} \quad (27)$$

with V_{cmax-M} and J_{max-M} the photosynthetic capacities at 25°C of unstressed mature leaves on a leaf dry mass basis, in μmol CO_2 g^{-1} s^{-1} and μmol e^- g^{-1} s^{-1}, respectively. N and P are leaf nitrogen and phosphorus concentrations in mg g^{-1}, and LMA is the leaf mass per area in g cm^{-2}. V_{cmax-M} and J_{max-M} can be converted into area-based V_{cmax} and J_{max} by multiplying by LMA. We used this leaf trait-based parameterization of $V_{cmax}(25°C)$ and $J_{max}(25°C)$ in the absence of water stress (as in Fyllas et al., 2014; Mercado et al., 2011). The dependence of V_{cmax} and J_{max} with temperature was given by equations in Bernacchi et al. (2003), and the dependence with water availability was modelled by a function of ψ_{pd} (WSF_{ns}, see section 2.5.3, Eq. (40)):

$$V_{cmax}(T_l, \psi_{pd}) = V_{cmax}(25°C) \times e^{\left(26.35 - \frac{65.33}{R \times (T_l + 273.15)}\right)} \times WSF_{ns}(\psi_{pd}) \quad (28)$$

$$J_{max}(T_l, \psi_{pd}) = J_{max}(25°C) \times e^{\left(17.57 - \frac{43.54}{R \times (T_l + 273.15)}\right)} \times WSF_{ns}(\psi_{pd}) \quad (29)$$

where R is the molar gas constant (0.008314 kJ K^{-1} mol^{-1}), and T_l is the internal leaf temperature in Celsius degrees. The temperature dependence of $\Gamma^*$and K_m followed von Caemmerer (2000):

$$\Gamma^*(T_l) = 37 \times e^{23.4 \times \frac{(T_l - 25)}{298 \times R \times (273 + T_l)}} \quad (30)$$

$$K_m(T_l) = 404 \times e^{59.36 \times \frac{(T_l - 25)}{298 \times R \times (273 + T_l)}} \times \left(1 + \frac{210}{248 \times e^{35.94 \times \frac{T_l - 25}{298 \times R \times (273 + T_l)}}}\right) \quad (31)$$

Temperature dependencies in Eqs (28)-(31) are consistent with Domingues et al. (2010), following recommendations from Rogers et al. (2017).

Leaf photorespiration rate R_p was assumed to be a fixed fraction (40%) of leaf dark respiration rate (Atkin et al., 2000). We used Atkin et al. (2015) 'broadleaved trees' empirical model to estimate mature leaf dark respiration rates as a function of plant functional traits:

$$R_{d-M}(25°C) = 8.5341 - 0.1306 \times N - 0.5670 \times P - 0.0137 \times LMA + 11.1 \times V_{cmax-M} + 0.1876 \times N \times P \quad (32)$$

with $R_{d\text{-}M}$ the leaf dark respiration rate on a dry mass basis and at reference temperature of 25°C (in nmol CO_2 $g^{-1}s^{-1}$). Multiplying $R_{d\text{-}M}$ by LMA gives the area-based leaf dark respiration R_d (in µmol C m^{-2} s^{-1}). The temperature dependence of mature leaf dark respiration rates was calculated as (Atkin et al., 2015, Eq. (1) therein; see also Heskel et al. 2016):

$$R_d(T_l) = R_d(25°C) \times \left[3.09 - 0.043 \times \frac{(T_l+25)}{2}\right]^{\frac{(T_l-25)}{10}} \quad (33)$$

Long-term acclimation to temperature is not considered in TROLL 4.0 (Kattge and Knorr, 2007; Smith and Dukes, 2013).

2.5.2 Stomatal conductance

Carbon assimilation by photosynthesis is limited by the CO_2 partial pressure at carboxylation sites, which is controlled by stomatal transport as modeled by the diffusion equation:

$$A_n = g_s(c_s - c_i) \quad (34)$$

with g_s the stomatal conductance to CO_2 (mol CO_2 m^{-2} s^{-1}). The representation of stomatal conductance varies greatly across vegetation models (Damour et al., 2010; Bonan et al., 2014; Rogers et al., 2017; see Appendix B, Table B1) and remains an active research topic (Anderegg et al., 2018; Dewar et al., 2018; Lamour et al., 2022; Sperry et al., 2017; Wolf et al., 2016; Sabot et al., 2022). In TROLL 4.0, stomatal conductance to water vapor is simulated as (Medlyn et al., 2011):

$$g_{sw} = g_0 + 1.6 \times \left(1 + \frac{g_1}{\sqrt{VPD_s}}\right) \times \frac{A_n}{c_s} \quad (35)$$

where g_{sw} is the stomatal conductance to water vapor in mol H_20 m^{-2} s^{-1}, 1.6 is the factor needed to convert one mole of CO_2 into one mole of H_20, VPD_s is the vapor pressure deficit at the leaf surface in kPa, A_n is the assimilation rate in µmol CO_2 m^{-2} s^{-1} (Eq. (24) above), c_s is the CO_2 concentration at the leaf surface in ppm, g_0 is the minimum conductance for water vapor in mol H_20 m^{-2} s^{-1} (Duursma et al., 2019), and g_1 is a model parameter in $kPa^{1/2}$. Equations 24, 34 and 35 taken together lead to two quadratic equations for c_i, one when Rubisco activity is limiting and one when RuBP regeneration is limiting, and the solution is the highest root.

The parameter g_1 varies with species ecological strategies and carbon cost of water use (Domingues et al., 2014; Franks et al., 2018; Héroult et al., 2013; Lin et al., 2015; Wolz et al., 2017). Consequently, it is expected that g_1 should differ across plant functional types (e.g. Xu et al., 2016). Here we assumed a dependence of g_1 with wood density (wsg, in g cm^{-3}) as in Lin et al. (2015). We also assumed a dependence with water availability, modelled by a function of ψ_{pd} (WSF_s; see section 2.5.3):

$$g_1 = (-3.97 \times wsg + 6.53) \times WSF_s(\psi_{pd}) \quad (36)$$

This parameterization of g_1 based on wood density is a matter of debate however, and alternatives have been proposed (Wu et al., 2020; Lamour et al., 2023).

The parameter g_0 quantifies water fluxes through the leaf cuticle (cuticular conductance) and from stomatal leaks. Although it is increasingly recognized as a key parameter explaining tree water loss in drought conditions (Cochard, 2021; Martin-StPaul et al., 2017), its values and variation with other functional traits is poorly documented (Duursma et al., 2019;

Slot et al., 2021; Nemetschek et al., 2024), and we here assumed a fixed value. Note that some previous studies have defined g_0 as cuticular conductance only, ignoring stomatal leak effects, and thus underestimating g_0.

Both g_0 and g_1 were assumed not to depend on temperature in the absence of clear empirical evidence for tropical forest trees (Duursma et al., 2019; Slot et al., 2021; Rogers et al., 2017), but this may be further explored in the future through measurement and experiment (Cochard, 2021).

2.5.3 Effect of water availability on leaf-level gas exchange

Under water stress, leaf-level gas exchanges and photosynthesis are impaired, but how this is represented varies greatly across models (Appendix B, Table B1; Powell et al., 2013; Trugman et al., 2018; Verhoef and Egea, 2014). A common approach is to define a single integrative water stress factor cumulating all effects along the soil-plant-atmosphere pathway, some of which being difficult to evaluate empirically (e.g. Fischer et al., 2014; Gutiérrez et al., 2014; Krinner et al., 2005; Clark et al., 2011). This factor is then used to modify the parameters of the stomatal conductance and/or photosynthesis models (Egea et al., 2011; Verhoef and Egea, 2014). Depending on models, water stress factors have been assumed to depend on soil water content or on soil water potential in the root zone (De Kauwe et al., 2015; Drake et al., 2017; Joetzjer et al., 2014; Powell et al., 2013; Trugman et al., 2018). Alternatively, some models have implemented a water stress factor as a function of leaf water potential (ψ_{leaf}; Christoffersen et al., 2016; Duursma and Medlyn, 2012; Kennedy et al., 2019; Xu et al., 2016; see also the pioneer work of Tuzet et al., 2003) or used optimization approaches (Williams et al., 1996; Anderegg et al., 2018; Sabot et al., 2020; Sperry et al., 2017; Wolf et al., 2016), to account for the cost of water uptake and transportation in the plant water column. The shape of such functions remains contentious however (Table B1), resulting in substantial differences in model predictions.

Also, there is no consensus on the relative role of stomatal and non-stomatal limitations on leaf CO_2 assimilation under drying conditions, reflecting contrasted experimental results (Drake et al., 2017; Zhou et al., 2014; Keenan et al., 2010; Appendix B, Table B2). Under stomatal limitation, stomatal closure reduces leaf gas exchanges, and the water stress factor is applied on stomatal conductance, or stomatal conductance model parameters (e.g. g_1). Under non-stomatal limitations, drought (leading to increased leaf temperature and/or decreased leaf water potential) impairs the biochemical photosynthesis apparatus, which results in a reduction of photosynthetic capacities, and/or mesophyll conductance (Flexas et al., 2004, 2012). In this latter case, the water stress factor is applied on V_{cmax} and J_{max} (Drake et al., 2017; Keenan et al., 2010). Some models consider only one limitation, and others both (Appendix B, Table B1).

In TROLL 4.0, two water stress factors are used, one for stomatal limitation, modifying the g_1 parameter (WSF_s; Eq. (36)), and one for non-stomatal limitations, modifying the V_{cmax} and J_{max} parameters of the photosynthesis model (WSF_{ns}; Eq. (28) and (29)). Both water stress factors are assumed to depend on the leaf predawn water potential (ψ_{pd}; De Kauwe et al., 2015; Verhoef and Egea, 2014), which is a function of the soil water potential in the root zone (ψ_{root}, Eq. (21)) (Stahl et al., 2013, but see Bucci et al., 2004; Donovan et al., 2003) as follows (Jones, 2013; Eq. (4.9) therein):

$$\psi_{pd} = \psi_{root} - \rho g h \simeq \psi_{root} - 0.01 \times h \quad (37)$$

where ρ is the density of water, g the gravitational force (g=9.81 m s^{-2}), and h total tree height in m. Here, WSF_s was computed as (Zhou et al., 2013; De Kauwe et al., 2015):

$$WSF_s = \exp(b \times \psi_{pd}) \quad (38)$$

where b is a parameter. To parameterize b, we used the relationship between the leaf water potential at turgor loss point (ψ_{tlp} in MPa) and the water potential causing 90% of stomatal closure (ψ_{gs90}, in MPa): $\psi_{tlp} = 0.97 \times \psi_{gs90}$ (P<0.01, R^2=0.4; Fig. 1 in Martin-StPaul et al. 2017), and assumed that $WSF_s \approx 0.1$ at ψ_{gs90} (an approximation given the shape of Eq. (35)), leading to:

$$WSF_s = \exp\left(-2.23 \times \frac{\psi_{pd}}{\psi_{tlp}}\right) \quad (39)$$

The link between the leaf water potential at stomatal closure and the leaf water potential at turgor loss point is supported by several studies (Bartlett et al., 2016b; Brodribb et al., 2003; Farrell et al., 2017; Martin-StPaul et al., 2017; Meinzer et al., 2016; Rodriguez-Dominguez et al., 2016; Trueba et al., 2019). The formulation of WSF_s in Eq (39) was preferred over alternatives, such as a linear relationship between WSF_s and ψ_{pd} (Oleson et al., 2008; Powell et al., 2013; Verhoef and Egea, 2014). The latter is less supported by data and leads to threshold responses as soil water content declines and similar responses across species, in contrast with empirical evidence (Kursar et al., 2009; Zhou et al., 2013).

The water stress factor for non-stomatal limitation (WSF_{ns}) was computed following Xu et al. (2016):

$$WSF_{ns} = \left(1 + \left(\frac{\psi_{pd}}{\psi_{tlp}}\right)^a\right)^{-1} \quad (40)$$

with a=6 estimated from data reported in Brodribb et al. (2003). In this formula, $WSF_{ns} = ½$ when $\psi_{pd} = \psi_{tlp}$, in agreement with empirical findings (Brodribb et al., 2002; Manzoni, 2014).

The parameterization of WSF_s and WSF_{ns} based on ψ_{tlp} is supported by the fact that leaf cells need to maintain turgor to sustain functioning (Hsiao, 1973). These functions do not depend on ψ_{tlp} when $\psi_{pd} = \psi_{tlp}$, so there a simple link between the leaf drought tolerance, as informed by ψ_{tlp}, and the response of leaf-level gas exchange to water availability. Also, these equations predict that the decline of stomatal conductance as water availability decreases precedes that of photochemistry, consistent with observations (Fig. 2; Fatichi et al., 2016; Trueba et al., 2019).

Note that, since mesophyll conductance is not explicitly represented here, the effect of water stress on photosynthetic capacities (WSF_{ns}) includes both direct effects on the photosynthetic machinery and indirect effects from the reduction of mesophyll conductance (Drake et al., 2017; Keenan et al., 2010). Alternative shapes of water stress factors could be explored in the future, and a more explicit representation of the water flow through the plant water column could be implemented (Paschalis et al., 2024). In the absence of a clear consensus on the effect of water stress on respiration, TROLL 4.0 does not assume that respiration depends on water availability (Flexas et al., 2006, 2005; Rowland et al., 2018, 2015; Santos et al., 2018; Stahl et al., 2013b).

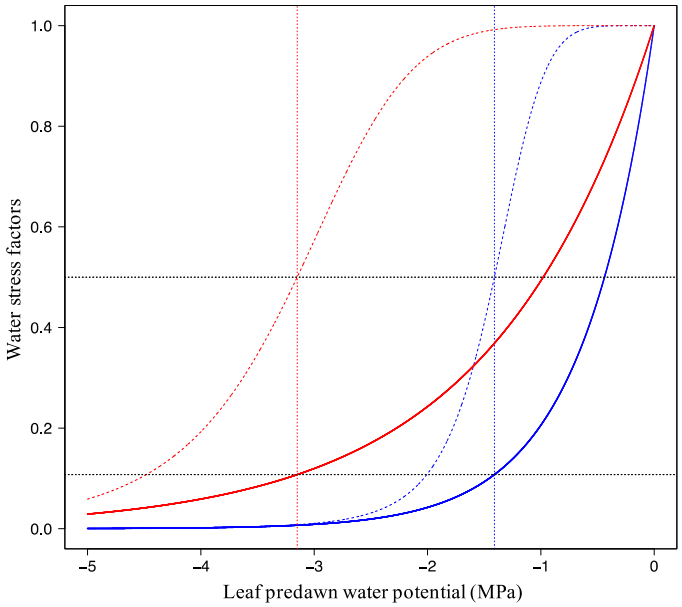

Figure 2: Responses of leaf-level gas exchange to water stress, depending on the leaf drought tolerance. Water stress factors for the stomatal conductance parameter g_1 (stomatal limitation, WSF_s, Eq. (39); solid lines) and for the photosynthetic capacities J_{max} and V_{cmax} (non-stomatal limitation, WSF_{ns}, Eq. (40); dashed lines) as a function of leaf predawn water potential (ψ_{pd}, in MPa). WSFs are shown for a a drought vulnerable species (ψ_{tlp}=-1.41 MPa, the least negative value reported in Maréchaux et al., 2015; blue lines), and for a drought tolerant species (ψ_{tlp}=-3.15 MPa, the most negative value reported in Maréchaux et al., 2015). Vertical dotted lines: ψ_{tlp}, horizontal dotted black lines: WSF_s and WSF_{ns} at ψ_{tlp}.

2.5.4 Leaf energy balance

In TROLL 4.0, leaf temperature (T_l), vapor pressure deficit (VPD_s) and CO_2 concentration (c_s) at the leaf surface are computed through an iterative scheme that solves the leaf energy balance (Medlyn et al., 2007; Wang and Leuning, 1998; Duursma, 2015; Vezy et al., 2018). This is an important step because the leaf boundary layer plays a key role on gas exchanges, and especially so in dense tropical moist forests, given the large size of tropical tree leaves and the low wind speeds within canopies (De Kauwe et al., 2017; Jarvis and McNaughton, 1986; Meinzer et al., 1997). The iterative scheme is as follows. Initially, T_l, VPD_s and c_s are set equal to surrounding air values (T, VPD and c_a). Leaf photosynthesis (A_n) and stomatal conductance (g_{sw}) are computed using Eqs (24), (34) and (35); next, the boundary layer conductance and radiation conductance are computed; and finally leaf-level transpiration rate is deduced from the Penman-Monteith equation (Eq. (41) below). After these steps, new values for T_l, VPD_s and c_s are computed, and the above steps are repeated until leaf temperature converges, i.e., when the absolute difference between the T_l of two consecutive iteration is lower than 0.01°C.

Leaf-level transpiration rate E_l (in mol H_20 m^{-2} s^{-1}) is calculated as:

$$E_l = \frac{1}{\lambda} \times \frac{sR_{ni} + VPD_a g_H C_p M_a}{s + \gamma \frac{g_H}{g_w}} \quad (41)$$

where λ is the latent heat of water vapor (in J mol^{-1}), s is the slope of the (locally linearized) relationship between saturated vapor pressure and temperature (in Pa K^{-1}, see Jones, 2013, Eq. (5.15) therein), R_{ni} is the isothermal net radiation (in J m^{-2} s^{-1}), g_H is the total leaf conductance to heat (in mol m^{-2} s^{-1}), C_p is the heat capacity of air (1010 J kg^{-1} K^{-1}), M_a is the molecular mass of air (28.96$\times 10^{-3}$ kg mol^{-1}), γ the psychrometric constant (in Pa K^{-1}), and g_w the total conductance to water vapor (mol H_20 m^{-2} s^{-1}). The latent heat of water vapor λ depends on air temperature as follows:

$$\lambda = (2.501 \times 10^3 - 2.365 \times \mathrm{T}) \times 18 \quad (42)$$

The isothermal net radiation R_{ni} has two components, the absorbed solar radiation (S_{abs}), including both PAR and NIR wavebands, and the net longwave radiation (Leuning et al., 1995; Appendix D therein):

$$R_{ni} = S_{abs} - B_{n,0} \times k_d \exp(-k_d LAI) \quad (43)$$

where $B_{n,0}$ is the net longwave radiation at the top of the canopy, and $k_d \exp(-k_d LAI)$ accounts for its extinction within the canopy, with k_d set equal to 0.8. To account for the absorbed NIR radiation at a given height within the canopy in S_{abs}, we used the relationship reported by Kume et al. (2011; Fig. 4 therein) that links the transmitted NIR to the transmitted and incident PAR, and assumed a leaf absorptance in the NIR equal to 0.1. $B_{n,0}$ is then computed as the absorbed minus the emitted longwave radiation:

$$B_{n,0} = \varepsilon_l(1 - \varepsilon_a)\sigma T_{top}^4 \quad (44)$$

where T_{top} is the top canopy air temperature in K, σ is the Stefan-Boltzmann constant ($\sigma = 5.67 \times 10^{-8}$ W m^{-2} K^{-4}), ε_l is the emissivity of the canopy leaves, here assumed to be 1, and ε_a the emissivity of the atmosphere. Several models exist for ε_a, with varying performance depending on the sky conditions (Marthews et al., 2012). We here used Dilley and O'Brien (1998), which compromises between parsimony and performance across sky conditions (Marthews et al., 2012; Tables 2 and 5 therein).

g_H, the total leaf conductance to heat, has three components, the boundary layer conductance for free convection g_{bHf}, the boundary layer for forced convection g_{bHu}, and the radiation conductance g_r (Leuning et al., 1995; Jones, 2013):

$$g_H = 2 \times \left(g_{bHf} + g_{bHu} + g_r \right) \quad (45)$$

where the factor 2 accounts for the two sides of the leaves. g_{bHf}, the boundary layer conductance for free convection, is given by:

$$g_{bHf} = 0.5 \times D_H \times \left(\frac{1.6 \times 10^8 \times |T_l - \mathrm{T}|}{w_l} \right)^{0.25} \times \frac{P_{ress}}{R\mathrm{T}} \quad (46)$$

where D_H is the molecular diffusivity to heat ($D_H = 21.5 \times 10^{-6}$ m^2 s^{-1}), P_{ress} the atmospheric pressure (in Pa), R the universal gas constant (R=8.314 J mol^{-1} K^{-1}) and T the temperature of surrounding air in K. Leaf width w_l (in m) is estimated as the square root of leaf area ($w_l = \sqrt{LA}$). g_{bHu}, the boundary layer for forced convection (in mol m^{-2} s^{-1}), is given by:

$$g_{bHu} = 0.003 \times \sqrt{\frac{u}{w_l}} \times \frac{P_{ress}}{R\mathrm{T}} \quad (47)$$

where u is the wind speed in m s^{-1} (see Eq. (9)). g_r, the radiation conductance in mol m^{-2} s^{-1} varies with T_a as follows (Jones, 2013, p.101 therein):

571 $g_r = \frac{4 \times \varepsilon_l \sigma T^3}{C_p M_a}$ (48)

572 g_w the total conductance to water vapor has two components that represent hydraulic resistances in series: the stomatal
573 conductance (g_{sw}, in mol H_20 m^{-2} s^{-1}, Eq. (35)) and the boundary layer conductance (g_{bw} in mol H_20 m^{-2} s^{-1}) to water vapor:

574 $g_w = \frac{g_{bw} \times g_{sw}}{g_{bw} + g_{sw}}$ (49)

575 with $g_{bw} = 1.075 \times \left(g_{bHf} + g_{bHu} \right)$ (50)

576 where 1.075 accounts for the relative diffusivities of heat and water vapor in air. Equations (49) and (50) assume that all leaves
577 are hypostomatous (stomates on the ground-facing side of the leaves only), a reasonable assumption in tropical forests (Drake
578 et al., 2019; Muir, 2015).

579 **2.6 Carbon allocation**

580 **2.6.1. Net carbon uptake: whole-tree integration and respiration**

581 At each daily timestep, the individual tree net primary productivity of carbon, NPP_{ind} (in gC), is obtained by the following
582 balance equation (Fig. 3):

583 $NPP_{ind} = GPP_{ind} - R_{maintenance} - R_{growth}$ (51)

584 GPP_{ind} (in gC) is computed each half hour as the carbon assimilation rate A_n (Eq. (19)), multiplied by the leaf area in each
585 tree crown layer (LA_l, in m^2), then summed over tree crown layers and cumulated across the day.

586 Young leaves and old leaves have been reported to have lower photosynthetic capacities and activities than mature
587 leaves (Doughty and Goulden, 2008; Kitajima et al., 2002, 1997b; Wu et al., 2016; Albert et al., 2018; Menezes et al., 2021).
588 For each tree, total leaf area (LA_t) is partitioned into three leaf age pools: young, mature and old leaves, so that $LA_t = LA_{young}$
589 + LA_{mature} + LA_{old} (all in m^2). These three leaf age pools are assumed to be uniformly distributed within the tree crown. In
590 young and old leaves, net assimilation rate is a fraction $\varrho < 1$ of that of mature leaves, so that:

591 $GPP_{ind} = C_{GPP} \times \frac{(\varrho \times LA_{young} + LA_{mature} + \varrho \times LA_{old})}{LA_t} \sum_l \sum_t A_n(t,l) \times LA_l$ (52)

592 where the factor C_{GPP} is a conversion factor, t depicts the daytime half-hours and l the tree crown layers. Here we assume that
593 the carbon uptake efficiency ϱ relative to mature leaves is the same in young and old leaves and $\varrho = 0.5$, a value consistent
594 with observations.

595 TROLL 4.0 partitions autotrophic respiration into maintenance respiration and growth respiration, even if both come
596 from the same biochemical pathways (Amthor, 1984; Thornley and Cannell, 2000). Maintenance respiration ($R_{maintenance}$) has
597 seldom been documented for stem and roots and is inferred empirically (Cavaleri et al., 2008; Meir et al., 2001; Slot et al.,
598 2013; Weerasinghe et al., 2014). Nighttime leaf maintenance respiration is computed using Eqs (32) and (33), using the mean
599 nighttime temperature. As stomatal conductance and dark respiration vary less with leaf age than carbon assimilation rate
600 (Albert et al., 2018; Kitajima et al., 2002; Villar et al., 1995), we assumed that young and old leaves have respiration and

transpiration rate equal to $\varrho' = 0.75$ that of mature leaves, leading to lower water use efficiency than mature leaves. Tree-level nighttime leaf respiration and daytime transpiration are computed as follows at each timestep:

$$X_{ind} = C_X \times \frac{(\varrho' \times LA_{young} + LA_{mature} + \varrho' \times LA_{old})}{LA_t} \sum_l (\sum_i \mathrm{X}(i,l)) \times LA_l \quad (53)$$

where X_{ind} is either the carbon respired by leaves during the night or the total water transpired by the tree, in gC or m^3 respectively, X being the leaf dark respiration (Eqs. (32) and (33)) or the leaf-level transpiration rate (Eq. (41)) respectively, and C_X is a conversion factor.

Stem maintenance respiration (R_{stem}, in μmol C s^{-1}) was modeled assuming a constant respiration rate per volume of sapwood (39.6 μmol m^{-3} s^{-1}, Ryan et al., 1994), so that:

$$R_{stem} = C_{sresp} \times 39.6 \times SA \times (h - cd) \quad (54)$$

where SA is the tree sapwood area (in m^2) and C_{sresp} is a conversion factor. Stem respiration response to temperature was modeled using a Q_{10} value of 2.0 (Meir and Grace, 2002; Ryan et al., 1994), and using mean daytime and nighttime temperatures. Stahl et al. (2011) reported that R_{stem} varies among individual trees, even when controlling for sapwood volume. However, in absence of a clear understanding of the drivers, Eq. (54) is a parsimonious choice. In TROLL 4.0, sapwood area is computed dynamically. We used an inversion of the pipe model to derive sapwood area from the tree's leaf area (LA_t, in m^2), height (h, in m) and wood density following Fyllas et al. (2014; Eqs (7) and (8) therein):

$$SA = C_{SA} \frac{2 \times LA_t}{\lambda_1 + \lambda_2 \times h + \delta_1 + \delta_2 \times wsg} \quad (55)$$

with λ_1= 0.066 m^2 cm^{-2}, λ_2=0.017 m cm^{-2}, δ_1=-0.018 m^2 cm^{-2}, and δ_2 =1.6 cm^3 g^{-1}, and C_{SA} a conversion factor. In addition to Eq. (55), there are both lower and upper limits on sapwood extent. Sapwood has a minimum thickness of 0.5 cm and any newly grown wood is always considered sapwood, irrespective of leaf area. TROLL 4.0 also imposes an upper limit on sapwood growth based on stem diameter growth, so that increases in living tissue cannot exceed increases in total tissue.

Other contributions of maintenance respiration were prescribed as proportions of leaf and stem maintenance respiration. Fine root maintenance respiration was assumed to be half of leaf maintenance respiration (Malhi, 2012), and coarse root and branch maintenance respirations were assumed to account for half of stem respiration (Asao et al., 2015; Cavaleri et al., 2006; Meir and Grace, 2002).

Growth respiration (R_{growth}) was assumed to account for 30% of the carbon uptake by photosynthesis (gross primary productivity) minus the maintenance respiration (Cannell and Thornley, 2000). These assumptions are commonly made in the literature, but remain a major source of uncertainty in the carbon flux modeling (Atkin et al., 2014; Huntingford et al., 2013).

Contrary to the last published version of TROLL, in which the allocation of NPP_{ind} to plant organs was fully prescribed by fixed factors (f_{canopy}= f_{leaves} + f_{fruit} + f_{twigs} and f_{wood}, Maréchaux and Chave, 2017), the allocation scheme implemented in TROLL 4.0 can now be additionally modulated depending on the current tree state and it includes an explicit carbon storage compartment (sections 2.6.2 and 2.6.3; Fig. 3).

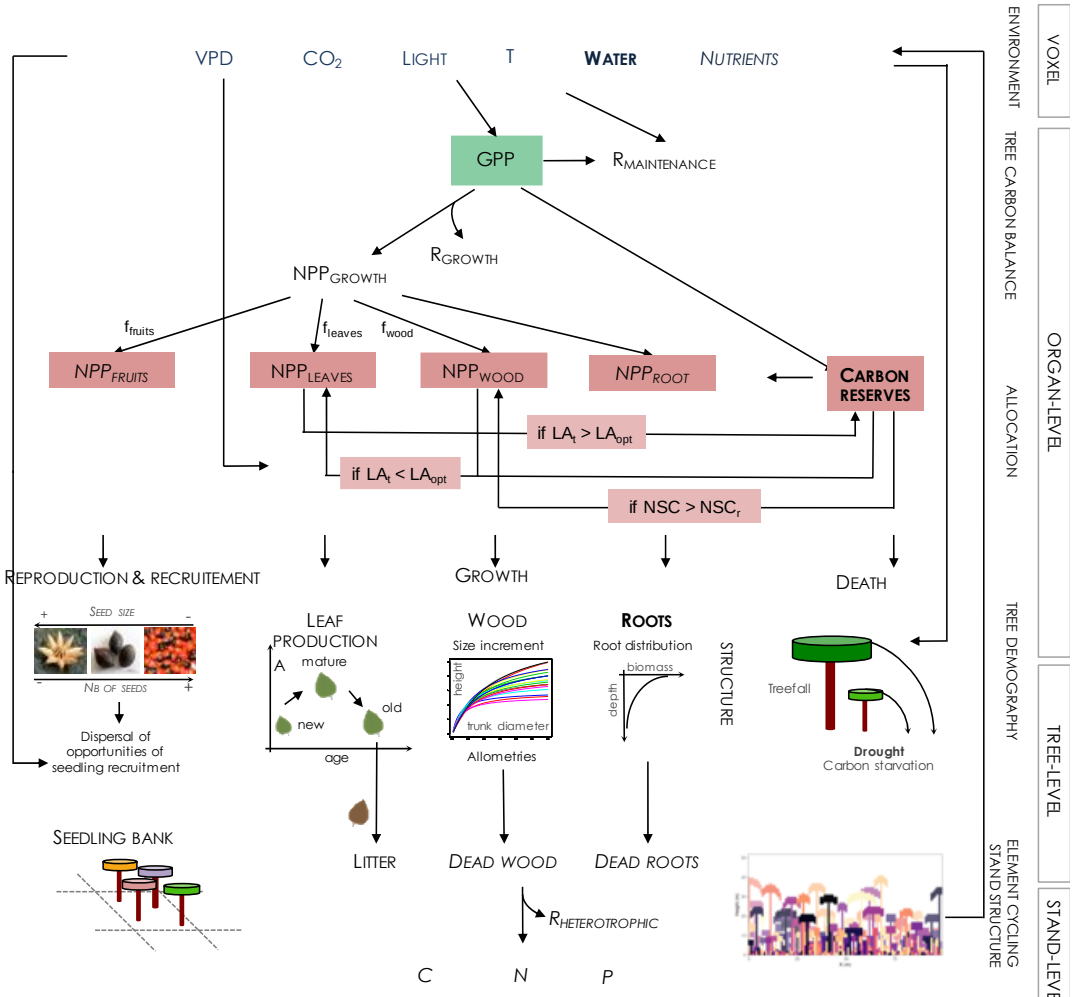

Figure 3: Diagram of structures and processes driving individual and community dynamics, as investigated under the modeling approach adopted in TROLL 4.0. Elements in bold letters refer to novel implementation in comparison to the previous published version, while italic letters refer to elements still not included in this present version. Abiotic environment is modeled at the voxel scale and drive C assimilation in the leaves (gross primary productivity, GPP) and maintenance respiration rates of the different plant organs ($R_{MAINTENANCE}$). The C amount resulting from the balance between GPP and $R_{MAINTENANCE}$ can be used for tissue production (NPP_{FRUITS}, NPP_{LEAVES}, NPP_{WOOD} and NPP_{ROOTS}) or stored (CARBON RESERVES) in the different tree organs. Both allocations induce metabolic costs (R_{GROWTH} and $R_{STORAGE}$; but the latter is not represented nor included). CARBON RESERVES represents non-structural carbohydrates (NSC), mainly stored as sugar or starch, and its maximal storage capacity is given by NSC_r. Allocation to these different compartments follows a hierarchical scheme initialized by default proportions (f_{fruits}, f_{leaves}, f_{wood}). If the tree leaf area (LA_t) exceeds the optimal leaf area (LA_{opt}, a function of both tree properties and its micro-environment), then the surplus of NPP_{LEAVES} is allocated to carbon reserves. If the tree leaf area is lower than optimal, then NPP_{WOOD}, and if further needed, carbon reserves, are mobilized for leaf production. If carbon reserves surpasses its storage capacity (NSC_r), then stored carbohydrates are used for woody growth. C allocated to tissue production leads to an increment of trunk diameter and height following allometric relationhips, and the production of new young leaves and roots. Simultaneously with tissue turnover, this leads to the update of leaf density and root biomass distribution, influencing both abiotic environment (eg. light diffusion and water interception) and light and element acquisition, and thus carbon assimilation and metabolism. C allocated to reproduction leads to the production of seeds, which are dispersed randomly. This generates a spatially-explicit seedling bank, from which winners are locally recruited depending on both light and water availability. Tree death may be triggered by environmental or mechanical

constraints, or carbon starvation. Litter decomposition, wood decay and nutrient mineralization, leading to soil nutrient availability for plant uptake, take place through the action of soil microorganisms, which activity, and hence respiration ($R_{HETEROTROPHIC}$), depends particularly on temperature and soil moisture.

2.6.2 Leaf production and leaf shedding

Leaf phenology is a key driver of the variation of tropical forest productivity (Manoli et al., 2018; Restrepo-Coupe et al., 2013; Wu et al., 2017). However, its underlying drivers remain poorly understood, and its representation in vegetation models remains challenging (Chen et al., 2020; Restrepo-Coupe et al., 2017). In ORCHIDEE, Chen et al. (2020, 2021) proposed a leaf phenological scheme in which the production of young leaves is partly controlled by incident shortwave radiation, while the shedding of old leaves is controlled by vapor pressure deficit. This scheme reproduces the simultaneous increase in leaf production and litterfall observed in many Amazonian rainforest sites where productivity increases during the dry season (Chave et al., 2010; Wagner et al., 2016; Yang et al., 2021), but not the observed seasonality in productivity at some sites (e.g. GUYAFLUX eddy-flux site in French Guiana, Chen et al., 2020). Additionally, this scheme overlooks the contrasted leaf phenological patterns observed across canopy individuals within and across species within communities (Nicolini et al., 2012; Loubry, 1994). In ED2, Xu et al. (2016) implemented a leaf phenological scheme driven by water availability in the root zone in a seasonally dry tropical forest. Since leaf shedding is often triggered by drought-induced loss of leaf turgor in these systems (Sobrado, 1986), leaf shedding and production are assumed to depend on the difference between leaf predawn water potential and leaf water potential at turgor loss point. However, such a scheme cannot simulate the simultaneous leaf production and shedding observed in moist tropical forests.

In TROLL 4.0, we propose an alternative approach. At each timestep, the optimal tree total leaf area (LA_{opt}) is estimated as the leaf area beyond which producing more leaves leads to a net carbon loss due to self-shading and respiration costs. LA_{opt} depends on tree crown size and leaf area density (section 2.4.2), leaf photosynthetic capacities and respiration rate (section 2.5.1), and local light environment. At each timestep, the amount of carbon allocated to the production of new young leaves, NPP_{leaves}, and to woody growth, NPP_{wood}, are determined by default as: $NPP_{leaves} = f_{leaves} \times NPP_{ind}$, with $f_{leaves} = 0.68 \times f_{canopy}$ (Chave et al., 2008, 2010; Maréchaux and Chave, 2017), and $NPP_{wood} = 0.6 \times f_{wood} \times NPP_{ind}$, where the factor 0.6 accounts for the fact that about 40% of woody NPP is actually used for branch fall repair (Malhi et al., 2011). When leaf area LA_t exceeds LA_{opt}, NPP_{leaves} is reduced so that $LA_t = LA_{opt}$. Second, if the carbon allocated to leaf production is not sufficient to compensate leaf loss, then the carbon attributed by default to tree woody growth is mobilized for leaf production until leaf loss is compensated. If not sufficient, the tree carbon storage (see section 2.6.3) is then also mobilized. Hence this scheme prioritizes the maintenance of the assimilating tissues over woody growth (Schippers et al., 2015). The variation of leaf area for each leaf age pool is then computed as follows:

$$\Delta LA_{young} = \frac{2 \times NPP_{leaves}}{LMA} - \frac{LA_{young}}{\tau_{young}}$$

$$\Delta LA_{mature} = \frac{LA_{young}}{\tau_{young}} - \frac{LA_{mature}}{\tau_{mature}}$$

$$\Delta LA_{old} = \frac{LA_{mature}}{\tau_{mature}} - \frac{LA_{old}}{\tau_{old}} \quad (56)$$

where τ_{young}, τ_{mature}, τ_{old} are the residence times in each class (in yr), so that LL= τ_{young}+τ_{mature}+τ_{old} with LL the maximal tree leaf lifespan (in yr). LL is inferred from the tree LMA, using the following empirical relationships (Schmitt, 2017):

$$LL = \frac{1}{12}\max(3, 12.755 \times \exp(0.007 \times LMA - 0.565 \times N)) \quad (57)$$

τ_{young} was fixed to min(LL/3, 1/12) yr (Doughty and Goulden, 2008; Wu et al., 2016), and τ_{mature} as a third of total leaf lifespan.

The loss term LA_{old}/τ_{old} corresponds to the rate of leaf litterfall at each timestep. In the previous TROLL version, litterfall resulted from the dynamics of leaf biomass with τ_{old}= LL - τ_{young}- τ_{mature}. This leaf shedding scheme is passive and does not simulate the observed seasonality in leaf litterfall. Here we propose a new approach to simulate leaf shedding. We first observed that within species and sites, canopy trees can shed their leaves at different times, suggesting that causal environmental drivers should display fine-scale heterogeneity in space (unlike atmospheric shortwave radiation and vapor pressure deficit). In addition, old leaves display nutrient resorption before abscission (Albert et al., 2018; Kitajima et al., 1997a; Urbina et al., 2021); similarly, solute translocation from older to younger leaves can lower osmotic potential and leaf water potential at turgor loss point, thus increasing the drought tolerance of younger leaves to the detriment of older leaves (Pantin et al., 2012). We therefore used predawn leaf water potential as a trigger of leaf shedding as in Xu et al., (2016), but with different thresholds for leaves of different ages, older leaves being more susceptible to a small decrease in tree water availability, while younger leaves can maintain turgor and grow at the same time. More specifically, we defined the following threshold:

$$\psi_{T,o} = \min(a_{T,o} \times \psi_{tlp}, -0.01 \times h - b_{T,o}) \quad (58)$$

The first term in $\psi_{T,o}$ with $a_{T,o} < 1$ represents old leaves' lower ability to maintain turgor as soil dries. The second term modulates this susceptibility to drought depending on tree height (Bennett et al., 2015): it induces a susceptibility to a (small) decrease $b_{T,o} > 0$ in soil water availability for large trees, while preventing them from constantly shedding their old leaves at fast pace (see Eq. (37)). τ_{old} is then updated using a multiplying factor f_o ($0.001 \leq f_o \leq 1$). Initially, $\tau'_{old} = f_o \tau_{old}$ with $f_o = 1$, which is updated daily as follows: $f'_o = f_o - \delta_o$ when $\psi_{pd} < \psi_{T,o}$ and $f'_o = f_o + \delta_o$ when $\psi_{pd} > \psi_{T,o}$, always assuming that f_o has 0.001 as a lower bound, and 1 as an upper bound.

We assumed no variation of ψ_{tlp} with tree height (Maréchaux et al., 2016). The threshold $\psi_{T,o}$ jointly depends on ψ_{tlp} and tree height h to account for drought tolerance and tree height on leaf-level water stress. Practically, the tree height above which old leaves becomes susceptible to a small decrease in soil water availability is $H_{T,o} = -100 \times (a_{T,o}\psi_{tlp} + b_{T,o})$ in m: 28 m at ψ_{tlp}=-1.5 MPa and 58m at ψ_{tlp}=-3 MPa (when $a_{T,o}$= 0.2 and $b_{T,o} = 0.02$). While this scheme is based on process-based observations, parameters $a_{T,o}$, $b_{T,o}$, and δ_o are currently calibrated (see Schmitt et al., submitted companion paper).

2.6.3 Carbon storage

In TROLL 4.0, trees can store carbon explicitly in non-structural carbohydrates. The maximal amount of carbon a tree can store and remobilize is determined as follows:

$$NSC_r = 1000 \times 0.5 \times 0.05 \times 1.25 \times AGB \quad (59)$$

where NSC_r stands for non-structural carbohydrates (in gC), AGB is the tree aboveground biomass (in kg), and 1000×0.5 converts biomass in kg into C in g (Elias and Potvin, 2003). It is assumed that NSC can account for 10% of the tree biomass, half of which is mobilizable (Martínez-Vilalta et al., 2016), hence the factor 0.05. The other half of NSC supports critical metabolic functions or is no longer accessible. The factor 1.25 accounts for an additional 25% biomass storage in coarse roots, so $1.25 \times AGB$ is total tree biomass (Ledo et al., 2018). AGB is computed following (Chave et al., 2014; Eq. (5) therein):

$$AGB = 0.0559 \times wsg \times dbh^2 \times h \quad (60)$$

where dbh is in cm, h in m and wsg in g cm^{-3}. The NSC storage compartment is filled by the potential carbon surplus resulting from the allocation to leaf production, i.e. $f_{leaves} \times NPP_{ind} - NPP_{leaves}$, if positive. If the storage compartment has reached its maximal capacity NSC_r, then the surplus is allocated to woody growth.

2.6.4 Growth

The net primary production allocated to woody growth, NPP_{wood}, depends on the outcome of allocation to leaf production and carbon reserves (see sections 2.6.2 and 2.6.3; Fig. 3). In TROLL 4.0, hydraulic control on carbon assimilation and leaf phenology both influence carbon allocation to trunk growth (e.g. Doughty et al., 2014; Farrior et al., 2013; Friedlingstein et al., 1999), but turgor-mediated processes are not explicitly modeled (Coussement et al., 2018; Peters et al., 2023; Muller et al., 2011; Körner, 2015). NPP_{wood} is converted into an increment of stem volume, ΔV in m^3, as follows:

$$\Delta V = 10^{-6} \times \frac{NPP_{wood}}{0.5 \times wsg} \times Senesc(dbh) \quad (61)$$

where the factor 0.5 converts dry biomass units into carbon units (Elias and Potvin, 2003). The function $Senesc(dbh)$ is designed so that the largest trees cannot allocate carbon as efficiently into growth, reflecting empirical evidence of a size-related relative growth decline in trees (Yoda et al., 1965; Ryan et al., 1997; Mencuccini et al., 2005; Woodruff and Meinzer, 2011; Stephenson et al., 2014). We assumed that trees cannot exceed a trunk diameter of $dbh_{max} = \frac{3}{2} dbh_{thresh}$, where dbh_{thresh} depends on species-specific information provided by the user (see section 2.4.1), so that:

$$\begin{aligned} Senesc(dbh) &= 1 && when\ dbh \leq dbh_{thresh} \\ Senesc(dbh) &= \max\left(0;\ 3 - 2\frac{dbh}{dbh_{thresh}}\right) && when\ dbh > dbh_{thresh} \end{aligned} \quad (62)$$

Trunk diameter growth increment Δdbh (in m), is computed from ΔV as follows. $V = C\,\pi(\frac{dbh}{2})^2 h$, where C is a form factor (Chave et al. 2014, Eq. (5) therein). The term h (in m) is total tree height inferred from the dbh following Eq. (16), this leads to an expression of V as a function of dbh only. This function can be inverted to estimate Δdbh as a function of ΔV, which is known from Eq. (61). Tree height and crown dimensions are then updated using Eqs (16), (17) and (18).

2.7 Tree demography

2.7.1 Seed production, dispersal and recruitment

The starting point for a tree life cycle, as represented in TROLL 4.0 is an event of seed dispersal into the seed bank. On each 1x1 m ground site and for each species *s*, a 'seed' bank stores all the seeds dispersed from the mature trees as well as from an external seed rain. The seed bank is updated once a year. Here, our conceptual 'seeds' represent opportunities of seedling recruitment rather than as true seeds, since not all seed dispersal events are modeled explicitly, and the seed-to-seedling transition is implicit.

In TROLL 4.0 trees are assumed to become fertile above a diameter threshold dbh_{mature} that depends on the tree maximal size (Visser et al., 2016) as follows:

$$dbh_{mature} = 0.5 \times dbh_{thresh} \quad (63)$$

This relationship is drawn from direct observations of reproductive status of tree species in the tropical forest of Barro Colorado Island, Panama, with maximal tree *dbh* spanning a range of 0.05 to 2 m (see Fig. S9 in Visser et al., 2016; R^2=0.81, n= 60 species). The number of reproduction opportunities per mature tree, n_s, is assumed fixed and equal for all individuals, and its value is user-defined. This assumption of a fixed reproductive opportunity per tree is predicated on the fact that there is a trade-off between seed number and seed size, itself related to seed and seedling survival. Thus, the probability of germination does not depend strongly on seed size or on the number of produced seeds and can be assumed a zero-sum game (Coomes and Grubb, 2003; Moles et al., 2004; Moles and Westoby, 2006). Each of the n_s events is scattered away from the tree in a random direction and at a distance randomly drawn from a Rayleigh distribution, thus allowing for potential long-dispersal events. Although seed dispersal distance is known to vary depending on dispersal syndrome and plant traits (Tamme et al., 2014; Seidler and Plotkin, 2006; Muller-Landau et al., 2008), the scale parameter σ_{disp} of the distribution is here fixed across species and individuals.

The intensity of the external seed rain is quantified by N_{tot} (in number of incoming seeds per hectare) and its species composition is defined by the relative abundances of species $f_{reg,s}$, both being user-defined. Hence, for each species s, $n_{ext,s}$ events of dispersal due to seeds immigrating from the outside occurred, with:

$$n_{ext,s} = N_{tot} \times f_{reg,s} \times n_{ha} \quad (64)$$

with n_{ha} the number of hectares of the simulated plot. These reproduction opportunities are uniformly distributed within the simulated area.

If several species are competing for recruitment in a local seed bank, one of the species is picked at random as the winner out of all the seeds present, as in a lottery model (Chesson and Warner, 1981). The recruitment event occurs only if ground-level light availability is sufficiently high. To test if this condition is met, the seedling is first attributed individual trait values depending on the species-specific averages (see section 2.4.1). These traits values are then used to determine the maximum LAI (LAI_{max}) the seedling would support under average environmental conditions, with LAI_{max} defined as the

threshold beyond which the seedling leaf assimilation would be less than respiration (see section 2.6.2). The seedling can be recruited if the site LAI at ground level is lower than LAI_{max}.

Water availability is also key to seedling performance (Engelbrecht et al., 2006; Johnson et al., 2017; Kupers et al., 2019), hence TROLL 4.0 now implements an additional water-dependent dependence on seedling establishment (Craine et al., 2012; Paine et al., 2018). Seedling recruitment is possible only if top-layer soil water potential is less negative than half the turgor loss point ($\psi_{tlp}/2$). Such parameterization is motivated by the fact that, at turgor loss point, the seedlings would not germinate, and a certain level of turgor is needed for germination and growth (Bradford, 1990; Daws et al., 2008; Coussement et al., 2018; Hsiao, 1973; Fatichi et al., 2016).

If both conditions on light and water availability are met, the newly recruited tree is initialized with a dbh=0.01m, a total leaf area $LA_t = 0.25 \times LA_{opt}$ distributed across the three leaf age pools in proportion to their relative span (τ_{young}/LL, τ_{mature}/LL, τ_{old}/LL; see section 2.6.2), and a carbon storage compartment filled at half its maximum NSC_r (see section 2.6.3).

The assumptions here made on tree reproduction largely reflect limited knowledge on these processes, which remains major sources of uncertainty in current models (König et al., 2022; Hanbury-Brown et al., 2022; Díaz-Yáñez et al., 2024).

2.7.2 Mortality

Mortality processes also play a key role in forest structure and carbon balance (Sevanto et al., 2014; Friend et al., 2014; Johnson et al., 2016; Esquivel-Muelbert et al., 2020; McDowell et al., 2022). TROLL 4.0 explicitly represents several important mechanisms of tree mortality. At each timestep, individual tree death rate (in events yr^{-1}; Sheil et al. 1995) is:

$$d = d_b + d_{starv} + d_{treefall} + d_{drought} \quad (65)$$

where d_b is a background death rate, d_{starv} represents death due to carbohydrate shortage (carbon starvation), $d_{treefall}$ represents death due to treefall (including trees indirectly killed by neighboring fallen trees), and $d_{drought}$ the drought-induced tree mortality.

Background mortality d_b encapsulates death events that are not attributed to any specific mechanism in the model. Mortality rate is known to vary greatly among species, and we here assume that it is negatively correlated with tree wood density, as observed pan-tropically (King et al., 2006; Kraft et al., 2010; Poorter et al., 2008; Wright et al., 2010). This dependence illustrates a trade-off between investment into construction costs and risk of mortality (Chave et al., 2009). We assumed the following relationship:

$$d_b = m \times \left(1 - \frac{wsg}{wsg_{lim}}\right) \quad (66)$$

where m (in events yr^{-1}) is the reference background mortality rate for a species with low wood density and is user-specified. wsg_{lim} is a value large enough so that d_b always remains positive (here set at 1 g cm^{-3}).

A tree can also die because of carbohydrate shortage in case of prolonged stress (d_{starv} in Eq. (65)). In TROLL 4.0 that includes an explicit carbohydrate storage compartment, the tree dies of carbon starvation when this compartment is empty and $NPP_{ind} \leq 0$ (Eq. (51)).

Tree death may be caused by treefalls (term $d_{treefall}$ in Eq. (65)). To simulate this process, we first define a stochastic threshold Θ, depending on the tree maximal height, and prescribed at tree birth. Then, the tree can fall with a probability equal to $1 - \frac{\theta}{h}$ (Chave, 1999) each month. As TROLL 4.0 uses a daily timestep, this probability is uniformly distributed across the days of one month. The parameter Θ is computed for each tree, as follows:

$$\Theta = h_{max} \times (1 - v_T \times |\zeta|) \quad (67)$$

where h_{max} is maximal tree height (i.e. the tree height computed using Eq. (16) at dbh_{max}), v_T is a variance term, $|\zeta|$ is the absolute value of a random Gaussian variable with zero mean and unit standard deviation. v_T is modified at tree level so that high risks of treefall (> 99.5th percentile of the Gaussian variable) occur at the same height for all individuals of the same species. This implicitly introduces a growth-mortality trade-off, as more slender trees (larger ratio of height to trunk diameter) should reach this height threshold quicker. The orientation of tree falls is random. Trees on the trajectory of the falling tree can be damaged, especially if they are smaller than the fallen tree (van der Meer and Bongers, 1996). To model this effect, an individual variable *hurt* is defined. If a tree is within the trajectory of the fallen stem or of the fallen crown, its variable *hurt* is updated to h and $\frac{h-CR}{2}$, respectively, if it was lower, where h and CR are the tree height and crown radius of the fallen tree, respectively. The probability to die due to another treefall is then $1 - \frac{1}{2}\frac{h}{hurt \times e^{\varepsilon_{h,j}}}$, where h is the height of the focal tree and $e^{\varepsilon_{h,j}}$ (see Eq. (16)) accounts for the fact that slender individuals (higher tree height deviation) would be more vulnerable to treefall. Such tree can either fall and itself damage other trees or dies standing, depending on the user choice. The *hurt* variable is reset to zero at each timestep.

Finally, prolonged drought is also a source of mortality. Drought-induced mortality is triggered when the leaf predawn water potential ψ_{pd} is below a lethal level (ψ_{lethal}), and ψ_{lethal} is computed from the leaf water potential at turgor loss point, using the relationship provided by the global meta-analysis of Bartlett et al. (2016; P=0.03, R^2=0.31, n=15 species from tropical dry and moist biomes), as follows:

$$\psi_{lethal} = -0.9842 + 3.1795 \times \psi_{tlp} \quad (68)$$

3 Modelling protocol

3.1 Model inputs

TROLL 4.0 requires five input files to run a simulation: (i) global parameters, (ii) species parameters, (iii) soil characteristics, and finally, meteorological drivers varying at (iv) half-hour and (v) daily step.

The global input file contains parameters that define the simulation set-up (e.g. the number of timesteps, size of the simulated plot and of the belowground voxels), and values for biophysical parameters that remain constant throughout the simulation and are not species- or tree-specific. These include the light attenuation coefficient, allocation parameters, minimal death rate, and more (see Table A1). Parameter values can be varied across simulations, to test model sensitivity, transfer across sites, or any other reason. The species input file contains mean functional traits for at least one species and with no upper bound (see Table A1). Functional trait values can be prescribed from local field measurements, or retrieved from global trait databases (e.g. Kattge et al., 2020; Díaz et al., 2022).

The soil input file contains the soil variables needed for the pedotransfer functions, i.e. soil texture (proportion of silt, clay and sand), soil organic matter content, dry bulk density, soil pH, and cation exchange capacity, for each soil layer, with thickness of each layer. The number of soil layers is at least one, and is not theoretically limited. Lacking local soil data, model users may retrieve soil parameters from online databases (e.g. Poggio et al., 2021), bearing in mind the uncertainties of such products, especially in tropical areas (Khan et al., 2024).

Meteorological drivers are provided in two files, depending on their temporal resolution in the model. Daytime temperature, vapor pressure deficit, incident irradiance and wind speed at a reference height above the canopy are provided for every half-hour, while average nighttime temperature and cumulative rainfall are provided at a daily timestep. Such data can typically be retrieved from meteorological stations embedded in eddy-flux towers, or from global products (Muñoz-Sabater et al., 2021), as in Schmitt et al. (2023).

3.2 Initial conditions

Two types of initial conditions are useful in most practical settings, and are implemented in TROLL 4.0. First, the user can simulate forest regeneration from bare ground. In this case, forest succession is initiated by the external seed rain, the composition and intensity of which are user-defined (see above). The steady-state forest composition and structure are thus emergent properties of the community assembly mechanisms embedded in the model, and the user-specified seed rain. The second option is to prescribe an initial forest state. This requires that an initial forest state be provided as an additional input file. The code is designed to adapt to the level of information provided by the inventory file, from a minimal requirement of tree *dbh* to the full list of individual variables for each tree. For individual variables missing in the input file, these are either computed from the model relationships or drawn at random. This second initial condition matches a real site forest state given the available data, but will require careful calibration to maintain the forest state over a longer time period (e.g. Fischer et al., 2019). A more common use case is to restart new simulations from an output of a previous simulation, e.g., to perform virtual experiments controlling the initial state.

3.3 Standard outputs

TROLL 4.0 provides a range of outputs related to forest structure, forest composition and diversity, and ecosystem functioning (e.g., carbon and water fluxes; Fig. 4). It simulates forest structure and composition and provides outputs comparable to those

measured in the field: tree size distribution, tree spatial distribution, biomass accumulation curve, functional trait distribution, canopy height and leaf area index maps (Maréchaux and Chave, 2017), and more generally all information that can be retrieved from a detailed field inventory or a meter-scale airborne laser scanning survey (Fischer et al., 2019). In TROLL 4.0, other outputs are also available: litterfall fluxes, carbon and water fluxes comparable to the one provided by eddy-flux towers, soil water state (content and water potential). An evaluation of these outputs for two Amazonian forest sites is provided in a companion paper (Schmitt et al., submitted companion paper).

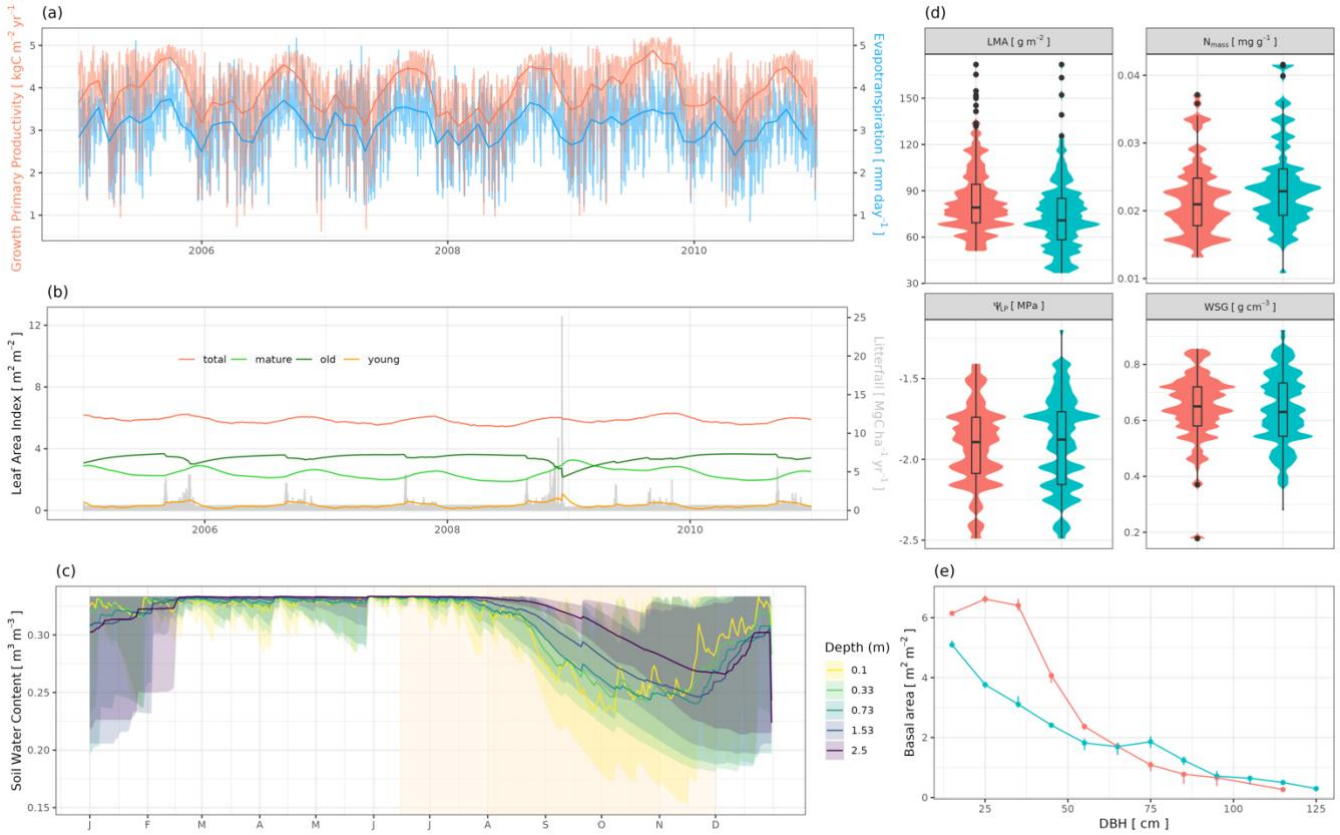

Figure 4: Examples of outputs provided by TROLL 4.0 and related to ecosystem functioning, diversity and structure. (a) Temporal variations of gross primary productivity (red) and evapotranspiration (blue) within and across years. (b) Variation in total leaf area index (red line) and leaf area index per leaf age cohort (young, mature, old; yellow, light green and dark green lines, respectively), together with litterfall (grey bars), within and across years. (c) Mean seasonal variations of water content in soil layers of different depths, with the vertical yellow band in the background depicting the dry season. (d) Distribution of functional traits. (e) Distributions of basal area per diameter class. Panels (a), (b) and (c) show outputs for an Amazonian forest site (Paracou), panels (d) and (e) show outputs for two Amazonian sites (Paracou, red; Tapajos, blue), see Schmitt et al., submitted companion paper. for details on similation set-ups.

4 Discussion

TROLL 4.0 is a novel generation of forest growth models designed to bridge the gap between traditional forest growth models and process-based models informed by ecophysiology. It includes an integration of processes underlying ecosystem fluxes closer to a modern DGVM than most other forest growth simulators. It also includes representation of plant community structure and diversity at a resolution similar to that used by ecologists in the field. This enables a direct comparison with a range of field data, including forest inventories, trait distribution, fine- and large-scale remote-sensing products, or eddy-covariance data. Here we discuss the assumptions of the water cycle newly included in the model, as well as transferability and limitations of the current model version.

4.1 Simulating water fluxes and forest responses to water availability

Previous versions of TROLL assume that water availability does not limit ecosystem fluxes and dynamics, a strong but reasonable assumption in a light-limited forest like in Eastern Amazonia (Guan et al., 2015; Wagner et al., 2016; Maréchaux and Chave, 2017). However, such a simplification does not allow to account for drought-induced inter-annual variability in forest dynamics (Bonal et al., 2008; Aguilos et al., 2018; Leitold et al., 2018) or to transfer the model to sites where water availability is limiting. As droughts will be important drivers for tropical ecosystems in the future (Duffy et al., 2015), such a simplification does not allow to project future states of forest under climate change.

In TROLL 4.0, we implemented a full water cycle. We introduced a belowground field with a hydraulic state coupled to the vegetation, and a representation of the response of leaf gas exchanges to local atmospheric conditions and their control by the leaf boundary layer. This detailed representation is commonplace DGVMs (Prentice et al., 2007) but to our knowledge, it is new for an individual-based spatially explicit forest dynamic simulator. This paves the way for explorations and projections of the independent effects of soil water availability and atmospheric demand on ecosystem functioning (Novick et al., 2016; Santos et al., 2018), community composition and structure (Esquivel-Muelbert et al., 2019; Fauset et al., 2012; Slik, 2004; Feeley et al., 2011).

These developments have striven to follow the parsimonious principle: more complex representations do not systematically result in increased model reliability and robustness, especially if the additional parameters are poorly constrained (Mahnken et al., 2022; Prentice et al., 2015). The soil hydraulic state is simulated using a bucket model (Budyko, 1961; Manabe1969; Vargas Godoy et al., 2021). In the future, more complex representations of soil water dynamics could be implemented at finer temporal and spatial resolutions, such as the implementation of Richards' equation (Richards, 1931), and integration of lateral flows, but this would be at a serious computational cost. These could be compared with the current simpler representation to assess the relevance of increasing complexity in various contexts and soil data availability (Van Nes and Scheffer, 2005). However, two aspects were considered to be needed in the current version, based on biological considerations. First, we implemented a multi-layer soil model, a more detailed representation compared with other models using a bucket model approach (e.g. Fischer et al., 2014; Laio et al., 2001). This was motivated by the need to account for contrasting rooting

strategies and access to water among coexisting plants, which is an under-explored, but likely key, aspect of community dynamics in forests (Brum et al., 2019; De Deurwaerder et al., 2018; Ivanov et al., 2012). Second, we assumed that the depth of tree water uptake is not only controlled by the distribution of root biomass (as in Naudts et al., 2015; Sakschewski et al., 2021; Paschalis et al., 2024), but also by soil water state and its vertical variation (as in Williams et al., 1996; Duursma and Medlyn, 2012). These improvements are relevant to the temporal variation of water retrieval depth (Bruno et al., 2006) and the sustained dry-season productivity in rainforest ecosystems (Restrepo-Coupe et al., 2017).

The control of leaf gas exchange by water availability has been implemented by means of multiplicative soil water stress factors. Although the use of such factors has been debated (Powell et al., 2013; Joetzjer et al., 2014), it has been preferred over a more explicit representation of the water flow through the plant column (e.g. Yao et al., 2022; Christoffersen et al., 2016; Cochard et al., 2021; De Cáceres et al., 2023). Although the stem hydraulic traits that would be needed for parameterizing an explicit plant water flow module have been increasingly measured over the past decades, data availability for tropical tree species remains low in regards to the actual number of species coexisting in these communities. Alternatively, correlative relationships have been used to infer these traits from more easily measured traits (Christoffersen et al., 2016; Xu et al., 2016). However these are context dependent (Brodribb, 2017; Rosas et al., 2019) and have at best low statistical support in rainforest communities that have been loosely constrained by water availability (Dwyer and Laughlin, 2017; Delhaye et al., 2020; Maréchaux et al., 2020), which plead against developing a parameterization based on more available structural traits. Innovative methods alleviate the difficulties of robustly measuring the vulnerability of tropical trees to embolism (Cochard et al., 2016; Sergent et al., 2020; Garcia et al., 2023), and this could provide a key motivation for a more explicit module of plant water flow in TROLL (Kennedy et al., 2019; Paschalis et al., 2024). Such developments could be necessary to correctly represent the legacy of drought in forest ecosystems (Paschalis et al., 2024; Anderegg et al., 2015). However, two important aspects were taken into account in the implementation of the multiplicative water stress factors in TROLL 4.0. These factors were parameterized based on soil water potential as independent variable, and not soil water content, the former directly controlling water availability for plants, while the effect of soil water content is strongly mediated by soil properties (Novick et al., 2022). Also, different water stress factors were used for stomatal and non-stomatal limitations, in order to capture the sequence of effects of decreasing water availability on plant function (Trueba et al., 2019; Fatichi et al., 2016; Hsiao, 1973).

The effects of water availability on plant function and tree demography were implemented through trait-based parameterization, which allows a range of responses between trees and species. This was made possible through the use of leaf water potential at turgor loss point (ψ_{tlp}), a leaf-level trait that is mechanistically linked to plant responses to water availability (Bartlett et al., 2016b) and that is measurable at the community scale in diverse systems through a well-validated method (Maréchaux et al., 2016; Griffin-Nolan et al., 2019; Sun et al., 2020; Bartlett et al., 2012a). Leaf water potential at turgor loss point varies greatly across species within Amazonian forest communities (Maréchaux et al., 2015; Ziegler et al., 2019), and this diversity explains contrasting responses to water availability at the leaf and plant levels (Martin-StPaul et al., 2017; Maréchaux et al., 2018; Powell et al., 2017), and species distribution at local, regional and global scales (Bartlett et al., 2016a; Baltzer et al., 2008; Lenz et al., 2006; Bartlett et al., 2012b). The relationships implemented here involving ψ_{tlp} have a

mechanistic basis, as discussed above. However, the relationships controlling the effect of water availability on (1) leaf shedding, (2) seed germination and seedling recruitment, and (3) drought-induced mortality would deserve in-depth exploration. More generally, these three processes remain key aspects of community dynamics and ecosystem functioning in high need of sustained empirical investigation (Albert et al., 2019; Díaz-Yáñez et al., 2024; McDowell et al., 2022).

4.2 Model-data integration, transferability and limitations

TROLL 4.0 simulates forest structure and diversity, while expanding the types of data with which its results can be compared (Schmitt et al., submitted companion paper). The individual-based species-specific representation of forest yields virtual forest inventories, including the location of each individual, their botanical identity, and their dimensions, and virtual airborne laser scanning point clouds (Fischer et al., 2019; Schmitt et al., 2023). TROLL 4.0 additionally provides water, carbon and litter flux dynamics that are directly comparable to eddy-flux tower data and litter trap monitoring at fine temporal resolutions, and this specificity has numerous advantages.

Data-driven knowledge can be directly assimilated in TROLL 4.0, offering new perspectives for inference or calibration (Dietze et al., 2013; Fer et al., 2018; Hartig et al., 2012; LeBauer et al., 2013; Fischer et al., 2019). TROLL 4.0 can help inform the development of DGVMs, in which the representation of vegetation does not allow this type of assimilation (Fischer et al., 2019). TROLL 4.0 is also easy to use and test by field ecologists as it simulates trees, not cohorts, PFTs, or gap patches: it can reproduce classical experiments in community or ecosystem ecology (e.g. Crawford et al., 2021; Schmitt et al., 2020) while overcoming known empirical challenges such as low repeatability (Schnitzer and Carson, 2016) or limited spatial footprint (Estes et al., 2018). TROLL 4.0 can be compared with data under the control of different biophysical processes supporting a more robust evaluation, and limiting equifinality issues (Franks et al., 1997; Medlyn et al., 2005). Finally, the model is parameterized based on traits directly measured in the field improving model transferability (Rau et al., 2022a).

The individual-scale and spatially-explicit representation of TROLL 4.0 comes with a computational burden. For a reference 4-ha area starting from bare ground, and 600 years of simulation, the computational cost of TROLL 4.0 is about 1820 min, compared with version TROLL2.3 (Maréchaux and Chave 2017) about 12 min. While the shift from a monthly to a daily timestep explains the multiplication by a factor of 30 between the two versions, the addition of a belowground field and of an iterative scheme to simulate leaf gas exchanges explains for a great part the remaining factor of five. Several developments should reduce this computational cost: tree demographic processes do not need to be simulated at the daily timestep, and could be represented at a monthly resolution; vegetation models already implement such nested time scales (Moorcroft, 2006). We are also confident that further computer time reduction will be brought about by code optimization. Finally, several strategies can be implemented to up-scale the outputs of individual-based models at reduced computational costs, especially by leveraging large scale remote sensing products (Rödig et al., 2017; Sato et al., 2007; Shugart et al., 2015).

4.3 Current and future developments

TROLL 4.0 is a reflection on the state of the art and knowledge gaps in plant physiology and ecology, resulting in an unbalanced representation across processes. TROLL is being continuously developed, as knowledge and data availability progress, specific questions to address with the model emerge, or important limitations are identified. In a companion paper (Schmitt et al., submitted companion paper), we use data from forest inventories, litter traps, eddy-flux towers and remote sensing products to evaluate and discuss the performance and limitations of TROLL 4.0 at two forest sites. We here mention several on-going or future developments.

Empirical findings suggest that the contribution of undisturbed tropical forests to the global carbon sink is declining (Hubau et al., 2020; Qie et al., 2017), pointing to the need of integrated modelling to understand and predict such trends (Yao et al., 2023, 2024; Koch et al., 2021). Among the possible steps forward with TROLL 4.0 are an improved representation of stomatal conductance and its coupling with photosynthesis (Lamour et al., 2022, 2023; Dewar et al., 2018), as well as respiration response and acclimation to climatic drivers (Smith and Dukes, 2013; Collalti et al., 2020; Slot et al., 2013; Rowland et al., 2015). Improvements on the carbon budget would also be important, with more explicit carbon allocation to reproductive organs and belowground structures, under the control of environmental drivers (Fig. 3). However, such developments would rely on limited empirical or experimental knowledge belowground (Cusack et al., 2024) and scarce information on tree reproductive strategies (Igarashi et al., 2024; Vacchiano et al., 2018; Norden et al., 2007). An improved representation and evaluation of drought-induced tree mortality would be another important step forward as it might play a key role in the observed changing dynamics and functional and floristic turnover (Esquivel-Muelbert et al., 2019; Feeley et al., 2011; Hubau et al., 2020; Qie et al., 2017). Information provided by long-term through fall exclusion experiments would offer interesting opportunities for model development and evaluation (Powell et al., 2013; Yao et al., 2022).

Tropical forest disturbance by land use change, fire regimes, and other degradations are an important source of C emissions (Lapola et al., 2023), and they must be represented in models. For instance, it is important to understand how edge effects affect the forest microclimate, and consequently forest dynamics, functioning and composition (Camargo and Kapos, 1995; Nunes et al., 2022). To this end, micro-climate models could be coupled to or embedded within TROLL (Gril et al., 2023a; Maclean and Klinges, 2021). Fragmentation also impacts seed dispersal, and thus seed rain and seed bank intensity and composition (Warneke et al., 2022; Cubiña and Aide, 2001). Improving TROLL's representation of seed dispersal ability and germination as a function of plant trait and dispersal mode is key to capture the effect of forest loss and fragmentation on forest functioning and biodiversity (Seidler and Plotkin, 2006; Muller-Landau et al., 2008; Tamme et al., 2014; Chase et al., 2020; Riva and Fahrig, 2023). More generally, one overarching objective is to improve model's representation of processes involved in forest regeneration, to simulate secondary forest dynamics and resilience to disturbances (Hanbury-Brown et al., 2022; Díaz-Yáñez et al., 2024; Poorter et al., 2023; Albrich et al., 2020).

Finally, TROLL 4.0 includes major developments that should facilitate its transferability across sites. The explicit integration of the ecosystem water balance and vegetation responses to soil water availability now allows to consider spatio-

temporal extrapolation along water stress gradients. The integration of soil topography and heterogeneity would also be an important advance for improved genericity. As nutrient availability is being altered by human activities (Peñuelas et al., 2013), the explicit integration of a nutrient cycle with nitrogen and phosphorous colimitation will be a useful advance in the future (Fernández-Martínez et al., 2014; Turner et al., 2018). Similarly, the extension of tree functioning responses to a broader range of temperatures, should support the transferability of TROLL to temperate and boreal forests.

5. Conclusion

TROLL 4.0 represents an advance over previous versions as it bridges across forest model types, while maintaining a representation consistent with field ecology and ecosystem science. TROLL 4.0 simulates the responses of tropical forests to water availability through the explicit representation of water dynamics belowground and its coupling with leaf-level gas exchanges and demographic processes. This comes at a computational cost, and a future task is to conduct code optimization and parallelization, and up-scaling in combination with remote-sensing products. The representation of processes in TROLL 4.0 mirrors an unbalanced state of the art, but its ability to dialogue with a range of data of various nature, makes it a valuable tool to take up the fundamental and applied research challenges on tropical forests. TROLL 4.0 has benefited from observations and field experiments that feed the development of models (Medlyn et al., 2015; Paschalis et al., 2020), while modeling exercises inform and guide empirical approaches (Medlyn et al., 2016; Norby et al., 2016; Pacala and Rees, 1998). This is possible because of the fine scale representation of forest structure and diversity and the trait-based parameterization of processes in the model.

Code and data availability. The code of TROLL 4.0 is available XXXXXXXgithub/TROLL, a DOI will be linked to this repository upon publication. Additionally, TROLL 4.0 can be set-up and run, and its outputs can be analyzed with an updated version of the R package rcontroll: https://github.com/sylvainschmitt/rcontroll/tree/TROLLV4, also available in R through the command devtools::install_github("sylvainschmitt/rcontroll", ref = "TROLLV4").

Supplement. The supplement related to this article will be available online upon publication acceptance.

Author contributions. IM led TROLL 4.0, and designed the implementation of the water cycle and its coupling to vegetation. FJF co-led TROLL 4.0 and designed the new implementation of intra-specific variability and crown shapes. SS and JC contributed ideas and discussions. IM wrote the paper with contributions from all authors.

Competing interests. The authors declare that they have no conflict of interest.

Acknowledgements. We acknowledge Nicolas Martin-StPaul and Rémi Vezy for useful discussions on the representation of gas exchanges and water fluxes in models; Nicolas Barbier, Gregoire Vincent, and James Ball for sharing data and useful discussions on leaf phenology; Philippe Verley and Thomas Arsouze for IT support. This work was carried out with the support of MESO@LR-Platform at the University of Montpellier.

Financial support. This research has been supported by fundings from ANR (the French National Research Agency) under the "Investissements d'avenir" program with the references ANR-16-IDEX-0006, ANR-10-LABX-25-01, ANR-10-LABX-0041, the Amazonian Landscapes in Transition ANR project (ALT), CNES Biomass-Valo project, and ESA CCI-BIOMASS.

References

Aguilos, M., Hérault, B., Burban, B., Wagner, F., and Bonal, D.: What drives long-term variations in carbon flux and balance in a tropical rainforest in French Guiana?, Agricultural and Forest Meteorology, 253–254, 114–123, https://doi.org/10.1016/j.agrformet.2018.02.009, 2018.

Albert, L. P., Restrepo-Coupe, N., Smith, M. N., Wu, J., Chavana-Bryant, C., Prohaska, N., Taylor, T. C., Martins, G. A., Ciais, P., Mao, J., Arain, M. A., Li, W., Shi, X., Ricciuto, D. M., Huxman, T. E., McMahon, S. M., and Saleska, S. R.: Cryptic phenology in plants: Case studies, implications, and recommendations, Global Change Biology, 25, 3591–3608, https://doi.org/10.1111/gcb.14759, 2019.

Albert, L. P., Wu, J., Prohaska, N., de Camargo, P. B., Huxman, T. E., Tribuzy, E. S., Ivanov, V. Y., Oliveira, R. S., Garcia, S., Smith, M. N., Oliveira Junior, R. C., Restrepo-Coupe, N., da Silva, R., Stark, S. C., Martins, G. A., Penha, D. V., and Saleska, S. R.: Age-dependent leaf physiology and consequences for crown-scale carbon uptake during the dry season in an Amazon evergreen forest, New Phytologist, 218, https://doi.org/10.1111/nph.15056, 2018.

Albrich, K., Rammer, W., Turner, M. G., Ratajczak, Z., Braziunas, K. H., Hansen, W. D., and Seidl, R.: Simulating forest resilience: A review, Global Ecology and Biogeography, 29, 2082–2096, https://doi.org/10.1111/geb.13197, 2020.

Amthor, J. S.: The role of maintenance respiration in plant growth, Plant, Cell & Environment, 7, 561–569, https://doi.org/10.1111/1365-3040.ep11591833, 1984.

Anderegg, W. R. L., Schwalm, C., Biondi, F., Camarero, J. J., Koch, G., Litvak, M., Ogle, K., Shaw, J. D., Shevliakova, E., Williams, A. P., Wolf, A., Ziaco, E., and Pacala, S.: Pervasive drought legacies in forest ecosystems and their implications for carbon cycle models, Science, 349, 528–532, https://doi.org/10.1126/science.aab1833, 2015.

Anderegg, W. R. L., Wolf, A., Arango-Velez, A., Choat, B., Chmura, D. J., Jansen, S., Kolb, T., Li, S., Meinzer, F., Pita, P., Dios, V. R. de, Sperry, J. S., Wolfe, B. T., and Pacala, S.: Plant water potential improves prediction of empirical stomatal models, PLOS ONE, 12, e0185481, https://doi.org/10.1371/journal.pone.0185481, 2017.

Anderegg, W. R. L., Wolf, A., Arango-Velez, A., Choat, B., Chmura, D. J., Jansen, S., Kolb, T., Li, S., Meinzer, F. C., Pita, P., Dios, V. R. de, Sperry, J. S., Wolfe, B. T., and Pacala, S.: Woody plants optimise stomatal behaviour relative to hydraulic risk, Ecology Letters, 21, 968–977, https://doi.org/10.1111/ele.12962, 2018.

Arora, V. K. and Boer, G. J.: A Representation of Variable Root Distribution in Dynamic Vegetation Models, Earth Interact., 7, 1–19, https://doi.org/10.1175/1087-3562(2003)007<0001:AROVRD>2.0.CO;2, 2003.

Asao, S., Bedoya-Arrieta, R., and Ryan, M. G.: Variation in foliar respiration and wood CO2 efflux rates among species and canopy layers in a wet tropical forest, Tree Physiol, 35, 148–159, https://doi.org/10.1093/treephys/tpu107, 2015.

Atkin, O. K., Evans, J. R., Ball, M. C., Lambers, H., and Pons, T. L.: Leaf respiration of snow gum in the light and dark. Interactions between temperature and irradiance., Plant Physiol., 122, 915–924, https://doi.org/10.1104/pp.122.3.915, 2000.

Atkin, O. K., Meir, P., and Turnbull, M. H.: Improving representation of leaf respiration in large-scale predictive climate–vegetation models, New Phytol, 202, 743–748, https://doi.org/10.1111/nph.12686, 2014.

Atkin, O. K., Bloomfield, K. J., Reich, P. B., Tjoelker, M. G., Asner, G. P., Bonal, D., Bönisch, G., Bradford, M. G., Cernusak, L. A., Cosio, E. G., Creek, D., Crous, K. Y., Domingues, T. F., Dukes, J. S., Egerton, J. J. G., Evans, J. R., Farquhar, G. D., Fyllas, N. M., Gauthier, P. P. G., Gloor, E., Gimeno, T. E., Griffin, K. L., Guerrieri, R., Heskel, M. A., Huntingford, C., Ishida, F. Y., Kattge, J., Lambers, H., Liddell, M. J., Lloyd, J., Lusk, C. H., Martin, R. E., Maksimov, A. P., Maximov, T. C., Malhi, Y., Medlyn, B. E., Meir, P., Mercado, L. M., Mirotchnick, N., Ng, D., Niinemets, Ü., O'Sullivan, O. S., Phillips, O. L., Poorter, L., Poot, P., Prentice, I. C., Salinas, N., Rowland, L. M., Ryan, M. G., Sitch, S., Slot, M., Smith, N. G., Turnbull, M. H., VanderWel, M. C., Valladares, F., Veneklaas, E. J., Weerasinghe, L. K., Wirth, C., Wright, I. J., Wythers, K. R., Xiang, J., Xiang, S., and Zaragoza-Castells, J.: Global variability in leaf respiration in relation to climate, plant functional types and leaf traits, New Phytol, 206, 614–636, https://doi.org/10.1111/nph.13253, 2015.

Baltzer, J. L., Davies, S. J., Bunyavejchewin, S., and Noor, N. S. M.: The role of desiccation tolerance in determining tree species distributions along the Malay–Thai Peninsula, Functional Ecology, 22, 221–231, https://doi.org/10.1111/j.1365-2435.2007.01374.x, 2008.

Baraloto, C., Paine, C. E. T., Patiño, S., Bonal, D., Hérault, B., and Chave, J.: Functional trait variation and sampling strategies in species-rich plant communities, Functional Ecology, 24, 208–216, https://doi.org/10.1111/j.1365-2435.2009.01600.x, 2010a.

Baraloto, C., Timothy Paine, C. E., Poorter, L., Beauchene, J., Bonal, D., Domenach, A.-M., Hérault, B., Patiño, S., Roggy, J.-C., and Chave, J.: Decoupled leaf and stem economics in rain forest trees, Ecology Letters, 13, 1338–1347, https://doi.org/10.1111/j.1461-0248.2010.01517.x, 2010b.

Bartlett, M. K., Scoffoni, C., Ardy, R., Zhang, Y., Sun, S., Cao, K., and Sack, L.: Rapid determination of comparative drought tolerance traits: using an osmometer to predict turgor loss point, Methods Ecol. Evol., 3, 880–888, https://doi.org/10.1111/j.2041-210X.2012.00230.x, 2012a.

Bartlett, M. K., Scoffoni, C., and Sack, L.: The determinants of leaf turgor loss point and prediction of drought tolerance of species and biomes: a global meta-analysis, Ecology Letters, 15, 393–405, https://doi.org/10.1111/j.1461-0248.2012.01751.x, 2012b.

Bartlett, M. K., Zhang, Y., Yang, J., Kreidler, N., Sun, S.-W., Lin, L., Hu, Y.-H., Cao, K.-F., and Sack, L.: Drought tolerance as a driver of tropical forest assembly: resolving spatial signatures for multiple processes, Ecology, 97, 503–514, https://doi.org/10.1890/15-0468.1, 2016a.

Bartlett, M. K., Klein, T., Jansen, S., Choat, B., and Sack, L.: The correlations and sequence of plant stomatal, hydraulic, and wilting responses to drought, PNAS, 113, 13098–13103, https://doi.org/10.1073/pnas.1604088113, 2016b.

Beer, C., Reichstein, M., Tomelleri, E., Ciais, P., Jung, M., Carvalhais, N., Rödenbeck, C., Arain, M. A., Baldocchi, D., Bonan, G. B., Bondeau, A., Cescatti, A., Lasslop, G., Lindroth, A., Lomas, M., Luyssaert, S., Margolis, H., Oleson, K. W., Roupsard, O., Veenendaal, E., Viovy, N., Williams, C., Woodward, F. I., and Papale, D.: Terrestrial gross carbon dioxide uptake: global distribution and covariation with climate, Science, 329, 834–838, https://doi.org/10.1126/science.1184984, 2010.

Bennett, A. C., McDowell, N. G., Allen, C. D., and Anderson-Teixeira, K. J.: Larger trees suffer most during drought in forests worldwide, Nature Plants, 1, https://doi.org/10.1038/nplants.2015.139, 2015.

Bernacchi, C. J., Pimentel, C., and Long, S. P.: In vivo temperature response functions of parameters required to model RuBP-limited photosynthesis, Plant, Cell & Environment, 26, 1419–1430, https://doi.org/10.1046/j.0016-8025.2003.01050.x, 2003.

Berzaghi, F., Wright, I. J., Kramer, K., Oddou-Muratorio, S., Bohn, F. J., Reyer, C. P. O., Sabaté, S., Sanders, T. G. M., and Hartig, F.: Towards a New Generation of Trait-Flexible Vegetation Models, Trends in Ecology & Evolution, 35, 191–205, https://doi.org/10.1016/j.tree.2019.11.006, 2020.

Blanchard, G., Barbier, N., Vieilledent, G., Ibanez, T., Hequet, V., McCoy, S., and Birnbaum, P.: UAV-Lidar reveals that canopy structure mediates the influence of edge effects on forest diversity, function and microclimate, Journal of Ecology, 111, 1411–1427, https://doi.org/10.1111/1365-2745.14105, 2023.

Bohlman, S. and O'Brien, S.: Allometry, adult stature and regeneration requirement of 65 tree species on Barro Colorado Island, Panama, Journal of Tropical Ecology, 22, 123–136, https://doi.org/10.1017/S0266467405003019, 2006.

Bonal, D., Bosc, A., Ponton, S., Goret, J.-Y., Burban, B., Gross, P., Bonnefond, J.-M., Elbers, J., Longdoz, B., Epron, D., Guehl, J.-M., and Granier, A.: Impact of severe dry season on net ecosystem exchange in the Neotropical rainforest of French Guiana, Global Change Biology, 14, 1917–1933, https://doi.org/10.1111/j.1365-2486.2008.01610.x, 2008.

Bonan, G. B.: Forests and Climate Change: Forcings, Feedbacks, and the Climate Benefits of Forests, Science, 320, 1444–1449, https://doi.org/10.1126/science.1155121, 2008.

Bonan, G. B., Williams, M., Fisher, R. A., and Oleson, K. W.: Modeling stomatal conductance in the earth system: linking leaf water-use efficiency and water transport along the soil–plant–atmosphere continuum, Geosci. Model Dev., 7, 2193–2222, https://doi.org/10.5194/gmd-7-2193-2014, 2014.

Botkin, D. B.: Functional groups of organisms in model ecosystems, Ecosystem Analysis and Prediction, 98–102, 1975.

Botkin, D. B., Janak, J. F., and Wallis, J. R.: Some Ecological Consequences of a Computer Model of Forest Growth, Journal of Ecology, 60, 849–872, https://doi.org/10.2307/2258570, 1972.

Bradford, K. J.: A Water Relations Analysis of Seed Germination Rates, Plant Physiol., 94, 840–849, https://doi.org/10.1104/pp.94.2.840, 1990.

Braghiere, R. K., Quaife, T., Black, E., He, L., and Chen, J. M.: Underestimation of Global Photosynthesis in Earth System Models Due to Representation of Vegetation Structure, Global Biogeochemical Cycles, 33, 1358–1369, https://doi.org/10.1029/2018GB006135, 2019.

Braghiere, R. K., Wang, Y., Doughty, R., Sousa, D., Magney, T., Widlowski, J.-L., Longo, M., Bloom, A. A., Worden, J., Gentine, P., and Frankenberg, C.: Accounting for canopy structure improves hyperspectral radiative transfer and sun-induced chlorophyll fluorescence representations in a new generation Earth System model, Remote Sensing of Environment, 261, 112497, https://doi.org/10.1016/j.rse.2021.112497, 2021.

Brodribb, T. J.: Progressing from 'functional' to mechanistic traits, New Phytol, 215, 9–11, https://doi.org/10.1111/nph.14620, 2017.

Brodribb, T. J., Holbrook, N. M., and Gutiérrez, M. V.: Hydraulic and photosynthetic co-ordination in seasonally dry tropical forest trees, Plant, Cell & Environment, 25, 1435–1444, https://doi.org/10.1046/j.1365-3040.2002.00919.x, 2002.

Brodribb, T. J., Holbrook, N. M., Edwards, E. J., and Gutiérrez, M. V.: Relations between stomatal closure, leaf turgor and xylem vulnerability in eight tropical dry forest trees, Plant, Cell & Environment, 26, 443–450, https://doi.org/10.1046/j.1365-3040.2003.00975.x, 2003.

Brooks, R. H. and Corey, A. T.: Hydraulic properties of porous media. Hydrology Paper No. 3, Civil Engineering Department, Colorado State University., Fort Collins, 1964.

Brum, M., Vadeboncoeur, M. A., Ivanov, V., Asbjornsen, H., Saleska, S., Alves, L. F., Penha, D., Dias, J. D., Aragão, L. E. O. C., Barros, F., Bittencourt, P., Pereira, L., and Oliveira, R. S.: Hydrological niche segregation defines forest structure and drought tolerance strategies in a seasonal Amazon forest, Journal of Ecology, 107, 318–333, https://doi.org/10.1111/1365-2745.13022, 2019.

Bruno, R. D., da Rocha, H. R., de Freitas, H. C., Goulden, M. L., and Miller, S. D.: Soil moisture dynamics in an eastern Amazonian tropical forest, Hydrol. Process., 20, 2477–2489, https://doi.org/10.1002/hyp.6211, 2006.

Bucci, S., Scholz, F. G., Goldstein, G., Meinzer, F. C., Hinojosa, J. A., Hoffman, W. A., and Franco, A. C. ; Processes preventing nocturnal equilibration between leaf and soil water potential in tropical savanna woody species., Tree Physiology, 24, 1119–1127, 2004.

Budyko, M. I.: The Heat Balance of the Earth's Surface, Soviet Geography, 1961.

Bugmann, H.: A review of forest gap models, Climatic Change, 51, 259–305, https://doi.org/10.1023/A:1012525626267, 2001.

Burgess, S. S. O., Adams, M. A., Turner, N. C., and Ong, C. K.: The redistribution of soil water by tree root systems, Oecologia, 115, 306–311, https://doi.org/10.1007/s004420050521, 1998.

von Caemmerer, S.: Biochemical models of leaf photosynthesis, Csiro Publishing, 184 pp., 2000.

Camargo, J. L. C. and Kapos, V.: Complex edge effects on soil moisture and microclimate in central Amazonian forest, Journal of Tropical Ecology, 11, 205–221, 1995.

Canadell, J., Jackson, R. B., Ehleringer, J. R., Mooney, H. A., Sala, O. E., and Schulze, E. D.: Maximum rooting depth of vegetation types at the global scale, Oecologia, 108, 583–595, https://doi.org/10.1007/BF00329030, 1996.

Cannell, M. G. R. and Thornley, J. H. M.: Modelling the components of plant respiration: some guiding principles, Ann Bot, 85, 45–54, https://doi.org/10.1006/anbo.1999.0996, 2000.

Cavaleri, M. A., Oberbauer, S. F., and Ryan, M. G.: Wood CO2 efflux in a primary tropical rain forest, Global Change Biology, 12, 2442–2458, https://doi.org/10.1111/j.1365-2486.2006.01269.x, 2006.

Cavaleri, M. A., Oberbauer, S. F., and Ryan, M. G.: Foliar and ecosystem respiration in an old-growth tropical rain forest, Plant, Cell & Environment, 31, 473–483, https://doi.org/10.1111/j.1365-3040.2008.01775.x, 2008.

Charney, J. G.: Dynamics of deserts and drought in the Sahel, Q.J.R. Meteorol. Soc., 101, 193–202, https://doi.org/10.1002/qj.49710142802, 1975.

Chase, J. M., Blowes, S. A., Knight, T. M., Gerstner, K., and May, F.: Ecosystem decay exacerbates biodiversity loss with habitat loss, Nature, 584, 238–243, https://doi.org/10.1038/s41586-020-2531-2, 2020.

Chave: Study of structural, successional and spatial patterns in tropical rain forests using TROLL, a spatially explicit forest model, Ecological Modelling, 124, 233–254, https://doi.org/10.1016/S0304-3800(99)00171-4, 1999.

Chave, J., Olivier, J., Bongers, F., Châtelet, P., Forget, P.-M., van der Meer, P., Norden, N., Riéra, B., and Charles-Dominique, P.: Above-ground biomass and productivity in a rain forest of eastern South America, Journal of Tropical Ecology, 24, 355–366, https://doi.org/10.1017/S0266467408005075, 2008.

Chave, J., Coomes, D., Jansen, S., Lewis, S. L., Swenson, N. G., and Zanne, A. E.: Towards a worldwide wood economics spectrum, Ecology Letters, 12, 351–366, https://doi.org/10.1111/j.1461-0248.2009.01285.x, 2009.

Chave, J., Navarrete, D., Almeida, S., Álvarez, E., Aragão, L. E. O. C., Bonal, D., Châtelet, P., Silva-Espejo, J. E., Goret, J.-Y., von Hildebrand, P., Jiménez, E., Patiño, S., Peñuela, M. C., Phillips, O. L., Stevenson, P., and Malhi, Y.: Regional and seasonal patterns of litterfall in tropical South America, Biogeosciences, 7, 43–55, https://doi.org/10.5194/bg-7-43-2010, 2010.

Chave, J., Réjou-Méchain, M., Búrquez, A., Chidumayo, E., Colgan, M. S., Delitti, W. B. C., Duque, A., Eid, T., Fearnside, P. M., Goodman, R. C., Henry, M., Martínez-Yrízar, A., Mugasha, W. A., Muller-Landau, H. C., Mencuccini, M., Nelson, B. W., Ngomanda, A., Nogueira, E. M., Ortiz-Malavassi, E., Pélissier, R., Ploton, P., Ryan, C. M., Saldarriaga, J. G., and Vieilledent, G.: Improved allometric models to estimate the aboveground biomass of tropical trees, Glob Change Biol, 20, 3177–3190, https://doi.org/10.1111/gcb.12629, 2014.

Chen, X., Maignan, F., Viovy, N., Bastos, A., Goll, D., Wu, J., Liu, L., Yue, C., Peng, S., Yuan, W., Conceição, A. C. da, O'Sullivan, M., and Ciais, P.: Novel Representation of Leaf Phenology Improves Simulation of Amazonian Evergreen

Forest Photosynthesis in a Land Surface Model, Journal of Advances in Modeling Earth Systems, 12, e2018MS001565, https://doi.org/10.1029/2018MS001565, 2020.

Chen, X., Ciais, P., Maignan, F., Zhang, Y., Bastos, A., Liu, L., Bacour, C., Fan, L., Gentine, P., Goll, D., Green, J., Kim, H., Li, L., Liu, Y., Peng, S., Tang, H., Viovy, N., Wigneron, J.-P., Wu, J., Yuan, W., and Zhang, H.: Vapor Pressure Deficit and Sunlight Explain Seasonality of Leaf Phenology and Photosynthesis Across Amazonian Evergreen Broadleaved Forest, Global Biogeochemical Cycles, 35, e2020GB006893, https://doi.org/10.1029/2020GB006893, 2021.

Chen, Y., Ryder, J., Bastrikov, V., McGrath, M. J., Naudts, K., Otto, J., Ottlé, C., Peylin, P., Polcher, J., Valade, A., Black, A., Elbers, J. A., Moors, E., Foken, T., van Gorsel, E., Haverd, V., Heinesch, B., Tiedemann, F., Knohl, A., Launiainen, S., Loustau, D., Ogée, J., Vessala, T., and Luyssaert, S.: Evaluating the performance of land surface model ORCHIDEE-CAN v1.0 on water and energy flux estimation with a single- and multi-layer energy budget scheme, Geoscientific Model Development, 9, 2951–2972, https://doi.org/10.5194/gmd-9-2951-2016, 2016.

Chesson, P. L. and Warner, R. R.: Environmental variability promotes coexistence in lottery competitive systems, The American Naturalist, 117, 923–943, 1981.

Christoffersen, B. O., Gloor, M., Fauset, S., Fyllas, N. M., Galbraith, D. R., Baker, T. R., Rowland, L., Fisher, R. A., Binks, O. J., Sevanto, S. A., Xu, C., Jansen, S., Choat, B., Mencuccini, M., McDowell, N. G., and Meir, P.: Linking hydraulic traits to tropical forest function in a size-structured and trait-driven model (TFS v.1-Hydro), Geoscientific Model Development Discussions, 0, 1–60, https://doi.org/10.5194/gmd-2016-128, 2016.

Chuine, I. and Beaubien, E. G.: Phenology is a major determinant of tree species range, Ecology Letters, 4, 500–510, https://doi.org/10.1046/j.1461-0248.2001.00261.x, 2001.

Clark, D. B., Mercado, L. M., Sitch, S., Jones, C. D., Gedney, N., Best, M. J., Pryor, M., Rooney, G. G., Essery, R. L. H., Blyth, E., Boucher, O., Harding, R. J., Huntingford, C., and Cox, P. M.: The Joint UK Land Environment Simulator (JULES), model description – Part 2: Carbon fluxes and vegetation dynamics, Geosci. Model Dev., 4, 701–722, https://doi.org/10.5194/gmd-4-701-2011, 2011.

Cochard, H.: A new mechanism for tree mortality due to drought and heatwaves, Peer Community Journal, 1, https://doi.org/10.24072/pcjournal.45, 2021.

Cochard, H., Torres-Ruiz, J. M., and Delzon, S.: Let plant hydraulics catch the wave, Journal of Plant Hydraulics, 3, 002, 2016.

Cochard, H., Pimont, F., Ruffault, J., and Martin-StPaul, N.: SurEau: a mechanistic model of plant water relations under extreme drought, Annals of Forest Science, 78, 55, https://doi.org/10.1007/s13595-021-01067-y, 2021.

Collalti, A., Tjoelker, M. G., Hoch, G., Mäkelä, A., Guidolotti, G., Heskel, M., Petit, G., Ryan, M. G., Battipaglia, G., Matteucci, G., and Prentice, I. C.: Plant respiration: Controlled by photosynthesis or biomass?, Global Change Biology, 26, 1739–1753, https://doi.org/10.1111/gcb.14857, 2020.

Coomes, D. A. and Grubb, P. J.: Colonization, tolerance, competition and seed-size variation within functional groups, Trends in Ecology & Evolution, 18, 283–291, https://doi.org/10.1016/S0169-5347(03)00072-7, 2003.

Cosby, B. J., Hornberger, G. M., Clapp, R. B., and Ginn, T. R.: A Statistical Exploration of the Relationships of Soil Moisture Characteristics to the Physical Properties of Soils, Water Resources Research, 20, 682–690, https://doi.org/10.1029/WR020i006p00682, 1984.

Costa, F. R. C., Schietti, J., Stark, S. C., and Smith, M. N.: The other side of tropical forest drought: do shallow water table regions of Amazonia act as large-scale hydrological refugia from drought?, New Phytologist, 237, 714–733, https://doi.org/10.1111/nph.17914, 2023.

Coussement, J. R., De Swaef, T., Lootens, P., Roldán-Ruiz, I., and Steppe, K.: Introducing turgor-driven growth dynamics into functional–structural plant models, Ann Bot, 121, 849–861, https://doi.org/10.1093/aob/mcx144, 2018.

Cox, P. M., Betts, R. A., Jones, C. D., Spall, S. A., and Totterdell, I. J.: Acceleration of global warming due to carbon-cycle feedbacks in a coupled climate model, Nature, 408, 184–187, https://doi.org/10.1038/35041539, 2000.

Craine, J. M., Engelbrecht, B. M. J., Lusk, C. H., McDowell, N. G., and Poorter, H.: Resource limitation, tolerance, and the future of ecological plant classification, Frontiers in Plant Science, 3, https://doi.org/10.3389/fpls.2012.00246, 2012.

Crawford, M. S., Barry, K. E., Clark, A. T., Farrior, C. E., Hines, J., Ladouceur, E., Lichstein, J. W., Maréchaux, I., May, F., Mori, A. S., Reineking, B., Turnbull, L. A., Wirth, C., and Rüger, N.: The function-dominance correlation drives the direction and strength of biodiversity–ecosystem functioning relationships, Ecology Letters, 24, 1762–1775, https://doi.org/10.1111/ele.13776, 2021.

Cubiña, A. and Aide, T. M.: The Effect of Distance from Forest Edge on Seed Rain and Soil Seed Bank in a Tropical Pasture, BIOTROPICA, 33, 260–267, https://doi.org/10.1646/0006-3606(2001)033[0260:TEODFF]2.0.CO;2, 2001.

Cusack, D. F., Christoffersen, B., Smith-Martin, C. M., Andersen, K. M., Cordeiro, A. L., Fleischer, K., Wright, S. J., Guerrero-Ramírez, N. R., Lugli, L. F., McCulloch, L. A., Sanchez-Julia, M., Batterman, S. A., Dallstream, C., Fortunel, C., Toro, L., Fuchslueger, L., Wong, M. Y., Yaffar, D., Fisher, J. B., Arnaud, M., Dietterich, L. H., Addo-Danso, S. D., Valverde-Barrantes, O. J., Weemstra, M., Ng, J. C., and Norby, R. J.: Toward a coordinated understanding of hydro-biogeochemical root functions in tropical forests for application in vegetation models, New Phytologist, n/a, https://doi.org/10.1111/nph.19561, 2024.

Damour, G., Simonneau, T., Cochard, H., and Urban, L.: An overview of models of stomatal conductance at the leaf level, Plant, Cell & Environment, 33, 1419–1438, https://doi.org/10.1111/j.1365-3040.2010.02181.x, 2010.

Daws, M. I., Crabtree, L. M., Dalling, J. W., Mullins, C. E., and Burslem, D. F. R. P.: Germination Responses to Water Potential in Neotropical Pioneers Suggest Large-seeded Species Take More Risks, Ann Bot, 102, 945–951, https://doi.org/10.1093/aob/mcn186, 2008.

Dawson, T. E.: Hydraulic lift and water use by plants: implications for water balance, performance and plant-plant interactions, Oecologia, 95, 565–574, https://doi.org/10.1007/BF00317442, 1993.

De Cáceres, M., Molowny-Horas, R., Cabon, A., Martínez-Vilalta, J., Mencuccini, M., García-Valdés, R., Nadal-Sala, D., Sabaté, S., Martin-StPaul, N., Morin, X., D'Adamo, F., Batllori, E., and Améztegui, A.: MEDFATE 2.9.3: a trait-enabled

model to simulate Mediterranean forest function and dynamics at regional scales, Geoscientific Model Development, 16, 3165–3201, https://doi.org/10.5194/gmd-16-3165-2023, 2023.

De Deurwaerder, H., Hervé-Fernández, P., Stahl, C., Burban, B., Petronelli, P., Hoffman, B., Bonal, D., Boeckx, P., and Verbeeck, H.: Liana and tree below-ground water competition—evidence for water resource partitioning during the dry season, Tree Physiol, 38, 1071–1083, https://doi.org/10.1093/treephys/tpy002, 2018.

De Frenne, P., Zellweger, F., Rodríguez-Sánchez, F., Scheffers, B. R., Hylander, K., Luoto, M., Vellend, M., Verheyen, K., and Lenoir, J.: Global buffering of temperatures under forest canopies, Nat Ecol Evol, 3, 744–749, https://doi.org/10.1038/s41559-019-0842-1, 2019.

De Kauwe, M. G., Zhou, S.-X., Medlyn, B. E., Pitman, A. J., Wang, Y.-P., Duursma, R. A., and Prentice, I. C.: Do land surface models need to include differential plant species responses to drought? Examining model predictions across a mesic-xeric gradient in Europe, Biogeosciences, 12, 7503–7518, https://doi.org/10.5194/bg-12-7503-2015, 2015.

De Kauwe, M. G., Medlyn, B. E., Knauer, J., and Williams, C. A.: Ideas and perspectives: how coupled is the vegetation to the boundary layer?, Biogeosciences, 14, 4435–4453, http://dx.doi.org/10.5194/bg-14-4435-2017, 2017.

Delhaye, G., Bauman, D., Séleck, M., Ilunga wa Ilunga, E., Mahy, G., and Meerts, P.: Interspecific trait integration increases with environmental harshness: A case study along a metal toxicity gradient, Functional Ecology, 34, 1428–1437, https://doi.org/10.1111/1365-2435.13570, 2020.

Dewar, R., Mauranen, A., Mäkelä, A., Hölttä, T., Medlyn, B., and Vesala, T.: New insights into the covariation of stomatal, mesophyll and hydraulic conductances from optimization models incorporating nonstomatal limitations to photosynthesis, New Phytologist, 217, 571–585, https://doi.org/10.1111/nph.14848, 2018.

Díaz, S., Kattge, J., Cornelissen, J. H. C., Wright, I. J., Lavorel, S., Dray, S., Reu, B., Kleyer, M., Wirth, C., Colin Prentice, I., Garnier, E., Bönisch, G., Westoby, M., Poorter, H., Reich, P. B., Moles, A. T., Dickie, J., Gillison, A. N., Zanne, A. E., Chave, J., Joseph Wright, S., Sheremet'ev, S. N., Jactel, H., Baraloto, C., Cerabolini, B., Pierce, S., Shipley, B., Kirkup, D., Casanoves, F., Joswig, J. S., Günther, A., Falczuk, V., Rüger, N., Mahecha, M. D., and Gorné, L. D.: The global spectrum of plant form and function, Nature, 529, 167–171, https://doi.org/10.1038/nature16489, 2016.

Díaz, S., Kattge, J., Cornelissen, J. H. C., Wright, I. J., Lavorel, S., Dray, S., Reu, B., Kleyer, M., Wirth, C., Prentice, I. C., Garnier, E., Bönisch, G., Westoby, M., Poorter, H., Reich, P. B., Moles, A. T., Dickie, J., Zanne, A. E., Chave, J., Wright, S. J., Sheremetiev, S. N., Jactel, H., Baraloto, C., Cerabolini, B. E. L., Pierce, S., Shipley, B., Casanoves, F., Joswig, J. S., Günther, A., Falczuk, V., Rüger, N., Mahecha, M. D., Gorné, L. D., Amiaud, B., Atkin, O. K., Bahn, M., Baldocchi, D., Beckmann, M., Blonder, B., Bond, W., Bond-Lamberty, B., Brown, K., Burrascano, S., Byun, C., Campetella, G., Cavender-Bares, J., Chapin, F. S., Choat, B., Coomes, D. A., Cornwell, W. K., Craine, J., Craven, D., Dainese, M., de Araujo, A. C., de Vries, F. T., Domingues, T. F., Enquist, B. J., Fagúndez, J., Fang, J., Fernández-Méndez, F., Fernandez-Piedade, M. T., Ford, H., Forey, E., Freschet, G. T., Gachet, S., Gallagher, R., Green, W., Guerin, G. R., Gutiérrez, A. G., Harrison, S. P., Hattingh, W. N., He, T., Hickler, T., Higgins, S. I., Higuchi, P., Ilic, J., Jackson, R. B., Jalili, A., Jansen, S., Koike, F., König, C., Kraft, N., Kramer, K., Kreft, H., Kühn, I., Kurokawa, H., Lamb, E. G., Laughlin, D. C., Leishman,

M., Lewis, S., Louault, F., Malhado, A. C. M., Manning, P., Meir, P., Mencuccini, M., Messier, J., Miller, R., Minden, V., Molofsky, J., et al.: The global spectrum of plant form and function: enhanced species-level trait dataset, Sci Data, 9, 755, https://doi.org/10.1038/s41597-022-01774-9, 2022.

Díaz-Yáñez, O., Käber, Y., Anders, T., Bohn, F., Braziunas, K. H., Brůna, J., Fischer, R., Fischer, S. M., Hetzer, J., Hickler, T., Hochauer, C., Lexer, M. J., Lischke, H., Mairota, P., Merganič, J., Merganičová, K., Mette, T., Mina, M., Morin, X., Nieberg, M., Rammer, W., Reyer, C. P. O., Scheiter, S., Scherrer, D., and Bugmann, H.: Tree regeneration in models of forest dynamics: A key priority for further research, Ecosphere, 15, e4807, https://doi.org/10.1002/ecs2.4807, 2024.

Dietze, M. C., Lebauer, D. S., and Kooper, R.: On improving the communication between models and data, Plant, Cell & Environment, 36, 1575–1585, https://doi.org/10.1111/pce.12043, 2013.

Dilley, A. C. and O'brien, D. M.: Estimating downward clear sky long-wave irradiance at the surface from screen temperature and precipitable water, Quarterly Journal of the Royal Meteorological Society, 124, 1391–1401, https://doi.org/10.1002/qj.49712454903, 1998.

Domingues, T. F., Meir, P., Feldpausch, T. R., Saiz, G., Veenendaal, E. M., Schrodt, F., Bird, M., Djagbletey, G., Hien, F., Compaore, H., Diallo, A., Grace, J., and Lloyd, J.: Co-limitation of photosynthetic capacity by nitrogen and phosphorus in West Africa woodlands, Plant, Cell & Environment, 33, 959–980, https://doi.org/10.1111/j.1365-3040.2010.02119.x, 2010.

Domingues, T. F., Martinelli, L. A., and Ehleringer, J. R.: Seasonal patterns of leaf-level photosynthetic gas exchange in an eastern Amazonian rain forest, Plant Ecology & Diversity, 7, 189–203, https://doi.org/10.1080/17550874.2012.748849, 2014.

Donovan, L. A., Richards, J. H., and Linton, M. J.: Magnitude and mechanisms of disequilibrium between predawn plant and soil water potentials, Ecology, 84, 463–470, https://doi.org/10.1890/0012-9658(2003)084[0463:MAMODB]2.0.CO;2, 2003.

Dormann, C. F., Schymanski, S. J., Cabral, J., Chuine, I., Graham, C., Hartig, F., Kearney, M., Morin, X., Römermann, C., Schröder, B., and Singer, A.: Correlation and process in species distribution models: bridging a dichotomy, Journal of Biogeography, 39, 2119–2131, https://doi.org/10.1111/j.1365-2699.2011.02659.x, 2012.

Doughty, C. E. and Goulden, M. L.: Seasonal patterns of tropical forest leaf area index and CO2 exchange, J. Geophys. Res., 113, G00B06, https://doi.org/10.1029/2007JG000590, 2008.

Doughty, C. E., Gaillard, C., Burns, P., Keany, J. M., Abraham, A. J., Malhi, Y., Aguirre-Gutierrez, J., Koch, G., Jantz, P., Shenkin, A., and Tang, H.: Tropical forests are mainly unstratified especially in Amazonia and regions with lower fertility or higher temperatures, Environ. Res.: Ecology, 2, 035002, https://doi.org/10.1088/2752-664X/ace723, 2023.

Drake, J. E., Power, S. A., Duursma, R. A., Medlyn, B. E., Aspinwall, M. J., Choat, B., Creek, D., Eamus, D., Maier, C., Pfautsch, S., Smith, R. A., Tjoelker, M. G., and Tissue, D. T.: Stomatal and non-stomatal limitations of photosynthesis for four tree species under drought: A comparison of model formulations, Agricultural and Forest Meteorology, 247, 454–466, https://doi.org/10.1016/j.agrformet.2017.08.026, 2017.

Drake, P. L., Boer, H. J. de, Schymanski, S. J., and Veneklaas, E. J.: Two sides to every leaf: water and CO2 transport in hypostomatous and amphistomatous leaves, New Phytologist, 222, 1179–1187, https://doi.org/10.1111/nph.15652, 2019.

Duffy, P. B., Brando, P., Asner, G. P., and Field, C. B.: Projections of future meteorological drought and wet periods in the Amazon, PNAS, 112, 13172–13177, https://doi.org/10.1073/pnas.1421010112, 2015.

Dunne, T. and Black, R. D.: An Experimental Investigation of Runoff Production in Permeable Soils, Water Resources Research, 6, 478–490, https://doi.org/10.1029/WR006i002p00478, 1970.

Duursma, R. A.: Plantecophys - An R Package for Analysing and Modelling Leaf Gas Exchange Data, PLOS ONE, 10, e0143346, https://doi.org/10.1371/journal.pone.0143346, 2015.

Duursma, R. A. and Medlyn, B. E.: MAESPA: a model to study interactions between water limitation, environmental drivers and vegetation function at tree and stand levels, with an example application to $[CO_2] \times$ drought interactions, Geoscientific Model Development, 5, 919–940, https://doi.org/10.5194/gmd-5-919-2012, 2012.

Duursma, R. A., Blackman, C. J., Lopéz, R., Martin-StPaul, N. K., Cochard, H., and Medlyn, B. E.: On the minimum leaf conductance: its role in models of plant water use, and ecological and environmental controls, New Phytologist, 221, 693–705, https://doi.org/10.1111/nph.15395, 2019.

Dwyer, J. M. and Laughlin, D. C.: Constraints on trait combinations explain climatic drivers of biodiversity: the importance of trait covariance in community assembly, Ecol Lett, 20, 872–882, https://doi.org/10.1111/ele.12781, 2017.

Egea, G., Verhoef, A., and Vidale, P. L.: Towards an improved and more flexible representation of water stress in coupled photosynthesis–stomatal conductance models, Agricultural and Forest Meteorology, 151, 1370–1384, https://doi.org/10.1016/j.agrformet.2011.05.019, 2011.

Elias, M. and Potvin, C.: Assessing inter- and intra-specific variation in trunk carbon concentration for 32 neotropical tree species, Can. J. For. Res., 33, 1039–1045, https://doi.org/10.1139/x03-018, 2003.

Elith, J. and Leathwick, J. R.: Species Distribution Models: Ecological Explanation and Prediction Across Space and Time, Annual Review of Ecology, Evolution, and Systematics, 40, 677–697, https://doi.org/10.1146/annurev.ecolsys.110308.120159, 2009.

Engelbrecht, B. M. J., Dalling, J. W., Pearson, T. R. H., Wolf, R. L., Galvez, D. A., Koehler, T., Tyree, M. T., and Kursar, T. A.: Short dry spells in the wet season increase mortality of tropical pioneer seedlings, Oecologia, 148, 258–269, https://doi.org/10.1007/s00442-006-0368-5, 2006.

Esquivel-Muelbert, A., Baker, T. R., Dexter, K. G., Lewis, S. L., Brienen, R. J. W., Feldpausch, T. R., Lloyd, J., Monteagudo-Mendoza, A., Arroyo, L., Álvarez-Dávila, E., Higuchi, N., Marimon, B. S., Marimon-Junior, B. H., Silveira, M., Vilanova, E., Gloor, E., Malhi, Y., Chave, J., Barlow, J., Bonal, D., Cardozo, N. D., Erwin, T., Fauset, S., Hérault, B., Laurance, S., Poorter, L., Qie, L., Stahl, C., Sullivan, M. J. P., Steege, H. ter, Vos, V. A., Zuidema, P. A., Almeida, E., Oliveira, E. A. de, Andrade, A., Vieira, S. A., Aragão, L., Araujo-Murakami, A., Arets, E., C, G. A. A., Baraloto, C., Camargo, P. B., Barroso, J. G., Bongers, F., Boot, R., Camargo, J. L., Castro, W., Moscoso, V. C., Comiskey, J., Valverde, F. C., Costa, A. C. L. da, Pasquel, J. del A., Fiore, A. D., Duque, L. F., Elias, F., Engel, J., Llampazo, G. F., Galbraith, D., Fernández, R.

H., Coronado, E. H., Hubau, W., Jimenez-Rojas, E., Lima, A. J. N., Umetsu, R. K., Laurance, W., Lopez-Gonzalez, G., Lovejoy, T., Cruz, O. A. M., Morandi, P. S., Neill, D., Vargas, P. N., Camacho, N. C. P., Gutierrez, A. P., Pardo, G., Peacock, J., Peña-Claros, M., Peñuela-Mora, M. C., Petronelli, P., Pickavance, G. C., Pitman, N., Prieto, A., Quesada, C., Ramírez-Angulo, H., Réjou-Méchain, M., Correa, Z. R., Roopsind, A., Rudas, A., Salomão, R., Silva, N., Espejo, J. S., Singh, J., Stropp, J., Terborgh, J., Thomas, R., Toledo, M., Torres-Lezama, A., Gamarra, L. V., Meer, P. J. van de, Heijden, G. van der, et al.: Compositional response of Amazon forests to climate change, Global Change Biology, 25, 39–56, https://doi.org/10.1111/gcb.14413, 2019.

Esquivel-Muelbert, A., Phillips, O. L., Brienen, R. J. W., Fauset, S., Sullivan, M. J. P., Baker, T. R., Chao, K.-J., Feldpausch, T. R., Gloor, E., Higuchi, N., Houwing-Duistermaat, J., Lloyd, J., Liu, H., Malhi, Y., Marimon, B., Marimon Junior, B. H., Monteagudo-Mendoza, A., Poorter, L., Silveira, M., Torre, E. V., Dávila, E. A., del Aguila Pasquel, J., Almeida, E., Loayza, P. A., Andrade, A., Aragão, L. E. O. C., Araujo-Murakami, A., Arets, E., Arroyo, L., C, G. A. A., Baisie, M., Baraloto, C., Camargo, P. B., Barroso, J., Blanc, L., Bonal, D., Bongers, F., Boot, R., Brown, F., Burban, B., Camargo, J. L., Castro, W., Moscoso, V. C., Chave, J., Comiskey, J., Valverde, F. C., da Costa, A. L., Cardozo, N. D., Di Fiore, A., Dourdain, A., Erwin, T., Llampazo, G. F., Vieira, I. C. G., Herrera, R., Honorio Coronado, E., Huamantupa-Chuquimaco, I., Jimenez-Rojas, E., Killeen, T., Laurance, S., Laurance, W., Levesley, A., Lewis, S. L., Ladvocat, K. L. L. M., Lopez-Gonzalez, G., Lovejoy, T., Meir, P., Mendoza, C., Morandi, P., Neill, D., Nogueira Lima, A. J., Vargas, P. N., de Oliveira, E. A., Camacho, N. P., Pardo, G., Peacock, J., Peña-Claros, M., Peñuela-Mora, M. C., Pickavance, G., Pipoly, J., Pitman, N., Prieto, A., Pugh, T. A. M., Quesada, C., Ramirez-Angulo, H., de Almeida Reis, S. M., Rejou-Machain, M., Correa, Z. R., Bayona, L. R., Rudas, A., Salomão, R., Serrano, J., Espejo, J. S., Silva, N., Singh, J., Stahl, C., Stropp, J., Swamy, V., Talbot, J., ter Steege, H., et al.: Tree mode of death and mortality risk factors across Amazon forests, Nature Communications, 11, 5515, https://doi.org/10.1038/s41467-020-18996-3, 2020.

Estes, L., Elsen, P. R., Treuer, T., Ahmed, L., Caylor, K., Chang, J., Choi, J. J., and Ellis, E. C.: The spatial and temporal domains of modern ecology, Nature Ecology & Evolution, 1, https://doi.org/10.1038/s41559-018-0524-4, 2018.

Evans, M. R.: Modelling ecological systems in a changing world, Phil. Trans. R. Soc. B, 367, 181–190, https://doi.org/10.1098/rstb.2011.0172, 2012.

Farquhar, G. D., Caemmerer, S. von, and Berry, J. A.: A biochemical model of photosynthetic CO2 assimilation in leaves of C3 species, Planta, 149, 78–90, 1980.

Farrell, C., Szota, C., and Arndt, S. K.: Does the turgor loss point characterize drought response in dryland plants?, Plant, Cell & Environment, 40, 1500–1511, https://doi.org/10.1111/pce.12948, 2017.

Fatichi, S., Pappas, C., and Ivanov, V. Y.: Modeling plant–water interactions: an ecohydrological overview from the cell to the global scale, WIREs Water, 3, 327–368, https://doi.org/10.1002/wat2.1125, 2016.

Fauset, S., Baker, T. R., Lewis, S. L., Feldpausch, T. R., Affum-Baffoe, K., Foli, E. G., Hamer, K. C., and Swaine, M. D.: Drought-induced shifts in the floristic and functional composition of tropical forests in Ghana, Ecol Lett, 15, 1120–1129, https://doi.org/10.1111/j.1461-0248.2012.01834.x, 2012.

Feeley, K. J., Davies, S. J., Perez, R., Hubbell, S. P., and Foster, R. B.: Directional changes in the species composition of a tropical forest, Ecology, 92, 871–882, 2011.

Fer, I., Kelly, R., Moorcroft, P. R., Richardson, A. D., Cowdery, E. M., and Dietze, M. C.: Linking big models to big data: efficient ecosystem model calibration through Bayesian model emulation, Biogeosciences, 15, 5801–5830, https://doi.org/10.5194/bg-15-5801-2018, 2018.

Fernández-Martínez, M., Vicca, S., Janssens, I. A., Sardans, J., Luyssaert, S., Campioli, M., Chapin Iii, F. S., Ciais, P., Malhi, Y., Obersteiner, M., Papale, D., Piao, S. L., Reichstein, M., Rodà, F., and Peñuelas, J.: Nutrient availability as the key regulator of global forest carbon balance, Nature Clim. Change, 4, 471–476, https://doi.org/10.1038/nclimate2177, 2014.

Ferrier, S. and Guisan, A.: Spatial modelling of biodiversity at the community level, Journal of Applied Ecology, 43, 393–404, https://doi.org/10.1111/j.1365-2664.2006.01149.x, 2006.

Fichtner, A., Härdtle, W., Bruelheide, H., Kunz, M., Li, Y., and Oheimb, G.: Neighbourhood interactions drive overyielding in mixed-species tree communities, Nature Communications, 9, 1144, https://doi.org/10.1038/s41467-018-03529-w, 2018.

Fischer, F. J.: Inferring the structure and dynamics of tropical rain forests with individual-based forest growth models, Doctoral Dissertation, Université Paul Sabatier-Toulouse III., 2019.

Fischer, F. J., Maréchaux, I., and Chave, J.: Improving plant allometry by fusing forest models and remote sensing, New Phytologist, 223, 1159–1165, https://doi.org/10.1111/nph.15810, 2019.

Fischer, F. J., Labrière, N., Vincent, G., Hérault, B., Alonso, A., Memiaghe, H., Bissiengou, P., Kenfack, D., Saatchi, S., and Chave, J.: A simulation method to infer tree allometry and forest structure from airborne laser scanning and forest inventories, Remote Sensing of Environment, 251, 112056, https://doi.org/10.1016/j.rse.2020.112056, 2020.

Fischer, R., Armstrong, A., Shugart, H. H., and Huth, A.: Simulating the impacts of reduced rainfall on carbon stocks and net ecosystem exchange in a tropical forest, Environmental Modelling & Software, 52, 200–206, https://doi.org/10.1016/j.envsoft.2013.10.026, 2014.

Fisher, J. B., Huntzinger, D. N., Schwalm, C. R., and Sitch, S.: Modeling the Terrestrial Biosphere, Annual Review of Environment and Resources, 39, 91–123, https://doi.org/10.1146/annurev-environ-012913-093456, 2014.

Fisher, R. A., Williams, M., Do Vale, R. L., Da Costa, A. L., and Meir, P.: Evidence from Amazonian forests is consistent with isohydric control of leaf water potential, Plant, Cell & Environment, 29, 151–165, https://doi.org/10.1111/j.1365-3040.2005.01407.x, 2006.

Fisher, R. A., Williams, M., Da Costa, A. L., Malhi, Y., Da Costa, R. F., Almeida, S., and Meir, P.: The response of an Eastern Amazonian rain forest to drought stress: results and modelling analyses from a throughfall exclusion experiment, Global Change Biology, 13, 2361–2378, https://doi.org/10.1111/j.1365-2486.2007.01417.x, 2007.

Fisher, R. A., Muszala, S., Verteinstein, M., Lawrence, P., Xu, C., McDowell, N. G., Knox, R. G., Koven, C., Holm, J., Rogers, B. M., Spessa, A., Lawrence, D., and Bonan, G.: Taking off the training wheels: the properties of a dynamic vegetation model without climate envelopes, CLM4.5(ED), Geosci. Model Dev., 8, 3593–3619, https://doi.org/10.5194/gmd-8-3593-2015, 2015.

Fisher, R. A., Koven, C. D., Anderegg, W. R. L., Christoffersen, B. O., Dietze, M. C., Farrior, C. E., Holm, J. A., Hurtt, G. C., Knox, R. G., Lawrence, P. J., Lichstein, J. W., Longo, M., Matheny, A. M., Medvigy, D., Muller-Landau, H. C., Powell, T. L., Serbin, S. P., Sato, H., Shuman, J. K., Smith, B., Trugman, A. T., Viskari, T., Verbeeck, H., Weng, E., Xu, C., Xu, X., Zhang, T., and Moorcroft, P. R.: Vegetation demographics in Earth System Models: A review of progress and priorities, Global Change Biology, 24, 35–54, https://doi.org/10.1111/gcb.13910, 2018.

Flexas, J., Bota, J., Loreto, F., Cornic, G., and Sharkey, T. D.: Diffusive and Metabolic Limitations to Photosynthesis under Drought and Salinity in C3 Plants, Plant biol (Stuttg), 6, 269–279, https://doi.org/10.1055/s-2004-820867, 2004.

Flexas, J., Galmes, J., Ribas-Carbo, M., and Medrano, H.: The Effects of Water Stress on Plant Respiration, in: Plant Respiration, Springer, Dordrecht, 85–94, https://doi.org/10.1007/1-4020-3589-6_6, 2005.

Flexas, J., Bota, J., Galmés, J., Medrano, H., and Ribas-Carbó, M.: Keeping a positive carbon balance under adverse conditions: responses of photosynthesis and respiration to water stress, Physiologia Plantarum, 127, 343–352, https://doi.org/10.1111/j.1399-3054.2006.00621.x, 2006.

Flexas, J., Barbour, M. M., Brendel, O., Cabrera, H. M., Carriquí, M., Díaz-Espejo, A., Douthe, C., Dreyer, E., Ferrio, J. P., Gago, J., Gallé, A., Galmés, J., Kodama, N., Medrano, H., Niinemets, Ü., Peguero-Pina, J. J., Pou, A., Ribas-Carbó, M., Tomás, M., Tosens, T., and Warren, C. R.: Mesophyll diffusion conductance to CO2: An unappreciated central player in photosynthesis, Plant Science, 193–194, 70–84, https://doi.org/10.1016/j.plantsci.2012.05.009, 2012.

Franks, P. J., Bonan, G. B., Berry, J. A., Lombardozzi, D. L., Holbrook, N. M., Herold, N., and Oleson, K. W.: Comparing optimal and empirical stomatal conductance models for application in Earth system models, Global Change Biology, 24, 5708–5723, https://doi.org/10.1111/gcb.14445, 2018.

Franks, S. W., Beven, K. J., Quinn, P. F., and Wright, I. R.: On the sensitivity of soil-vegetation-atmosphere transfer (SVAT) schemes: equifinality and the problem of robust calibration, Agricultural and Forest Meteorology, 86, 63–75, https://doi.org/10.1016/S0168-1923(96)02421-5, 1997.

Friend, A. D., Lucht, W., Rademacher, T. T., Keribin, R., Betts, R., Cadule, P., Ciais, P., Clark, D. B., Dankers, R., Falloon, P. D., Ito, A., Kahana, R., Kleidon, A., Lomas, M. R., Nishina, K., Ostberg, S., Pavlick, R., Peylin, P., Schaphoff, S., Vuichard, N., Warszawski, L., Wiltshire, A., and Woodward, F. I.: Carbon residence time dominates uncertainty in terrestrial vegetation responses to future climate and atmospheric CO2, Proc. Natl. Acad. Sci. U. S. A., 111, 3280–3285, https://doi.org/10.1073/pnas.1222477110, 2014.

Fyllas, N. M., Gloor, E., Mercado, L. M., Sitch, S., Quesada, C. A., Domingues, T. F., Galbraith, D. R., Torre-Lezama, A., Vilanova, E., Ramírez-Angulo, H., Higuchi, N., Neill, D. A., Silveira, M., Ferreira, L., Aymard C., G. A., Malhi, Y., Phillips, O. L., and Lloyd, J.: Analysing Amazonian forest productivity using a new individual and trait-based model (TFS v.1), Geosci. Model Dev., 7, 1251–1269, https://doi.org/10.5194/gmd-7-1251-2014, 2014.

Garcia, M. N., Domingues, T. F., Oliveira, R. S., and Costa, F. R. C.: The biogeography of embolism resistance across resource gradients in the Amazon, Global Ecology and Biogeography, 32, 2199–2211, https://doi.org/10.1111/geb.13765, 2023.

Gardner, W. R.: Relation of Root Distribution to Water Uptake and Availability, Agronomy Journal, 56, 41–45, https://doi.org/10.2134/agronj1964.00021962005600010013x, 1964.

Gash, J. H. C.: An analytical model of rainfall interception by forests, Q.J.R. Meteorol. Soc., 105, 43–55, https://doi.org/10.1002/qj.49710544304, 1979.

Gash, J. H. C., Lloyd, C. R., and Lachaud, G.: Estimating sparse forest rainfall interception with an analytical model, Journal of Hydrology, 170, 79–86, https://doi.org/10.1016/0022-1694(95)02697-N, 1995.

van Genuchten, M. Th.: A Closed-form Equation for Predicting the Hydraulic Conductivity of Unsaturated Soils1, Soil Science Society of America Journal, 44, 892–898, https://doi.org/10.2136/sssaj1980.03615995004400050002x, 1980.

Girard-Tercieux, C., Maréchaux, I., Clark, A. T., Clark, J. S., Courbaud, B., Fortunel, C., Guillemot, J., Künstler, G., le Maire, G., Pélissier, R., Rüger, N., and Vieilledent, G.: Rethinking the nature of intraspecific variability and its consequences on species coexistence, Ecology and Evolution, 13, e9860, https://doi.org/10.1002/ece3.9860, 2023.

Gourlet-Fleury, S., Blanc, L., Picard, N., Sist, P., Dick, J., Nasi, R., Swaine, M. D., and Forni, E.: Grouping species for predicting mixed tropical forest dynamics: looking for a strategy, Annals of Forest Science, 62, 12, https://doi.org/10.1051/forest:2005084, 2005.

Griffin-Nolan, R. J., Ocheltree, T. W., Mueller, K. E., Blumenthal, D. M., Kray, J. A., and Knapp, A. K.: Extending the osmometer method for assessing drought tolerance in herbaceous species, Oecologia, 189, 353–363, https://doi.org/10.1007/s00442-019-04336-w, 2019.

Gril, E., Spicher, F., Greiser, C., Ashcroft, M. B., Pincebourde, S., Durrieu, S., Nicolas, M., Richard, B., Decocq, G., Marrec, R., and Lenoir, J.: Slope and equilibrium: A parsimonious and flexible approach to model microclimate, Methods in Ecology and Evolution, 14, 885–897, https://doi.org/10.1111/2041-210X.14048, 2023a.

Gril, E., Laslier, M., Gallet-Moron, E., Durrieu, S., Spicher, F., Le Roux, V., Brasseur, B., Haesen, S., Van Meerbeek, K., Decocq, G., Marrec, R., and Lenoir, J.: Using airborne LiDAR to map forest microclimate temperature buffering or amplification, Remote Sensing of Environment, 298, 113820, https://doi.org/10.1016/j.rse.2023.113820, 2023b.

Grisebach, A.: Die Vegetation der Erde nach ihrer klimatischen Anordnung: Ein Abriss der vergleichenden Geographie der Pflanzen. Bd. I und II., Verlag von Wilhelm Engelmann, Leipzig, 1872.

Gu, L., Shugart, H. H., Fuentes, J. D., Black, T. A., and Shewchuk, S. R.: Micrometeorology, biophysical exchanges and NEE decomposition in a two-story boreal forest — development and test of an integrated model, Agricultural and Forest Meteorology, 94, 123–148, https://doi.org/10.1016/S0168-1923(99)00006-4, 1999.

Guan, K., Pan, M., Li, H., Wolf, A., Wu, J., Medvigy, D., Caylor, K. K., Sheffield, J., Wood, E. F., Malhi, Y., Liang, M., Kimball, J. S., Saleska, S. R., Berry, J., Joiner, J., and Lyapustin, A. I.: Photosynthetic seasonality of global tropical forests constrained by hydroclimate, Nature Geosci, 8, 284–289, https://doi.org/10.1038/ngeo2382, 2015.

Guerrero-Ramírez, N. R., Mommer, L., Freschet, G. T., Iversen, C. M., McCormack, M. L., Kattge, J., Poorter, H., van der Plas, F., Bergmann, J., Kuyper, T. W., York, L. M., Bruelheide, H., Laughlin, D. C., Meier, I. C., Roumet, C., Semchenko, M., Sweeney, C. J., van Ruijven, J., Valverde-Barrantes, O. J., Aubin, I., Catford, J. A., Manning, P., Martin, A., Milla, R.,

Minden, V., Pausas, J. G., Smith, S. W., Soudzilovskaia, N. A., Ammer, C., Butterfield, B., Craine, J., Cornelissen, J. H. C., de Vries, F. T., Isaac, M. E., Kramer, K., König, C., Lamb, E. G., Onipchenko, V. G., Peñuelas, J., Reich, P. B., Rillig, M. C., Sack, L., Shipley, B., Tedersoo, L., Valladares, F., van Bodegom, P., Weigelt, P., Wright, J. P., and Weigelt, A.: Global root traits (GRooT) database, Global Ecology and Biogeography, 30, 25–37, https://doi.org/10.1111/geb.13179, 2021.

Guillemot, J., Kunz, M., Schnabel, F., Fichtner, A., Madsen, C. P., Gebauer, T., Härdtle, W., von Oheimb, G., and Potvin, C.: Neighbourhood-mediated shifts in tree biomass allocation drive overyielding in tropical species mixtures, New Phytologist, 228, 1256–1268, https://doi.org/10.1111/nph.16722, 2020.

Guimberteau, M., Ducharne, A., Ciais, P., Boisier, J.-P., Peng, S., De Weirdt, M., and Verbeeck, H.: Testing conceptual and physically based soil hydrology schemes against observations for the Amazon Basin, Geoscientific Model Development, 7, 1115–1136, https://doi.org/10.5194/gmd-7-1115-2014, 2014.

Guisan, A. and Thuiller, W.: Predicting species distribution: offering more than simple habitat models, Ecology Letters, 8, 993–1009, https://doi.org/10.1111/j.1461-0248.2005.00792.x, 2005.

Guisan, A., Thuiller, W., and Zimmermann, N. E.: Habitat Suitability and Distribution Models: with Applications in R, Cambridge University Press, 513 pp., 2017.

Gutiérrez, A. G., Armesto, J. J., Díaz, M. F., and Huth, A.: Increased Drought Impacts on Temperate Rainforests from Southern South America: Results of a Process-Based, Dynamic Forest Model, PLOS ONE, 9, e103226, https://doi.org/10.1371/journal.pone.0103226, 2014.

Hanbury-Brown, A. R., Ward, R. E., and Kueppers, L. M.: Forest regeneration within Earth system models: current process representations and ways forward, New Phytologist, 235, 20–40, https://doi.org/10.1111/nph.18131, 2022.

Harper, A., Baker, I. T., Denning, A. S., Randall, D. A., Dazlich, D., and Branson, M.: Impact of evapotranspiration on dry season climate in the Amazon forest, Journal of Climate, 27, 574–591, https://doi.org/10.1175/JCLI-D-13-00074.1, 2013.

Hartig, F., Dyke, J., Hickler, T., Higgins, S. I., O'Hara, R. B., Scheiter, S., and Huth, A.: Connecting dynamic vegetation models to data – an inverse perspective, Journal of Biogeography, 39, 2240–2252, https://doi.org/10.1111/j.1365-2699.2012.02745.x, 2012.

Hasselquist, N. J., Allen, M. F., and Santiago, L. S.: Water relations of evergreen and drought-deciduous trees along a seasonally dry tropical forest chronosequence, Oecologia, 164, 881–890, https://doi.org/10.1007/s00442-010-1725-y, 2010.

Hengl, T., Jesus, J. M. de, Heuvelink, G. B. M., Gonzalez, M. R., Kilibarda, M., Blagotić, A., Shangguan, W., Wright, M. N., Geng, X., Bauer-Marschallinger, B., Guevara, M. A., Vargas, R., MacMillan, R. A., Batjes, N. H., Leenaars, J. G. B., Ribeiro, E., Wheeler, I., Mantel, S., and Kempen, B.: SoilGrids250m: Global gridded soil information based on machine learning, PLOS ONE, 12, e0169748, https://doi.org/10.1371/journal.pone.0169748, 2017.

Héroult, A., Lin, Y.-S., Bourne, A., Medlyn, B. E., and Ellsworth, D. S.: Optimal stomatal conductance in relation to photosynthesis in climatically contrasting Eucalyptus species under drought, Plant, Cell & Environment, 36, 262–274, https://doi.org/10.1111/j.1365-3040.2012.02570.x, 2013.

Heskel, M. A., O'Sullivan, O. S., Reich, P. B., Tjoelker, M. G., Weerasinghe, L. K., Penillard, A., Egerton, J. J. G., Creek, D., Bloomfield, K. J., Xiang, J., Sinca, F., Stangl, Z. R., Torre, A. M. la, Griffin, K. L., Huntingford, C., Hurry, V., Meir, P., Turnbull, M. H., and Atkin, O. K.: Convergence in the temperature response of leaf respiration across biomes and plant functional types, PNAS, 201520282, https://doi.org/10.1073/pnas.1520282113, 2016.

Hodnett, M. G. and Tomasella, J.: Marked differences between van Genuchten soil water-retention parameters for temperate and tropical soils: a new water-retention pedo-transfer functions developed for tropical soils, Geoderma, 108, 155–180, https://doi.org/10.1016/S0016-7061(02)00105-2, 2002.

Horton, R. E.: The role of infiltration in the hydrologic cycle, Eos, Transactions American Geophysical Union, 14, 446–460, https://doi.org/10.1029/TR014i001p00446, 1933.

Hsiao, T. C.: Plant Responses to Water Stress, Annual Review of Plant Physiology, 24, 519–570, https://doi.org/10.1146/annurev.pp.24.060173.002511, 1973.

Huaraca Huasco, W., Riutta, T., Girardin, C. A. J., Hancco Pacha, F., Puma Vilca, B. L., Moore, S., Rifai, S. W., del Aguila-Pasquel, J., Araujo Murakami, A., Freitag, R., Morel, A. C., Demissie, S., Doughty, C. E., Oliveras, I., Galiano Cabrera, D. F., Durand Baca, L., Farfán Amézquita, F., Silva Espejo, J. E., da Costa, A. C. L., Oblitas Mendoza, E., Quesada, C. A., Evouna Ondo, F., Edzang Ndong, J., Jeffery, K. J., Mihindou, V., White, L. J. T., N'ssi Bengone, N., Ibrahim, F., Addo-Danso, S. D., Duah-Gyamfi, A., Djaney Djagbletey, G., Owusu-Afriyie, K., Amissah, L., Mbou, A. T., Marthews, T. R., Metcalfe, D. B., Aragão, L. E. O., Marimon-Junior, B. H., Marimon, B. S., Majalap, N., Adu-Bredu, S., Abernethy, K. A., Silman, M., Ewers, R. M., Meir, P., and Malhi, Y.: Fine root dynamics across pantropical rainforest ecosystems, Global Change Biology, 27, 3657–3680, https://doi.org/10.1111/gcb.15677, 2021.

Hubau, W., Lewis, S. L., Phillips, O. L., Affum-Baffoe, K., Beeckman, H., Cuní-Sanchez, A., Daniels, A. K., Ewango, C. E. N., Fauset, S., Mukinzi, J. M., Sheil, D., Sonké, B., Sullivan, M. J. P., Sunderland, T. C. H., Taedoumg, H., Thomas, S. C., White, L. J. T., Abernethy, K. A., Adu-Bredu, S., Amani, C. A., Baker, T. R., Banin, L. F., Baya, F., Begne, S. K., Bennett, A. C., Benedet, F., Bitariho, R., Bocko, Y. E., Boeckx, P., Boundja, P., Brienen, R. J. W., Brncic, T., Chezeaux, E., Chuyong, G. B., Clark, C. J., Collins, M., Comiskey, J. A., Coomes, D. A., Dargie, G. C., de Haulleville, T., Kamdem, M. N. D., Doucet, J.-L., Esquivel-Muelbert, A., Feldpausch, T. R., Fofanah, A., Foli, E. G., Gilpin, M., Gloor, E., Gonmadje, C., Gourlet-Fleury, S., Hall, J. S., Hamilton, A. C., Harris, D. J., Hart, T. B., Hockemba, M. B. N., Hladik, A., Ifo, S. A., Jeffery, K. J., Jucker, T., Yakusu, E. K., Kearsley, E., Kenfack, D., Koch, A., Leal, M. E., Levesley, A., Lindsell, J. A., Lisingo, J., Lopez-Gonzalez, G., Lovett, J. C., Makana, J.-R., Malhi, Y., Marshall, A. R., Martin, J., Martin, E. H., Mbayu, F. M., Medjibe, V. P., Mihindou, V., Mitchard, E. T. A., Moore, S., Munishi, P. K. T., Bengone, N. N., Ojo, L., Ondo, F. E., Peh, K. S.-H., Pickavance, G. C., Poulsen, A. D., Poulsen, J. R., Qie, L., Reitsma, J., Rovero, F., Swaine, M. D., Talbot, J., Taplin, J., Taylor, D. M., Thomas, D. W., Toirambe, B., Mukendi, J. T., Tuagben, D., Umunay, P. M., et al.:

Asynchronous carbon sink saturation in African and Amazonian tropical forests, Nature, 579, 80–87, https://doi.org/10.1038/s41586-020-2035-0, 2020.

Humbel, F.-X.: Caractérisation, par des mesures physiques, hydriques et d'enracinement, de sols de Guyane francaise à dynamique de l'eau superficielle, Sciences du sol, 2, 83–94, 1978.

Humboldt, A. von: Aspects of nature, in different lands and different climates; with scientific elucidations, Lea and Blanchard, 512 pp., 1849.

Huntingford, C., Zelazowski, P., Galbraith, D., Mercado, L. M., Sitch, S., Fisher, R., Lomas, M., Walker, A. P., Jones, C. D., Booth, B. B. B., Malhi, Y., Hemming, D., Kay, G., Good, P., Lewis, S. L., Phillips, O. L., Atkin, O. K., Lloyd, J., Gloor, E., Zaragoza-Castells, J., Meir, P., Betts, R., Harris, P. P., Nobre, C., Marengo, J., and Cox, P. M.: Simulated resilience of tropical rainforests to CO2-induced climate change, Nature Geosci, 6, 268–273, https://doi.org/10.1038/ngeo1741, 2013.

Hutchinson, G. E.: Concluding remarks, Cold Spring Harbor Symposia on Quantitative Biology, 22, 415–427, 1957.

Igarashi, S., Yoshida, S., Kenzo, T., Sakai, S., Nagamasu, H., Hyodo, F., Tayasu, I., Mohamad, M., and Ichie, T.: No evidence of carbon storage usage for seed production in 18 dipterocarp masting species in a tropical rain forest, Oecologia, https://doi.org/10.1007/s00442-024-05527-w, 2024.

Iida, Y., Poorter, L., Sterck, F. J., Kassim, A. R., Kubo, T., Potts, M. D., and Kohyama, T. S.: Wood density explains architectural differentiation across 145 co-occurring tropical tree species, Funct. Ecol., 26, 274–282, https://doi.org/10.1111/j.1365-2435.2011.01921.x, 2012.

Ivanov, V. Y., Hutyra, L. R., Wofsy, S. C., Munger, J. W., Saleska, S. R., Oliveira, R. C. de, and Camargo, P. B. de: Root niche separation can explain avoidance of seasonal drought stress and vulnerability of overstory trees to extended drought in a mature Amazonian forest, Water Resources Research, 48, https://doi.org/10.1029/2012WR011972, 2012.

Jackson, R. B., Canadell, J., Ehleringer, J. R., Mooney, H. A., Sala, O. E., and Schulze, E. D.: A global analysis of root distributions for terrestrial biomes, Oecologia, 108, 389–411, https://doi.org/10.1007/BF00333714, 1996.

Jackson, R. B., Moore, L. A., Hoffmann, W. A., Pockman, W. T., and Linder, C. R.: Ecosystem rooting depth determined with caves and DNA, PNAS, 96, 11387–11392, https://doi.org/10.1073/pnas.96.20.11387, 1999.

Jarvis, P. G. and McNaughton, K. G.: Stomatal Control of Transpiration: Scaling Up from Leaf to Region, Advances in Ecological Research, 15, 1–49, https://doi.org/10.1016/S0065-2504(08)60119-1, 1986.

Joetzjer, E., Delire, C., Douville, H., Ciais, P., Decharme, B., Fisher, R., Christoffersen, B., Calvet, J. C., da Costa, A. C. L., Ferreira, L. V., and Meir, P.: Predicting the response of the Amazon rainforest to persistent drought conditions under current and future climates: a major challenge for global land surface models, Geosci. Model Dev., 7, 2933–2950, https://doi.org/10.5194/gmd-7-2933-2014, 2014.

Joetzjer, E., Maignan, F., Chave, J., Goll, D., Poulter, B., Barichivich, J., Maréchaux, I., Luyssaert, S., Guimberteau, M., Naudts, K., Bonal, D., and Ciais, P.: Effect of tree demography and flexible root water uptake for modeling the carbon and water cycles of Amazonia, Ecological Modelling, 469, 109969, https://doi.org/10.1016/j.ecolmodel.2022.109969, 2022.

Johnson, D. J., Condit, R., Hubbell, S. P., and Comita, L. S.: Abiotic niche partitioning and negative density dependence drive tree seedling survival in a tropical forest, Proc. R. Soc. B, 284, 20172210, https://doi.org/10.1098/rspb.2017.2210, 2017.

Johnson, M. O., Galbraith, D., Gloor, M., De Deurwaerder, H., Guimberteau, M., Rammig, A., Thonicke, K., Verbeeck, H., von Randow, C., Monteagudo, A., Phillips, O. L., Brienen, R. J. W., Feldpausch, T. R., Lopez Gonzalez, G., Fauset, S., Quesada, C. A., Christoffersen, B., Ciais, P., Sampaio, G., Kruijt, B., Meir, P., Moorcroft, P., Zhang, K., Alvarez-Davila, E., Alves de Oliveira, A., Amaral, I., Andrade, A., Aragao, L. E. O. C., Araujo-Murakami, A., Arets, E. J. M. M., Arroyo, L., Aymard, G. A., Baraloto, C., Barroso, J., Bonal, D., Boot, R., Camargo, J., Chave, J., Cogollo, A., Cornejo Valverde, F., Lola da Costa, A. C., Di Fiore, A., Ferreira, L., Higuchi, N., Honorio, E. N., Killeen, T. J., Laurance, S. G., Laurance, W. F., Licona, J., Lovejoy, T., Malhi, Y., Marimon, B., Marimon, B. H., Matos, D. C. L., Mendoza, C., Neill, D. A., Pardo, G., Peña-Claros, M., Pitman, N. C. A., Poorter, L., Prieto, A., Ramirez-Angulo, H., Roopsind, A., Rudas, A., Salomao, R. P., Silveira, M., Stropp, J., ter Steege, H., Terborgh, J., Thomas, R., Toledo, M., Torres-Lezama, A., van der Heijden, G. M. F., Vasquez, R., Guimarães Vieira, I. C., Vilanova, E., Vos, V. A., and Baker, T. R.: Variation in stem mortality rates determines patterns of above-ground biomass in Amazonian forests: implications for dynamic global vegetation models, Glob Change Biol, 22, 3996–4013, https://doi.org/10.1111/gcb.13315, 2016.

Jones, H. G.: Plants and Microclimate: A Quantitative Approach to Environmental Plant Physiology, 3rd ed., Cambridge University Press, Cambridge, https://doi.org/10.1017/CBO9780511845727, 2013.

Jourdan, M., Kunstler, G., and Morin, X.: How neighbourhood interactions control the temporal stability and resilience to drought of trees in mountain forests, Journal of Ecology, 108, 666–677, https://doi.org/10.1111/1365-2745.13294, 2020.

Journé, V., Barnagaud, J.-Y., Bernard, C., Crochet, P.-A., and Morin, X.: Correlative climatic niche models predict real and virtual species distributions equally well, Ecology, 101, e02912, https://doi.org/10.1002/ecy.2912, 2020.

Jucker, T., Caspersen, J., Chave, J., Antin, C., Barbier, N., Bongers, F., Dalponte, M., van Ewijk, K. Y., Forrester, D. I., Haeni, M., Higgins, S. I., Holdaway, R. J., Iida, Y., Lorimer, C., Marshall, P. L., Momo, S., Moncrieff, G. R., Ploton, P., Poorter, L., Rahman, K. A., Schlund, M., Sonké, B., Sterck, F. J., Trugman, A. T., Usoltsev, V. A., Vanderwel, M. C., Waldner, P., Wedeux, B. M. M., Wirth, C., Wöll, H., Woods, M., Xiang, W., Zimmermann, N. E., and Coomes, D. A.: Allometric equations for integrating remote sensing imagery into forest monitoring programmes, Glob Change Biol, 23, 177–190, https://doi.org/10.1111/gcb.13388, 2017.

Jucker, T., Hardwick, S. R., Both, S., Elias, D. M. O., Ewers, R. M., Milodowski, D. T., Swinfield, T., and Coomes, D. A.: Canopy structure and topography jointly constrain the microclimate of human-modified tropical landscapes, Global Change Biology, 24, 5243–5258, https://doi.org/10.1111/gcb.14415, 2018.

Jucker, T., Fischer, F. J., Chave, J., Coomes, D. A., Caspersen, J., Ali, A., Loubota Panzou, G. J., Feldpausch, T. R., Falster, D., Usoltsev, V. A., Adu-Bredu, S., Alves, L. F., Aminpour, M., Angoboy, I. B., Anten, N. P. R., Antin, C., Askari, Y., Muñoz, R., Ayyappan, N., Balvanera, P., Banin, L., Barbier, N., Battles, J. J., Beeckman, H., Bocko, Y. E., Bond-Lamberty, B., Bongers, F., Bowers, S., Brade, T., van Breugel, M., Chantrain, A., Chaudhary, R., Dai, J., Dalponte, M., Dimobe, K., Domec, J.-C., Doucet, J.-L., Duursma, R. A., Enríquez, M., van Ewijk, K. Y., Farfán-Rios, W., Fayolle, A., Forni, E.,

Forrester, D. I., Gilani, H., Godlee, J. L., Gourlet-Fleury, S., Haeni, M., Hall, J. S., He, J.-K., Hemp, A., Hernández-Stefanoni, J. L., Higgins, S. I., Holdaway, R. J., Hussain, K., Hutley, L. B., Ichie, T., Iida, Y., Jiang, H., Joshi, P. R., Kaboli, H., Larsary, M. K., Kenzo, T., Kloeppel, B. D., Kohyama, T., Kunwar, S., Kuyah, S., Kvasnica, J., Lin, S., Lines, E. R., Liu, H., Lorimer, C., Loumeto, J.-J., Malhi, Y., Marshall, P. L., Mattsson, E., Matula, R., Meave, J. A., Mensah, S., Mi, X., Momo, S., Moncrieff, G. R., Mora, F., Nissanka, S. P., O'Hara, K. L., Pearce, S., Pelissier, R., Peri, P. L., Ploton, P., Poorter, L., Pour, M. J., Pourbabaei, H., Dupuy-Rada, J. M., Ribeiro, S. C., Ryan, C., Sanaei, A., Sanger, J., Schlund, M., Sellan, G., et al.: Tallo: A global tree allometry and crown architecture database, Global Change Biology, 28, 5254–5268, https://doi.org/10.1111/gcb.16302, 2022.

Kattge, J. and Knorr, W.: Temperature acclimation in a biochemical model of photosynthesis: a reanalysis of data from 36 species, Plant, Cell & Environment, 30, 1176–1190, https://doi.org/10.1111/j.1365-3040.2007.01690.x, 2007.

Kattge, J., Díaz, S., Lavorel, S., Prentice, I. C., Leadley, P., Bönisch, G., Garnier, E., Westoby, M., Reich, P. B., Wright, I. J., Cornelissen, J. H. C., Violle, C., Harrison, S. P., Van Bodegom, P. M., Reichstein, M., Enquist, B. J., Soudzilovskaia, N. A., Ackerly, D. D., Anand, M., Atkin, O., Bahn, M., Baker, T. R., Baldocchi, D., Bekker, R., Blanco, C. C., Blonder, B., Bond, W. J., Bradstock, R., Bunker, D. E., Casanoves, F., Cavender-bares, J., Chambers, J. Q., Chapin Iii, F. S., Chave, J., Coomes, D., Cornwell, W. K., Craine, J. M., Dobrin, B. H., Duarte, L., Durka, W., Elser, J., Esser, G., Estiarte, M., Fagan, W. F., Fang, J., Fernández-méndez, F., Fidelis, A., Finegan, B., Flores, O., Ford, H., Frank, D., Freschet, G. T., Fyllas, N. M., Gallagher, R. V., Green, W. A., Gutierrez, A. G., Hickler, T., Higgins, S. I., Hodgson, J. G., Jalili, A., Jansen, S., Joly, C. A., Kerkhoff, A. J., Kirkup, D., Kitajima, K., Kleyer, M., Klotz, S., Knops, J. M. H., Kramer, K., Kühn, I., Kurokawa, H., Laughlin, D., Lee, T. D., Leishman, M., Lens, F., Lenz, T., Lewis, S. L., Lloyd, J., Llusià, J., Louault, F., Ma, S., Mahecha, M. D., Manning, P., Massad, T., Medlyn, B. E., Messier, J., Moles, A. T., Müller, S. C., Nadrowski, K., Naeem, S., Niinemets, Ü., Nöllert, S., Nüske, A., Ogaya, R., Oleksyn, J., Onipchenko, V. G., Onoda, Y., Ordoñez, J., Overbeck, G., et al.: TRY – a global database of plant traits, Global Change Biology, 17, 2905–2935, https://doi.org/10.1111/j.1365-2486.2011.02451.x, 2011.

Kattge, J., Bönisch, G., Díaz, S., Lavorel, S., Prentice, I. C., Leadley, P., Tautenhahn, S., Werner, G. D. A., Aakala, T., Abedi, M., Acosta, A. T. R., Adamidis, G. C., Adamson, K., Aiba, M., Albert, C. H., Alcántara, J. M., C, C. A., Aleixo, I., Ali, H., Amiaud, B., Ammer, C., Amoroso, M. M., Anand, M., Anderson, C., Anten, N., Antos, J., Apgaua, D. M. G., Ashman, T.-L., Asmara, D. H., Asner, G. P., Aspinwall, M., Atkin, O., Aubin, I., Baastrup-Spohr, L., Bahalkeh, K., Bahn, M., Baker, T., Baker, W. J., Bakker, J. P., Baldocchi, D., Baltzer, J., Banerjee, A., Baranger, A., Barlow, J., Barneche, D. R., Baruch, Z., Bastianelli, D., Battles, J., Bauerle, W., Bauters, M., Bazzato, E., Beckmann, M., Beeckman, H., Beierkuhnlein, C., Bekker, R., Belfry, G., Belluau, M., Beloiu, M., Benavides, R., Benomar, L., Berdugo-Lattke, M. L., Berenguer, E., Bergamin, R., Bergmann, J., Carlucci, M. B., Berner, L., Bernhardt-Römermann, M., Bigler, C., Bjorkman, A. D., Blackman, C., Blanco, C., Blonder, B., Blumenthal, D., Bocanegra-González, K. T., Boeckx, P., Bohlman, S., Böhning-Gaese, K., Boisvert-Marsh, L., Bond, W., Bond-Lamberty, B., Boom, A., Boonman, C. C. F., Bordin, K., Boughton, E. H., Boukili, V., Bowman, D. M. J. S., Bravo, S., Brendel, M. R., Broadley, M. R., Brown, K. A., Bruelheide, H., Brumnich,

F., Bruun, H. H., Bruy, D., Buchanan, S. W., Bucher, S. F., Buchmann, N., Buitenwerf, R., Bunker, D. E., et al.: TRY plant trait database – enhanced coverage and open access, Global Change Biology, 26, 119–188, https://doi.org/10.1111/gcb.14904, 2020.

Kazmierczak, M., Wiegand, T., and Huth, A.: A neutral vs. non-neutral parametrizations of a physiological forest gap model, Ecological Modelling, 288, 94–102, https://doi.org/10.1016/j.ecolmodel.2014.05.002, 2014.

Kearney, M. and Porter, W.: Mechanistic niche modelling: combining physiological and spatial data to predict species' ranges, Ecology Letters, 12, 334–350, https://doi.org/10.1111/j.1461-0248.2008.01277.x, 2009.

Keenan, T., Sabate, S., and Gracia, C.: Soil water stress and coupled photosynthesis–conductance models: Bridging the gap between conflicting reports on the relative roles of stomatal, mesophyll conductance and biochemical limitations to photosynthesis, Agricultural and Forest Meteorology, 150, 443–453, https://doi.org/10.1016/j.agrformet.2010.01.008, 2010.

Kennedy, D., Swenson, S., Oleson, K. W., Lawrence, D. M., Fisher, R., Costa, A. C. L. da, and Gentine, P.: Implementing Plant Hydraulics in the Community Land Model, Version 5, Journal of Advances in Modeling Earth Systems, 11, 485–513, https://doi.org/10.1029/2018MS001500, 2019.

Kenzo, T., Ichie, T., Hattori, D., Itioka, T., Handa, C., Ohkubo, T., Kendawang, J. J., Nakamura, M., Sakaguchi, M., Takahashi, N., Okamoto, M., Tanaka-Oda, A., Sakurai, K., and Ninomiya, I.: Development of allometric relationships for accurate estimation of above- and below-ground biomass in tropical secondary forests in Sarawak, Malaysia, Journal of Tropical Ecology, 25, 371–386, https://doi.org/10.1017/S0266467409006129, 2009.

Khan, S., Maréchaux, I., Vieilledent, G., Guitet, S., Brunaux, O., Ferry, B., Soulard, F., Stahl, C., Baraloto, C., Fortunel, C., and Freycon, V.: Regional Soil Profile Data Reveals the Predominant Role of Geomorphology and Geology in Accurately Deriving Digital Soil Texture Maps in a Tropical Area, https://doi.org/10.2139/ssrn.4789279, 9 April 2024.

King, D. A., Davies, S. J., Tan, S., and Noor, N. S. Md.: The role of wood density and stem support costs in the growth and mortality of tropical trees, Journal of Ecology, 94, 670–680, https://doi.org/10.1111/j.1365-2745.2006.01112.x, 2006.

Kitajima, K., Mulkey, S., and Wright, S.: Decline of photosynthetic capacity with leaf age in relation to leaf longevities for five tropical canopy tree species., Am. J. Bot., 84, 702–702, 1997a.

Kitajima, K., Mulkey, S. S., and Wright, S. J.: Seasonal leaf phenotypes in the canopy of a tropical dry forest: photosynthetic characteristics and associated traits, Oecologia, 109, 490–498, https://doi.org/10.1007/s004420050109, 1997b.

Kitajima, K., Mulkey, S. S., Samaniego, M., and Wright, S. J.: Decline of photosynthetic capacity with leaf age and position in two tropical pioneer tree species, Am. J. Bot., 89, 1925–1932, https://doi.org/10.3732/ajb.89.12.1925, 2002.

Kitajima, K., Mulkey, S. S., and Wright, S. J.: Variation in crown light utilization characteristics among tropical canopy trees, Ann Bot, 95, 535–547, https://doi.org/10.1093/aob/mci051, 2005.

Koch, A., Hubau, W., and Lewis, S. L.: Earth System Models Are Not Capturing Present-Day Tropical Forest Carbon Dynamics, Earth's Future, 9, e2020EF001874, https://doi.org/10.1029/2020EF001874, 2021.

Köhler, P. and Huth, A.: The effects of tree species grouping in tropical rainforest modelling: simulations with the individual-based model Formind, Ecological Modelling, 109, 301–321, https://doi.org/10.1016/S0304-3800(98)00066-0, 1998.

Köhler, P., Ditzer, T., and Huth, A.: Concepts for the aggregation of tropical tree species into functional types and the application to Sabah's lowland rain forests, Journal of Tropical Ecology, 16, 591–602, https://doi.org/null, 2000.

König, L. A., Mohren, F., Schelhaas, M.-J., Bugmann, H., and Nabuurs, G.-J.: Tree regeneration in models of forest dynamics – Suitability to assess climate change impacts on European forests, Forest Ecology and Management, 520, 120390, https://doi.org/10.1016/j.foreco.2022.120390, 2022.

Körner, C.: Paradigm shift in plant growth control, Current Opinion in Plant Biology, 25, 107–114, https://doi.org/10.1016/j.pbi.2015.05.003, 2015.

Kraft, N. J. B., Metz, M. R., Condit, R. S., and Chave, J.: The relationship between wood density and mortality in a global tropical forest data set, New Phytologist, 188, 1124–1136, https://doi.org/10.1111/j.1469-8137.2010.03444.x, 2010.

Krinner, G., Viovy, N., de Noblet-Ducoudré, N., Ogée, J., Polcher, J., Friedlingstein, P., Ciais, P., Sitch, S., and Prentice, I. C.: A dynamic global vegetation model for studies of the coupled atmosphere-biosphere system, Global Biogeochem. Cycles, 19, GB1015, https://doi.org/10.1029/2003GB002199, 2005.

Kume, A., Nasahara, K. N., Nagai, S., and Muraoka, H.: The ratio of transmitted near-infrared radiation to photosynthetically active radiation (PAR) increases in proportion to the adsorbed PAR in the canopy, J Plant Res, 124, 99–106, https://doi.org/10.1007/s10265-010-0346-1, 2011.

Kupers, S. J., Engelbrecht, B. M. J., Hernández, A., Wright, S. J., Wirth, C., and Rüger, N.: Growth responses to soil water potential indirectly shape local species distributions of tropical forest seedlings, Journal of Ecology, 107, 860–874, https://doi.org/10.1111/1365-2745.13096, 2019.

Kursar, T. A., Engelbrecht, B. M. J., Burke, A., Tyree, M. T., EI Omari, B., and Giraldo, J. P.: Tolerance to low leaf water status of tropical tree seedlings is related to drought performance and distribution, Functional Ecology, 23, 93–102, https://doi.org/10.1111/j.1365-2435.2008.01483.x, 2009.

Lagarrigues, G., Jabot, F., Lafond, V., and Courbaud, B.: Approximate Bayesian computation to recalibrate individual-based models with population data: illustration with a forest simulation model, Ecological Modelling, 306, 278–286, https://doi.org/10.1016/j.ecolmodel.2014.09.023, 2015.

Laio, F., Porporato, A., Ridolfi, L., and Rodriguez-Iturbe, I.: Plants in water-controlled ecosystems: active role in hydrologic processes and response to water stress: II. Probabilistic soil moisture dynamics, Advances in Water Resources, 24, 707–723, https://doi.org/10.1016/S0309-1708(01)00005-7, 2001.

Lamour, J., Davidson, K. J., Ely, K. S., Le Moguédec, G., Leakey, A. D. B., Li, Q., Serbin, S. P., and Rogers, A.: An improved representation of the relationship between photosynthesis and stomatal conductance leads to more stable estimation of conductance parameters and improves the goodness-of-fit across diverse data sets, Global Change Biology, 28, 3537–3556, https://doi.org/10.1111/gcb.16103, 2022.

Lamour, J., Souza, D. C., Gimenez, B. O., Higuchi, N., Chave, J., Chambers, J., and Rogers, A.: Wood-density has no effect on stomatal control of leaf-level water use efficiency in an Amazonian forest, Plant, Cell & Environment, 46, 3806–3821, https://doi.org/10.1111/pce.14704, 2023.

Lapola, D. M., Pinho, P., Barlow, J., Aragão, L. E. O. C., Berenguer, E., Carmenta, R., Liddy, H. M., Seixas, H., Silva, C. V. J., Silva-Junior, C. H. L., Alencar, A. A. C., Anderson, L. O., Armenteras, D., Brovkin, V., Calders, K., Chambers, J., Chini, L., Costa, M. H., Faria, B. L., Fearnside, P. M., Ferreira, J., Gatti, L., Gutierrez-Velez, V. H., Han, Z., Hibbard, K., Koven, C., Lawrence, P., Pongratz, J., Portela, B. T. T., Rounsevell, M., Ruane, A. C., Schaldach, R., da Silva, S. S., von Randow, C., and Walker, W. S.: The drivers and impacts of Amazon forest degradation, Science, 379, eabp8622, https://doi.org/10.1126/science.abp8622, 2023.

Laurans, M., Munoz, F., Charles-Dominique, T., Heuret, P., Fortunel, C., Isnard, S., Sabatier, S.-A., Caraglio, Y., and Violle, C.: Why incorporate plant architecture into trait-based ecology?, Trends in Ecology & Evolution, 0, https://doi.org/10.1016/j.tree.2023.11.011, 2024.

LeBauer, D. S., Wang, D., Richter, K. T., Davidson, C. C., and Dietze, M. C.: Facilitating feedbacks between field measurements and ecosystem models, Ecological Monographs, 83, 133–154, https://doi.org/10.1890/12-0137.1, 2013.

Ledo, A., Paul, K. I., Burslem, D. F. R. P., Ewel, J. J., Barton, C., Battaglia, M., Brooksbank, K., Carter, J., Eid, T. H., England, J. R., Fitzgerald, A., Jonson, J., Mencuccini, M., Montagu, K. D., Montero, G., Mugasha, W. A., Pinkard, E., Roxburgh, S., Ryan, C. M., Ruiz-Peinado, R., Sochacki, S., Specht, A., Wildy, D., Wirth, C., Zerihun, A., and Chave, J.: Tree size and climatic water deficit control root to shoot ratio in individual trees globally, New Phytologist, 217, 8–11, https://doi.org/10.1111/nph.14863, 2018.

Leitold, V., Morton, D. C., Longo, M., dos-Santos, M. N., Keller, M., and Scaranello, M.: El Niño drought increased canopy turnover in Amazon forests, New Phytologist, 219, 959–971, https://doi.org/10.1111/nph.15110, 2018.

Lenz, T. I., Wright, I. J., and Westoby, M.: Interrelations among pressure–volume curve traits across species and water availability gradients, Physiologia Plantarum, 127, 423–433, https://doi.org/10.1111/j.1399-3054.2006.00680.x, 2006.

Leuning, R., Kelliher, F. M., Pury, D. G. G., and Schulze, E. -d: Leaf nitrogen, photosynthesis, conductance and transpiration: scaling from leaves to canopies, Plant, Cell & Environment, 18, 1183–1200, https://doi.org/10.1111/j.1365-3040.1995.tb00628.x, 1995.

Li, Q., Serbin, S. P., Lamour, J., Davidson, K. J., Ely, K. S., and Rogers, A.: Implementation and evaluation of the unified stomatal optimization approach in the Functionally Assembled Terrestrial Ecosystem Simulator (FATES), Geoscientific Model Development, 15, 4313–4329, https://doi.org/10.5194/gmd-15-4313-2022, 2022.

Liang, J. and Picard, N.: Matrix Model of Forest Dynamics: An Overview and Outlook, Forest Science, 59, 359–378, https://doi.org/10.5849/forsci.11-123, 2013.

Liang, X., Lettenmaier, D. P., Wood, E. F., and Burges, S. J.: A simple hydrologically based model of land surface water and energy fluxes for general circulation models, J. Geophys. Res., 99, 14415–14428, https://doi.org/10.1029/94JD00483, 1994.

Lin, Y.-S., Medlyn, B. E., Duursma, R. A., Prentice, I. C., Wang, H., Baig, S., Eamus, D., de Dios, V. R., Mitchell, P., Ellsworth, D. S., de Beeck, M. O., Wallin, G., Uddling, J., Tarvainen, L., Linderson, M.-L., Cernusak, L. A., Nippert, J. B., Ocheltree, T. W., Tissue, D. T., Martin-StPaul, N. K., Rogers, A., Warren, J. M., De Angelis, P., Hikosaka, K., Han, Q., Onoda, Y., Gimeno, T. E., Barton, C. V. M., Bennie, J., Bonal, D., Bosc, A., Löw, M., Macinins-Ng, C., Rey, A., Rowland, L., Setterfield, S. A., Tausz-Posch, S., Zaragoza-Castells, J., Broadmeadow, M. S. J., Drake, J. E., Freeman, M., Ghannoum, O., Hutley, L. B., Kelly, J. W., Kikuzawa, K., Kolari, P., Koyama, K., Limousin, J.-M., Meir, P., Lola da Costa, A. C., Mikkelsen, T. N., Salinas, N., Sun, W., and Wingate, L.: Optimal stomatal behaviour around the world, Nature Clim. Change, 5, 459–464, https://doi.org/10.1038/nclimate2550, 2015.

Liu, Y., Parolari, A. J., Kumar, M., Huang, C.-W., Katul, G. G., and Porporato, A.: Increasing atmospheric humidity and CO2 concentration alleviate forest mortality risk, PNAS, 114, 9918–9923, https://doi.org/10.1073/pnas.1704811114, 2017.

Long, S. P., Postl, W. F., and Bolhár-Nordenkampf, H. R.: Quantum yields for uptake of carbon dioxide in C3 vascular plants of contrasting habitats and taxonomic groupings, Planta, 189, 226–234, https://doi.org/10.1007/BF00195081, 1993.

Longo, M., Knox, R. G., Medvigy, D. M., Levine, N. M., Dietze, M. C., Kim, Y., Swann, A. L. S., Zhang, K., Rollinson, C. R., Bras, R. L., Wofsy, S. C., and Moorcroft, P. R.: The biophysics, ecology, and biogeochemistry of functionally diverse, vertically and horizontally heterogeneous ecosystems: the Ecosystem Demography model, version 2.2 – Part 1: Model description, Geoscientific Model Development, 12, 4309–4346, https://doi.org/10.5194/gmd-12-4309-2019, 2019.

Loubry, D.: La phénologie des arbres caducifoliés en forêt guyanaise (5° de latitude nord) : illustration d'un déterminisme à composantes endogène et exogène, Can. J. Bot., 72, 1843–1857, https://doi.org/10.1139/b94-226, 1994.

Maclean, I. M. D. and Klinges, D. H.: Microclimc: A mechanistic model of above, below and within-canopy microclimate, Ecological Modelling, 451, 109567, https://doi.org/10.1016/j.ecolmodel.2021.109567, 2021.

Mahnken, M., Cailleret, M., Collalti, A., Trotta, C., Biondo, C., D'Andrea, E., Dalmonech, D., Marano, G., Mäkelä, A., Minunno, F., Peltoniemi, M., Trotsiuk, V., Nadal-Sala, D., Sabaté, S., Vallet, P., Aussenac, R., Cameron, D. R., Bohn, F. J., Grote, R., Augustynczik, A. L. D., Yousefpour, R., Huber, N., Bugmann, H., Merganičová, K., Merganic, J., Valent, P., Lasch-Born, P., Hartig, F., Vega del Valle, I. D., Volkholz, J., Gutsch, M., Matteucci, G., Krejza, J., Ibrom, A., Meesenburg, H., Rötzer, T., van der Maaten-Theunissen, M., van der Maaten, E., and Reyer, C. P. O.: Accuracy, realism and general applicability of European forest models, Global Change Biology, 28, 6921–6943, https://doi.org/10.1111/gcb.16384, 2022.

Malhi, Y.: The productivity, metabolism and carbon cycle of tropical forest vegetation, Journal of Ecology, 100, 65–75, https://doi.org/10.1111/j.1365-2745.2011.01916.x, 2012.

Malhi, Y., Doughty, C., and Galbraith, D.: The allocation of ecosystem net primary productivity in tropical forests, Philosophical Transactions of the Royal Society of London B: Biological Sciences, 366, 3225–3245, https://doi.org/10.1098/rstb.2011.0062, 2011.

Manabe, S.: Climate and the ocean circulation: I. The atmospheric circulation and the hydrology of the earth's surface, Mon. Wea. Rev., 97, 739–774, https://doi.org/10.1175/1520-0493(1969)097<0739:CATOC>2.3.CO;2, 1969.

Manoli, G., Ivanov, V. Y., and Fatichi, S.: Dry-Season Greening and Water Stress in Amazonia: The Role of Modeling Leaf Phenology, Journal of Geophysical Research: Biogeosciences, 123, 1909–1926, https://doi.org/10.1029/2017JG004282, 2018.

Manzoni, S.: Integrating plant hydraulics and gas exchange along the drought-response trait spectrum, Tree Physiol, tpu088, https://doi.org/10.1093/treephys/tpu088, 2014.

Maréchaux, I. and Chave, J.: An individual-based forest model to jointly simulate carbon and tree diversity in Amazonia: description and applications, Ecol Monogr, 87, 632–664, https://doi.org/10.1002/ecm.1271, 2017.

Maréchaux, I., Bartlett, M. K., Sack, L., Baraloto, C., Engel, J., Joetzjer, E., and Chave, J.: Drought tolerance as predicted by leaf water potential at turgor loss point varies strongly across species within an Amazonian forest, Funct Ecol, 29, 1268–1277, https://doi.org/10.1111/1365-2435.12452, 2015.

Maréchaux, I., Bartlett, M. K., Gaucher, P., Sack, L., and Chave, J.: Causes of variation in leaf-level drought tolerance within an Amazonian forest, Journal of Plant Hydraulics, 3, e004, 2016.

Maréchaux, I., Bonal, D., Bartlett, M. K., Burban, B., Coste, S., Courtois, E. A., Dulormne, M., Goret, J.-Y., Mira, E., Mirabel, A., Sack, L., Stahl, C., and Chave, J.: Dry-season decline in tree sapflux is correlated with leaf turgor loss point in a tropical rainforest, Functional Ecology, 32, 2285–2297, https://doi.org/10.1111/1365-2435.13188, 2018.

Maréchaux, I., Saint-André, L., Bartlett, M. K., Sack, L., and Chave, J.: Leaf drought tolerance cannot be inferred from classic leaf traits in a tropical rainforest, Journal of Ecology, 108, 1030–1045, https://doi.org/10.1111/1365-2745.13321, 2020.

Maréchaux, I., Langerwisch, F., Huth, A., Bugmann, H., Morin, X., Reyer, C. P. O., Seidl, R., Collalti, A., Paula, M. D. de, Fischer, R., Gutsch, M., Lexer, M. J., Lischke, H., Rammig, A., Rödig, E., Sakschewski, B., Taubert, F., Thonicke, K., Vacchiano, G., and Bohn, F. J.: Tackling unresolved questions in forest ecology: The past and future role of simulation models, Ecology and Evolution, 11, 3746–3770, https://doi.org/10.1002/ece3.7391, 2021.

Marthews, T. R., Malhi, Y., and Iwata, H.: Calculating downward longwave radiation under clear and cloudy conditions over a tropical lowland forest site: an evaluation of model schemes for hourly data, Theor Appl Climatol, 107, 461–477, https://doi.org/10.1007/s00704-011-0486-9, 2012.

Marthews, T. R., Quesada, C. A., Galbraith, D. R., Malhi, Y., Mullins, C. E., Hodnett, M. G., and Dharssi, I.: High-resolution hydraulic parameter maps for surface soils in tropical South America, Geoscientific Model Development, 7, 711, 2014.

Martínez-Vilalta, J., Sala, A., Asensio, D., Galiano, L., Hoch, G., Palacio, S., Piper, F. I., and Lloret, F.: Dynamics of non-structural carbohydrates in terrestrial plants: a global synthesis, Ecol Monogr, 86, 495–516, https://doi.org/10.1002/ecm.1231, 2016.

Martin-StPaul, N., Delzon, S., and Cochard, H.: Plant resistance to drought depends on timely stomatal closure, Ecol Lett, 20, 1437–1447, https://doi.org/10.1111/ele.12851, 2017.

McDowell, N. G., Sapes, G., Pivovaroff, A., Adams, H. D., Allen, C. D., Anderegg, W. R. L., Arend, M., Breshears, D. D., Brodribb, T., Choat, B., Cochard, H., De Cáceres, M., De Kauwe, M. G., Grossiord, C., Hammond, W. M., Hartmann, H., Hoch, G., Kahmen, A., Klein, T., Mackay, D. S., Mantova, M., Martínez-Vilalta, J., Medlyn, B. E., Mencuccini, M.,

Nardini, A., Oliveira, R. S., Sala, A., Tissue, D. T., Torres-Ruiz, J. M., Trowbridge, A. M., Trugman, A. T., Wiley, E., and Xu, C.: Mechanisms of woody-plant mortality under rising drought, CO2 and vapour pressure deficit, Nat Rev Earth Environ, 1–15, https://doi.org/10.1038/s43017-022-00272-1, 2022.

McMahon, S. M., Harrison, S. P., Armbruster, W. S., Bartlein, P. J., Beale, C. M., Edwards, M. E., Kattge, J., Midgley, G., Morin, X., and Prentice, I. C.: Improving assessment and modelling of climate change impacts on global terrestrial biodiversity, Trends in Ecology & Evolution, 26, 249–259, https://doi.org/10.1016/j.tree.2011.02.012, 2011.

Medlyn, B. E., Robinson, A. P., Clement, R., and McMurtrie, R. E.: On the validation of models of forest CO2 exchange using eddy covariance data: some perils and pitfalls, Tree Physiol, 25, 839–857, https://doi.org/10.1093/treephys/25.7.839, 2005.

Medlyn, B. E., Pepper, D. A., O'Grady, A. P., and Keith, H.: Linking leaf and tree water use with an individual-tree model, Tree Physiol, 27, 1687–1699, https://doi.org/10.1093/treephys/27.12.1687, 2007.

Medlyn, B. E., Duursma, R. A., Eamus, D., Ellsworth, D. S., Prentice, I. C., Barton, C. V. M., Crous, K. Y., De Angelis, P., Freeman, M., and Wingate, L.: Reconciling the optimal and empirical approaches to modelling stomatal conductance, Global Change Biology, 17, 2134–2144, https://doi.org/10.1111/j.1365-2486.2010.02375.x, 2011.

Medlyn, B. E., Zaehle, S., De Kauwe, M. G., Walker, A. P., Dietze, M. C., Hanson, P. J., Hickler, T., Jain, A. K., Luo, Y., Parton, W., Prentice, I. C., Thornton, P. E., Wang, S., Wang, Y.-P., Weng, E., Iversen, C. M., McCarthy, H. R., Warren, J. M., Oren, R., and Norby, R. J.: Using ecosystem experiments to improve vegetation models, Nature Clim. Change, 5, 528–534, https://doi.org/10.1038/nclimate2621, 2015.

Medlyn, B. E., De Kauwe, M. G., Zaehle, S., Walker, A. P., Duursma, R. A., Luus, K., Mishurov, M., Pak, B., Smith, B., Wang, Y.-P., Yang, X., Crous, K. Y., Drake, J. E., Gimeno, T. E., Macdonald, C. A., Norby, R. J., Power, S. A., Tjoelker, M. G., and Ellsworth, D. S.: Using models to guide field experiments: a priori predictions for the CO2 response of a nutrient- and water-limited native Eucalypt woodland, Glob Change Biol, 22, 2834–2851, https://doi.org/10.1111/gcb.13268, 2016.

van der Meer, P. J. and Bongers, F.: Patterns of tree-fall and branch-fall in a tropical rain forest in French Guiana, Journal of Ecology, 84, 19–29, https://doi.org/10.2307/2261696, 1996.

Meinzer, F. C., Andrade, J. L., Goldstein, G., Holbrook, N. M., Cavelier, J., and Jackson, P.: Control of transpiration from the upper canopy of a tropical forest: the role of stomatal, boundary layer and hydraulic architecture components, Plant, Cell & Environment, 20, 1242–1252, https://doi.org/10.1046/j.1365-3040.1997.d01-26.x, 1997.

Meinzer, F. C., Woodruff, D. R., Marias, D. E., Smith, D. D., McCulloh, K. A., Howard, A. R., and Magedman, A. L.: Mapping 'hydroscapes' along the iso- to anisohydric continuum of stomatal regulation of plant water status, Ecol Lett, 19, 1343–1352, https://doi.org/10.1111/ele.12670, 2016.

Meir, P. and Grace, J.: Scaling relationships for woody tissue respiration in two tropical rain forests, Plant, Cell & Environment, 25, 963–973, https://doi.org/10.1046/j.1365-3040.2002.00877.x, 2002.

Meir, P., Grace, J., and Miranda, A. C.: Leaf respiration in two tropical rainforests: constraints on physiology by phosphorus, nitrogen and temperature, Functional Ecology, 15, 378–387, https://doi.org/10.1046/j.1365-2435.2001.00534.x, 2001.

Meir, P., Cox, P., and Grace, J.: The influence of terrestrial ecosystems on climate, Trends in Ecology & Evolution, 21, 254–260, https://doi.org/10.1016/j.tree.2006.03.005, 2006.

Mencuccini, M., Martínez-Vilalta, J., Vanderklein, D., Hamid, H. A., Korakaki, E., Lee, S., and Michiels, B.: Size-mediated ageing reduces vigour in trees, Ecology Letters, 8, 1183–1190, https://doi.org/10.1111/j.1461-0248.2005.00819.x, 2005.

Menezes, J., Garcia, S., Grandis, A., Nascimento, H., Domingues, T. F., Guedes, A. V., Aleixo, I., Camargo, P., Campos, J., Damasceno, A., Dias-Silva, R., Fleischer, K., Kruijt, B., Cordeiro, A. L., Martins, N. P., Meir, P., Norby, R. J., Pereira, I., Portela, B., Rammig, A., Ribeiro, A. G., Lapola, D. M., and Quesada, C. A.: Changes in leaf functional traits with leaf age: when do leaves decrease their photosynthetic capacity in Amazonian trees?, Tree Physiology, tpab042, https://doi.org/10.1093/treephys/tpab042, 2021.

Mercado, L. M., Lloyd, J., Dolman, A. J., Sitch, S., and Patiño, S.: Modelling basin-wide variations in Amazon forest productivity – Part 1: model calibration, evaluation and upscaling functions for canopy photosynthesis, Biogeosciences, 6, 1247–1272, https://doi.org/10.5194/bg-6-1247-2009, 2009.

Mercado, L. M., Patiño, S., Domingues, T. F., Fyllas, N. M., Weedon, G. P., Sitch, S., Quesada, C. A., Phillips, O. L., Aragão, L. E. O. C., Malhi, Y., Dolman, A. J., Restrepo-Coupe, N., Saleska, S. R., Baker, T. R., Almeida, S., Higuchi, N., and Lloyd, J.: Variations in Amazon forest productivity correlated with foliar nutrients and modelled rates of photosynthetic carbon supply, Phil. Trans. R. Soc. B, 366, 3316–3329, https://doi.org/10.1098/rstb.2011.0045, 2011.

Merganičová, K., Merganič, J., Lehtonen, A., Vacchiano, G., Zorana, M., Ostrogović, S., Augustynczik, A. L. D., Grote, R., Kyselová, I., Mäkelä, A., Yousefpour, R., Krejza, J., Collalti, A., and Reyer, C.: Forest carbon allocation modelling under climate change, Tree Physiology, https://doi.org/10.1093/treephys/tpz105, 2019.

Merlin, O., Stefan, V. G., Amazirh, A., Chanzy, A., Ceschia, E., Er-Raki, S., Gentine, P., Tallec, T., Ezzahar, J., Bircher, S., Beringer, J., and Khabba, S.: Modeling soil evaporation efficiency in a range of soil and atmospheric conditions using a meta-analysis approach, Water Resources Research, 52, 3663–3684, https://doi.org/10.1002/2015WR018233, 2016.

Metcalfe, D. B., Meir, P., Aragão, L. E. O. C., Costa, A. C. L. da, Braga, A. P., Gonçalves, P. H. L., Junior, J. de A. S., Almeida, S. S. de, Dawson, L. A., Malhi, Y., and Williams, M.: The effects of water availability on root growth and morphology in an Amazon rainforest, Plant and Soil, 311, 189–199, https://doi.org/10.1007/s11104-008-9670-9, 2008.

Mokany, K., Ferrier, S., Connolly, S. R., Dunstan, P. K., Fulton, E. A., Harfoot, M. B., Harwood, T. D., Richardson, A. J., Roxburgh, S. H., Scharlemann, J. P. W., Tittensor, D. P., Westcott, D. A., and Wintle, B. A.: Integrating modelling of biodiversity composition and ecosystem function, Oikos, 125, 10–19, https://doi.org/10.1111/oik.02792, 2016.

Moles, A. T. and Westoby, M.: Seed size and plant strategy across the whole life cycle, Oikos, 113, 91–105, https://doi.org/10.1111/j.0030-1299.2006.14194.x, 2006.

Moles, A. T., Falster, D. S., Leishman, M. R., and Westoby, M.: Small-seeded species produce more seeds per square metre of canopy per year, but not per individual per lifetime, Journal of Ecology, 92, 384–396, https://doi.org/10.1111/j.0022-0477.2004.00880.x, 2004.

Moorcroft, P. R.: Recent advances in ecosystem-atmosphere interactions: an ecological perspective, Proceedings of the Royal Society of London B: Biological Sciences, 270, 1215–1227, https://doi.org/10.1098/rspb.2002.2251, 2003.

Moorcroft, P. R.: How close are we to a predictive science of the biosphere?, Trends in Ecology & Evolution, 21, 400–407, https://doi.org/10.1016/j.tree.2006.04.009, 2006.

Moorcroft, P. R., Hurtt, G. C., and Pacala, S. W.: A method for scaling vegetation dynamics: the ecosystem demography model (ed), Ecological Monographs, 71, 557–586, https://doi.org/10.1890/0012-9615(2001)071[0557:AMFSVD]2.0.CO;2, 2001.

Morin, X. and Lechowicz, M. J.: Contemporary perspectives on the niche that can improve models of species range shifts under climate change, Biology Letters, 4, 573–576, https://doi.org/10.1098/rsbl.2008.0181, 2008.

Morin, X. and Thuiller, W.: Comparing niche-and process-based models to reduce prediction uncertainty in species range shifts under climate change, Ecology, 90, 1301–1313, 2009.

Mualem, Y.: A new model for predicting the hydraulic conductivity of unsaturated porous media, Water Resources Research, 12, 513–522, https://doi.org/10.1029/WR012i003p00513, 1976.

Muir, C. D.: Making pore choices: repeated regime shifts in stomatal ratio, Proceedings of the Royal Society B: Biological Sciences, 282, 20151498, https://doi.org/10.1098/rspb.2015.1498, 2015.

Muller, B., Pantin, F., Génard, M., Turc, O., Freixes, S., Piques, M., and Gibon, Y.: Water deficits uncouple growth from photosynthesis, increase C content, and modify the relationships between C and growth in sink organs, J. Exp. Bot., erq438, https://doi.org/10.1093/jxb/erq438, 2011.

Muller-Landau, H. C., Wright, S. J., Calderón, O., Condit, R., and Hubbell, S. P.: Interspecific variation in primary seed dispersal in a tropical forest, Journal of Ecology, 96, 653–667, https://doi.org/10.1111/j.1365-2745.2008.01399.x, 2008.

Muñoz-Sabater, J., Dutra, E., Agustí-Panareda, A., Albergel, C., Arduini, G., Balsamo, G., Boussetta, S., Choulga, M., Harrigan, S., Hersbach, H., Martens, B., Miralles, D. G., Piles, M., Rodríguez-Fernández, N. J., Zsoter, E., Buontempo, C., and Thépaut, J.-N.: ERA5-Land: a state-of-the-art global reanalysis dataset for land applications, Earth System Science Data, 13, 4349–4383, https://doi.org/10.5194/essd-13-4349-2021, 2021.

Naudts, K., Ryder, J., McGrath, M. J., Otto, J., Chen, Y., Valade, A., Bellasen, V., Berhongaray, G., Bönisch, G., Campioli, M., Ghattas, J., De Groote, T., Haverd, V., Kattge, J., MacBean, N., Maignan, F., Merilä, P., Penuelas, J., Peylin, P., Pinty, B., Pretzsch, H., Schulze, E. D., Solyga, D., Vuichard, N., Yan, Y., and Luyssaert, S.: A vertically discretised canopy description for ORCHIDEE (SVN r2290) and the modifications to the energy, water and carbon fluxes, Geosci. Model Dev., 8, 2035–2065, https://doi.org/10.5194/gmd-8-2035-2015, 2015.

Nemetschek, D., Derroire, G., Marcon, E., Aubry-Kientz, M., Auer, J., Badouard, V., Baraloto, C., Bauman, D., Le Blaye, Q., Boisseaux, M., Bonal, D., Coste, S., Dardevet, E., Heuret, P., Hietz, P., Levionnois, S., Maréchaux, I., McMahon, S. M., Stahl, C., Vleminckx, J., Wanek, W., Ziegler, C., and Fortunel, C.: Climate anomalies and neighbourhood crowding interact in shaping tree growth in old-growth and selectively logged tropical forests, Journal of Ecology, 112, 590–612, https://doi.org/10.1111/1365-2745.14256, 2024.

Nemetschek, D., Fortunel, C., Marcon, E., Auer, J., Badouard, V., Baraloto, C., Boisseaux, M., Bonal, D., Coste, S., Dardevette, E., Heuret, P., Hietz, P., Levionnois, S., Maréchaux, I., Stahl, C., Vleminckx, J., Wanek, W., Ziegler, C., and Derroire, G.: Love thy neighbour? Tropical tree growth and its response to climate anomalies is mediated by neighbourhood hierarchy and dissimilarity in carbon and water related traits., https://doi.org/10.22541/au.171366417.71658960/v1, 21 April 2024.

Nepstad, D. C., de Carvalho, C. R., Davidson, E. A., Jipp, P. H., Lefebvre, P. A., Negreiros, G. H., da Silva, E. D., Stone, T. A., Trumbore, S. E., and Vieira, S.: The role of deep roots in the hydrological and carbon cycles of Amazonian forests and pastures, Nature, 372, 666–669, https://doi.org/10.1038/372666a0, 1994.

Newman, E. I.: Resistance to Water Flow in Soil and Plant. I. Soil Resistance in Relation to Amounts of Root: Theoretical Estimates, Journal of Applied Ecology, 6, 1–12, https://doi.org/10.2307/2401297, 1969.

Nicolini, E., Beauchêne, J., de la Vallée, B. L., Ruelle, J., Mangenet, T., and Heuret, P.: Dating branch growth units in a tropical tree using morphological and anatomical markers: the case of Parkia velutina Benoist (Mimosoïdeae), Annals of Forest Science, 69, 543–555, https://doi.org/10.1007/s13595-011-0172-1, 2012.

Norby, R. J., De Kauwe, M. G., Domingues, T. F., Duursma, R. A., Ellsworth, D. S., Goll, D. S., Lapola, D. M., Luus, K. A., MacKenzie, A. R., Medlyn, B. E., Pavlick, R., Rammig, A., Smith, B., Thomas, R., Thonicke, K., Walker, A. P., Yang, X., and Zaehle, S.: Model–data synthesis for the next generation of forest free-air CO2 enrichment (FACE) experiments, New Phytol, 209, 17–28, https://doi.org/10.1111/nph.13593, 2016.

Norden, N., Chave, J., Belbenoit, P., Caubère, A., Châtelet, P., Forget, P.-M., and Thébaud, C.: Mast fruiting is a frequent strategy in woody species of eastern South America, PLOS ONE, 2, e1079, https://doi.org/10.1371/journal.pone.0001079, 2007.

Novick, K. A., Ficklin, D. L., Stoy, P. C., Williams, C. A., Bohrer, G., Oishi, A. C., Papuga, S. A., Blanken, P. D., Noormets, A., Sulman, B. N., Scott, R. L., Wang, L., and Phillips, R. P.: The increasing importance of atmospheric demand for ecosystem water and carbon fluxes, Nature Climate Change, 6, 1023–1027, https://doi.org/10.1038/nclimate3114, 2016.

Novick, K. A., Ficklin, D. L., Baldocchi, D., Davis, K. J., Ghezzehei, T. A., Konings, A. G., MacBean, N., Raoult, N., Scott, R. L., Shi, Y., Sulman, B. N., and Wood, J. D.: Confronting the water potential information gap, Nat. Geosci., 15, 158–164, https://doi.org/10.1038/s41561-022-00909-2, 2022.

Nunes, M. H., Camargo, J. L. C., Vincent, G., Calders, K., Oliveira, R. S., Huete, A., Mendes de Moura, Y., Nelson, B., Smith, M. N., Stark, S. C., and Maeda, E. E.: Forest fragmentation impacts the seasonality of Amazonian evergreen canopies, Nat Commun, 13, 917, https://doi.org/10.1038/s41467-022-28490-7, 2022.

Ogée, J., Brunet, Y., Loustau, D., Berbigier, P., and Delzon, S.: MuSICA, a CO2, water and energy multilayer, multileaf pine forest model: evaluation from hourly to yearly time scales and sensitivity analysis, Global Change Biology, 9, 697–717, https://doi.org/10.1046/j.1365-2486.2003.00628.x, 2003.

Oleson, K. W., Niu, G.-Y., Yang, Z.-L., Lawrence, D. M., Thornton, P. E., Lawrence, P. J., Stöckli, R., Dickinson, R. E., Bonan, G. B., Levis, S., Dai, A., and Qian, T.: Improvements to the Community Land Model and their impact on the hydrological cycle, J. Geophys. Res., 113, G01021, https://doi.org/10.1029/2007JG000563, 2008.

Oliveira, R. S., Dawson, T. E., Burgess, S. S. O., and Nepstad, D. C.: Hydraulic redistribution in three Amazonian trees, Oecologia, 145, 354–363, https://doi.org/10.1007/s00442-005-0108-2, 2005.

d'Orgeval, T., Polcher, J., and de Rosnay, P.: Sensitivity of the West African hydrological cycle in ORCHIDEE to infiltration processes, Hydrol. Earth Syst. Sci., 12, 1387–1401, https://doi.org/10.5194/hess-12-1387-2008, 2008.

Pacala, S. W. and Rees, M.: Models Suggesting Field Experiments to Test Two Hypotheses Explaining Successional Diversity, The American Naturalist, 152, 729–737, https://doi.org/10.1086/286203, 1998.

Paine, C. E. T., Deasey, A., and Duthie, A. B.: Towards the general mechanistic prediction of community dynamics, Functional Ecology, 32, 1681–1692, https://doi.org/10.1111/1365-2435.13096, 2018.

Pan, Y., Birdsey, R. A., Fang, J., Houghton, R., Kauppi, P. E., Kurz, W. A., Phillips, O. L., Shvidenko, A., Lewis, S. L., Canadell, J. G., Ciais, P., Jackson, R. B., Pacala, S. W., McGuire, A. D., Piao, S., Rautiainen, A., Sitch, S., and Hayes, D.: A Large and Persistent Carbon Sink in the World's Forests, Science, 333, 988–993, https://doi.org/10.1126/science.1201609, 2011.

Pantin, F., Simonneau, T., and Muller, B.: Coming of leaf age: control of growth by hydraulics and metabolics during leaf ontogeny, New Phytologist, 196, 349–366, https://doi.org/10.1111/j.1469-8137.2012.04273.x, 2012.

Paschalis, A., Fatichi, S., Zscheischler, J., Ciais, P., Bahn, M., Boysen, L., Chang, J., De Kauwe, M., Estiarte, M., Goll, D., Hanson, P. J., Harper, A. B., Hou, E., Kigel, J., Knapp, A. K., Larsen, K. S., Li, W., Lienert, S., Luo, Y., Meir, P., Nabel, J. E. M. S., Ogaya, R., Parolari, A. J., Peng, C., Peñuelas, J., Pongratz, J., Rambal, S., Schmidt, I. K., Shi, H., Sternberg, M., Tian, H., Tschumi, E., Ukkola, A., Vicca, S., Viovy, N., Wang, Y.-P., Wang, Z., Williams, K., Wu, D., and Zhu, Q.: Rainfall manipulation experiments as simulated by terrestrial biosphere models: Where do we stand?, Global Change Biology, 26, 3336–3355, https://doi.org/10.1111/gcb.15024, 2020.

Paschalis, A., De Kauwe, M. G., Sabot, M., and Fatichi, S.: When do plant hydraulics matter in terrestrial biosphere modelling?, Global Change Biology, 30, e17022, https://doi.org/10.1111/gcb.17022, 2024.

Pavlick, R., Drewry, D. T., Bohn, K., Reu, B., and Kleidon, A.: The Jena Diversity-Dynamic Global Vegetation Model (JeDi-DGVM): a diverse approach to representing terrestrial biogeography and biogeochemistry based on plant functional trade-offs, Biogeosciences, 10, 4137–4177, https://doi.org/10.5194/bg-10-4137-2013, 2013.

Peters, R. L., Kaewmano, A., Fu, P.-L., Fan, Z.-X., Sterck, F., Steppe, K., and Zuidema, P. A.: High vapour pressure deficit enhances turgor limitation of stem growth in an Asian tropical rainforest tree, Plant, Cell & Environment, 46, 2747–2762, https://doi.org/10.1111/pce.14661, 2023.

Picard, N. and Franc, A.: Are ecological groups of species optimal for forest dynamics modelling?, Ecological Modelling, 163, 175–186, https://doi.org/10.1016/S0304-3800(03)00010-3, 2003.

Picard, N., Köhler, P., Mortier, F., and Gourlet-Fleury, S.: A comparison of five classifications of species into functional groups in tropical forests of French Guiana, Ecological Complexity, 11, 75–83, https://doi.org/10.1016/j.ecocom.2012.03.003, 2012.

Pitman, A. J.: The evolution of, and revolution in, land surface schemes designed for climate models, Int. J. Climatol., 23, 479–510, https://doi.org/10.1002/joc.893, 2003.

Poggio, L., de Sousa, L. M., Batjes, N. H., Heuvelink, G. B. M., Kempen, B., Ribeiro, E., and Rossiter, D.: SoilGrids 2.0: producing soil information for the globe with quantified spatial uncertainty, SOIL, 7, 217–240, https://doi.org/10.5194/soil-7-217-2021, 2021.

Poorter, L., Bongers, L., and Bongers, F.: Architecture of 54 moist-forest tree species: traits, trade-offs, and functional groups, Ecology, 87, 1289–1301, https://doi.org/10.1890/0012-9658(2006)87[1289:AOMTST]2.0.CO;2, 2006.

Poorter, L., Wright, S. J., Paz, H., Ackerly, D. D., Condit, R., Ibarra-Manríquez, G., Harms, K. E., Licona, J. C., Martínez-Ramos, M., Mazer, S. J., Muller-Landau, H. C., Peña-Claros, M., Webb, C. O., and Wright, I. J.: Are functional traits good predictors of demographic rates? Evidence from five Neotropical forests, Ecology, 89, 1908–1920, https://doi.org/10.1890/07-0207.1, 2008.

Poorter, L., Oberbauer, S. F., and Clark, D. B.: Leaf optical properties along a vertical gradient in a tropical rain forest canopy in Costa Rica, American Journal of Botany, 82, 1257–1263, https://doi.org/10.2307/2446248, 1995.

Poorter, L., van der Sande, M. T., Thompson, J., Arets, E. J. M. M., Alarcón, A., Álvarez-Sánchez, J., Ascarrunz, N., Balvanera, P., Barajas-Guzmán, G., Boit, A., Bongers, F., Carvalho, F. A., Casanoves, F., Cornejo-Tenorio, G., Costa, F. R. C., de Castilho, C. V., Duivenvoorden, J. F., Dutrieux, L. P., Enquist, B. J., Fernández-Méndez, F., Finegan, B., Gormley, L. H. L., Healey, J. R., Hoosbeek, M. R., Ibarra-Manríquez, G., Junqueira, A. B., Levis, C., Licona, J. C., Lisboa, L. S., Magnusson, W. E., Martínez-Ramos, M., Martínez-Yrizar, A., Martorano, L. G., Maskell, L. C., Mazzei, L., Meave, J. A., Mora, F., Muñoz, R., Nytch, C., Pansonato, M. P., Parr, T. W., Paz, H., Pérez-García, E. A., Rentería, L. Y., Rodríguez-Velazquez, J., Rozendaal, D. M. A., Ruschel, A. R., Sakschewski, B., Salgado-Negret, B., Schietti, J., Simões, M., Sinclair, F. L., Souza, P. F., Souza, F. C., Stropp, J., ter Steege, H., Swenson, N. G., Thonicke, K., Toledo, M., Uriarte, M., van der Hout, P., Walker, P., Zamora, N., and Peña-Claros, M.: Diversity enhances carbon storage in tropical forests, Global Ecology and Biogeography, 24, 1314–1328, https://doi.org/10.1111/geb.12364, 2015.

Poorter, L., Amissah, L., Bongers, F., Hordijk, I., Kok, J., Laurance, S. G. W., Lohbeck, M., Martínez-Ramos, M., Matsuo, T., Meave, J. A., Muñoz, R., Peña-Claros, M., and van der Sande, M. T.: Successional theories, Biological Reviews, 98, 2049–2077, https://doi.org/10.1111/brv.12995, 2023.

Porté, A. and Bartelink, H. H.: Modelling mixed forest growth: a review of models for forest management, Ecological Modelling, 150, 141–188, https://doi.org/10.1016/S0304-3800(01)00476-8, 2002.

Poulter, B., Ciais, P., Hodson, E., Lischke, H., Maignan, F., Plummer, S., and Zimmermann, N. E.: Plant functional type mapping for earth system models, Geosci. Model Dev., 4, 993–1010, https://doi.org/10.5194/gmd-4-993-2011, 2011.

Powell, T. L., Galbraith, D. R., Christoffersen, B. O., Harper, A., Imbuzeiro, H. M. A., Rowland, L., Almeida, S., Brando, P. M., da Costa, A. C. L., Costa, M. H., Levine, N. M., Malhi, Y., Saleska, S. R., Sotta, E., Williams, M., Meir, P., and Moorcroft, P. R.: Confronting model predictions of carbon fluxes with measurements of Amazon forests subjected to experimental drought, New Phytologist, 200, 350–365, https://doi.org/10.1111/nph.12390, 2013.

Powell, T. L., Wheeler, J. K., Oliveira, A. A. R. de, Costa, A. C. L. da, Saleska, S. R., Meir, P., and Moorcroft, P. R.: Differences in xylem and leaf hydraulic traits explain differences in drought tolerance among mature Amazon rainforest trees, Global Change Biology, 23, 4280–4293, https://doi.org/10.1111/gcb.13731, 2017.

Prentice, I. C., Bondeau, A., Cramer, W., Harrison, S. P., Hickler, T., Lucht, W., Sitch, S., Smith, B., and Sykes, M. T.: Dynamic Global Vegetation Modeling: Quantifying Terrestrial Ecosystem Responses to Large-Scale Environmental Change, in: Terrestrial ecosystems in a changing world, edited by: Canadell, J. G., Pataki, D. E., and Pitelka, L. F., Springer Berlin Heidelberg, 175–192, 2007.

Prentice, I. C., Liang, X., Medlyn, B. E., and Wang, Y.-P.: Reliable, robust and realistic: the three R's of next-generation land-surface modelling, Atmos. Chem. Phys., 15, 5987–6005, https://doi.org/10.5194/acp-15-5987-2015, 2015.

Purves, D. and Pacala, S.: Predictive models of forest dynamics, Science, 320, 1452–1453, https://doi.org/10.1126/science.1155359, 2008.

Qie, L., Lewis, S. L., Sullivan, M. J. P., Lopez-Gonzalez, G., Pickavance, G. C., Sunderland, T., Ashton, P., Hubau, W., Salim, K. A., Aiba, S.-I., Banin, L. F., Berry, N., Brearley, F. Q., Burslem, D. F. R. P., Dančák, M., Davies, S. J., Fredriksson, G., Hamer, K. C., Hédl, R., Kho, L. K., Kitayama, K., Krisnawati, H., Lhota, S., Malhi, Y., Maycock, C., Metali, F., Mirmanto, E., Nagy, L., Nilus, R., Ong, R., Pendry, C. A., Poulsen, A. D., Primack, R. B., Rutishauser, E., Samsoedin, I., Saragih, B., Sist, P., Slik, J. W. F., Sukri, R. S., Svátek, M., Tan, S., Tjoa, A., Nieuwstadt, M. van, Vernimmen, R. R. E., Yassir, I., Kidd, P. S., Fitriadi, M., Ideris, N. K. H., Serudin, R. M., Lim, L. S. A., Saparudin, M. S., and Phillips, O. L.: Long-term carbon sink in Borneo's forests halted by drought and vulnerable to edge effects, Nature Communications, 8, 1966, https://doi.org/10.1038/s41467-017-01997-0, 2017.

Rau, E.-P., Fischer, F., Joetzjer, É., Maréchaux, I., Sun, I. F., and Chave, J.: Transferability of an individual- and trait-based forest dynamics model: A test case across the tropics, Ecological Modelling, 463, 109801, https://doi.org/10.1016/j.ecolmodel.2021.109801, 2022a.

Rau, E.-P., Gardiner, B. A., Fischer, F. J., Maréchaux, I., Joetzjer, E., Sun, I.-F., and Chave, J.: Wind Speed Controls Forest Structure in a Subtropical Forest Exposed to Cyclones: A Case Study Using an Individual-Based Model, Frontiers in Forests and Global Change, 5, 2022b.

Restrepo-Coupe, N., da Rocha, H. R., Hutyra, L. R., da Araujo, A. C., Borma, L. S., Christoffersen, B., Cabral, O. M. R., de Camargo, P. B., Cardoso, F. L., da Costa, A. C. L., Fitzjarrald, D. R., Goulden, M. L., Kruijt, B., Maia, J. M. F., Malhi, Y. S., Manzi, A. O., Miller, S. D., Nobre, A. D., von Randow, C., Sá, L. D. A., Sakai, R. K., Tota, J., Wofsy, S. C., Zanchi, F. B., and Saleska, S. R.: What drives the seasonality of photosynthesis across the Amazon basin? A cross-site analysis of

eddy flux tower measurements from the Brasil flux network, Agricultural and Forest Meteorology, 182–183, 128–144, https://doi.org/10.1016/j.agrformet.2013.04.031, 2013.

Restrepo-Coupe, N., Levine, N. M., Christoffersen, B. O., Albert, L. P., Wu, J., Costa, M. H., Galbraith, D., Imbuzeiro, H., Martins, G., da Araujo, A. C., Malhi, Y. S., Zeng, X., Moorcroft, P., and Saleska, S. R.: Do dynamic global vegetation models capture the seasonality of carbon fluxes in the Amazon basin? A data-model intercomparison, Glob Change Biol, 23, 191–208, https://doi.org/10.1111/gcb.13442, 2017.

Richards, L. A.: Capillary conduction of liquids through porous mediums, Physics, 1, 318–333, https://doi.org/10.1063/1.1745010, 1931.

Riva, F. and Fahrig, L.: Landscape-scale habitat fragmentation is positively related to biodiversity, despite patch-scale ecosystem decay, Ecology Letters, 26, 268–277, https://doi.org/10.1111/ele.14145, 2023.

Rödig, E., Cuntz, M., Heinke, J., Rammig, A., and Huth, A.: Spatial heterogeneity of biomass and forest structure of the Amazon rain forest: Linking remote sensing, forest modelling and field inventory, Global Ecology and Biogeography, 26, 1292–1302, https://doi.org/10.1111/geb.12639, 2017.

Rodriguez-Dominguez, C. M., Buckley, T. N., Egea, G., de Cires, A., Hernandez-Santana, V., Martorell, S., and Diaz-Espejo, A.: Most stomatal closure in woody species under moderate drought can be explained by stomatal responses to leaf turgor, Plant, Cell & Environment, 39, 2014–2026, https://doi.org/10.1111/pce.12774, 2016.

Rodriguez-Iturbe, I., Porporato, A., Ridolfi, L., Isham, V., and Coxi, D. R.: Probabilistic modelling of water balance at a point: the role of climate, soil and vegetation, Proceedings of the Royal Society of London A: Mathematical, Physical and Engineering Sciences, 455, 3789–3805, https://doi.org/10.1098/rspa.1999.0477, 1999.

Rogers, A., Medlyn, B. E., Dukes, J. S., Bonan, G., von Caemmerer, S., Dietze, M. C., Kattge, J., Leakey, A. D. B., Mercado, L. M., Niinemets, Ü., Prentice, I. C., Serbin, S. P., Sitch, S., Way, D. A., and Zaehle, S.: A roadmap for improving the representation of photosynthesis in Earth system models, New Phytol, 213, 22–42, https://doi.org/10.1111/nph.14283, 2017.

Rosas, T., Mencuccini, M., Barba, J., Cochard, H., Saura-Mas, S., and Martínez-Vilalta, J.: Adjustments and coordination of hydraulic, leaf and stem traits along a water availability gradient, New Phytologist, 223, 632–646, https://doi.org/10.1111/nph.15684, 2019.

Ross, J.: The radiation regime and architecture of plant stands, The Hague, The Netherlands, 1981.

Rowland, L., Lobo-do-Vale, R. L., Christoffersen, B. O., Melém, E. A., Kruijt, B., Vasconcelos, S. S., Domingues, T., Binks, O. J., Oliveira, A. A. R., Metcalfe, D., da Costa, A. C. L., Mencuccini, M., and Meir, P.: After more than a decade of soil moisture deficit, tropical rainforest trees maintain photosynthetic capacity, despite increased leaf respiration, Glob Change Biol, 21, 4662–4672, https://doi.org/10.1111/gcb.13035, 2015.

Rowland, L., Costa, A. C. L. da, Oliveira, A. A. R., Oliveira, R. S., Bittencourt, P. L., Costa, P. B., Giles, A. L., Sosa, A. I., Coughlin, I., Godlee, J. L., Vasconcelos, S. S., Junior, J. A. S., Ferreira, L. V., Mencuccini, M., and Meir, P.: Drought

stress and tree size determine stem CO2 efflux in a tropical forest, New Phytologist, 218, 1393–1405, https://doi.org/10.1111/nph.15024, 2018.

Rowland, L., Ramírez-Valiente, J.-A., Hartley, I. P., and Mencuccini, M.: How woody plants adjust above- and below-ground traits in response to sustained drought, New Phytologist, 239, 1173–1189, https://doi.org/10.1111/nph.19000, 2023.

Rutter, A. J. and Morton, A. J.: A Predictive Model of Rainfall Interception in Forests. III. Sensitivity of The Model to Stand Parameters and Meteorological Variables, Journal of Applied Ecology, 14, 567–588, https://doi.org/10.2307/2402568, 1977.

Ryan, M. G., Hubbard, R. M., Clark, D. A., and Jr, R. L. S.: Woody-tissue respiration for Simarouba amara and Minquartia guianensis, two tropical wet forest trees with different growth habits, Oecologia, 100, 213–220, https://doi.org/10.1007/BF00316947, 1994.

Ryan, M. G., Binkley, D., and Fownes, J. H.: Age-related decline in forest productivity., Adv. Ecol. Res., 27, 213–262, 1997.

Sabot, M. E. B., Kauwe, M. G. D., Pitman, A. J., Medlyn, B. E., Verhoef, A., Ukkola, A. M., and Abramowitz, G.: Plant profit maximization improves predictions of European forest responses to drought, New Phytologist, 226, 1638–1655, https://doi.org/10.1111/nph.16376, 2020.

Sabot, M. E. B., De Kauwe, M. G., Pitman, A. J., Medlyn, B. E., Ellsworth, D. S., Martin-StPaul, N. K., Wu, J., Choat, B., Limousin, J.-M., Mitchell, P. J., Rogers, A., and Serbin, S. P.: One Stomatal Model to Rule Them All? Toward Improved Representation of Carbon and Water Exchange in Global Models, Journal of Advances in Modeling Earth Systems, 14, e2021MS002761, https://doi.org/10.1029/2021MS002761, 2022.

Sakschewski, B., von Bloh, W., Boit, A., Rammig, A., Kattge, J., Poorter, L., Peñuelas, J., and Thonicke, K.: Leaf and stem economics spectra drive diversity of functional plant traits in a dynamic global vegetation model, Glob Change Biol, 21, 2711–2725, https://doi.org/10.1111/gcb.12870, 2015.

Sakschewski, B., von Bloh, W., Drüke, M., Sörensson, A. A., Ruscica, R., Langerwisch, F., Billing, M., Bereswill, S., Hirota, M., Oliveira, R. S., Heinke, J., and Thonicke, K.: Variable tree rooting strategies are key for modelling the distribution, productivity and evapotranspiration of tropical evergreen forests, Biogeosciences, 18, 4091–4116, https://doi.org/10.5194/bg-18-4091-2021, 2021.

Sander, H.: The porosity of tropical soils and implications for geomorphological and pedogenetic processes and the movement of solutions within the weathering cover, CATENA, 49, 129–137, https://doi.org/10.1016/S0341-8162(02)00021-8, 2002.

Santos, V. A. H. F. dos, Ferreira, M. J., Rodrigues, J. V. F. C., Garcia, M. N., Ceron, J. V. B., Nelson, B. W., and Saleska, S. R.: Causes of reduced leaf-level photosynthesis during strong El Niño drought in a Central Amazon forest, Global Change Biology, 24, 4266–4279, https://doi.org/10.1111/gcb.14293, 2018.

Sato, H., Itoh, A., and Kohyama, T.: SEIB-DGVM: a new dynamic global vegetation model using a spatially explicit individual-based approach, Ecol. Model., 200, 279–307, https://doi.org/10.1016/j.ecolmodel.2006.09.006, 2007.

Schaphoff, S., von Bloh, W., Rammig, A., Thonicke, K., Biemans, H., Forkel, M., Gerten, D., Heinke, J., Jägermeyr, J., Knauer, J., Langerwisch, F., Lucht, W., Müller, C., Rolinski, S., and Waha, K.: LPJmL4 – a dynamic global vegetation model with managed land – Part 1: Model description, Geoscientific Model Development, 11, 1343–1375, https://doi.org/Schaphoff, Sibyll, von Bloh, Werner, Rammig, Anja, Thonicke, Kirsten, Biemans, Hester, Forkel, Matthias, Gerten, Dieter, Heinke, Jens, Jägermeyr, Jonas, Knauer, Jürgen, Langerwisch, Fanny, Lucht, Wolfgang, Müller, Christoph, Rolinski, Susanne and Waha, Katharina (2018) LPJmL4 – a dynamic global vegetation model with managed land – Part 1: Model description. Open Access Geoscientific Model Development, 11 (4). pp. 1343-1375. DOI 10.5194/gmd-11-1343-2018 <http://dx.doi.org/10.5194/gmd-11-1343-2018>., 2018.

Scheiter, S., Langan, L., and Higgins, S. I.: Next-generation dynamic global vegetation models: learning from community ecology, New Phytol, 198, 957–969, https://doi.org/10.1111/nph.12210, 2013.

Schimel, D., Pavlick, R., Fisher, J. B., Asner, G. P., Saatchi, S., Townsend, P., Miller, C., Frankenberg, C., Hibbard, K., and Cox, P.: Observing terrestrial ecosystems and the carbon cycle from space, Global Change Biology, 21, 1762–1776, https://doi.org/10.1111/gcb.12822, 2015.

Schippers, P., Vlam, M., Zuidema, P. A., and Sterck, F.: Sapwood allocation in tropical trees: a test of hypotheses, Functional Plant Biol., 42, 697–709, https://doi.org/10.1071/FP14127, 2015.

Schmidhalter, U.: The gradient between pre-dawn rhizoplane and bulk soil matric potentials, and its relation to the pre-dawn root and leaf water potentials of four species, Plant, Cell & Environment, 20, 953–960, https://doi.org/10.1046/j.1365-3040.1997.d01-136.x, 1997.

Schmitt, S., Maréchaux, I., Chave, J., Fischer, F. J., Piponiot, C., Traissac, S., and Hérault, B.: Functional diversity improves tropical forest resilience: Insights from a long-term virtual experiment, Journal of Ecology, 108, 831–843, https://doi.org/10.1111/1365-2745.13320, 2020.

Schmitt, S.: Rôle de la biodiversité dans la résilience des écosystèmes forestiers tropicaux après perturbations, AgroParisTech, Université de Montpellier, Kourou, 2017.

Schmitt, S., Salzet, G., Fischer, F. J., Maréchaux, I., and Chave, J.: rcontroll: An R interface for the individual-based forest dynamics simulator TROLL, Methods in Ecology and Evolution, 14, 2749–2757, https://doi.org/10.1111/2041-210X.14215, 2023.

Schnabel, F., Schwarz, J. A., Dănescu, A., Fichtner, A., Nock, C. A., Bauhus, J., and Potvin, C.: Drivers of productivity and its temporal stability in a tropical tree diversity experiment, Global Change Biology, 25, 4257–4272, https://doi.org/10.1111/gcb.14792, 2019.

Schnitzer, S. A. and Carson, W. P.: Would Ecology Fail the Repeatability Test?, BioScience, 66, 98–99, https://doi.org/10.1093/biosci/biv176, 2016.

Seidl, R., Rammer, W., and Blennow, K.: Simulating wind disturbance impacts on forest landscapes: Tree-level heterogeneity matters, Environmental Modelling & Software, 51, 1–11, https://doi.org/10.1016/j.envsoft.2013.09.018, 2014.

Seidler, T. G. and Plotkin, J. B.: Seed Dispersal and Spatial Pattern in Tropical Trees, PLOS Biology, 4, e344, https://doi.org/10.1371/journal.pbio.0040344, 2006.

Sellers, P. J., Mintz, Y., Sud, Y. C., and Dalcher, A.: A Simple Biosphere Model (SIB) for Use within General Circulation Models, J. Atmos. Sci., 43, 505–531, https://doi.org/10.1175/1520-0469(1986)043<0505:ASBMFU>2.0.CO;2, 1986.

Sellers, P. J., Heiser, M. D., and Hall, F. G.: Relations between surface conductance and spectral vegetation indices at intermediate (100 m2 to 15 km2) length scales, Journal of Geophysical Research: Atmospheres, 97, 19033–19059, https://doi.org/10.1029/92JD01096, 1992.

Sellers, P. J., Dickinson, R. E., Randall, D. A., Betts, A. K., Hall, F. G., Berry, J. A., Collatz, G. J., Denning, A. S., Mooney, H. A., Nobre, C. A., Sato, N., Field, C. B., and Henderson-Sellers, A.: Modeling the Exchanges of Energy, Water, and Carbon Between Continents and the Atmosphere, Science, 275, 502–509, https://doi.org/10.1126/science.275.5299.502, 1997.

Sergent, A. S., Varela, S. A., Barigah, T. S., Badel, E., Cochard, H., Dalla-Salda, G., Delzon, S., Fernández, M. E., Guillemot, J., Gyenge, J., Lamarque, L. J., Martinez-Meier, A., Rozenberg, P., Torres-Ruiz, J. M., and Martin-StPaul, N. K.: A comparison of five methods to assess embolism resistance in trees, Forest Ecology and Management, 468, 118175, https://doi.org/10.1016/j.foreco.2020.118175, 2020.

Sevanto, S., Mcdowell, N. G., Dickman, L. T., Pangle, R., and Pockman, W. T.: How do trees die? A test of the hydraulic failure and carbon starvation hypotheses, Plant Cell Environ, 37, 153–161, https://doi.org/10.1111/pce.12141, 2014.

Sheil, D., Burslem, D. F. R. P., and Alder, D.: The interpretation and misinterpretation of mortality rate measures, Journal of Ecology, 83, 331–333, https://doi.org/10.2307/2261571, 1995.

Shugart, H. H., Asner, G. P., Fischer, R., Huth, A., Knapp, N., Le Toan, T., and Shuman, J. K.: Computer and remote-sensing infrastructure to enhance large-scale testing of individual-based forest models, Frontiers in Ecology and the Environment, 13, 503–511, 2015.

Shuttleworth, W. J.: Daily variations of temperature and humidity within and above Amazonian forest, Weather, 40, 102–108, https://doi.org/10.1002/j.1477-8696.1985.tb07489.x, 1985.

Shuttleworth, W. J., Leuning, R., Black, T. A., Grace, J., Jarvis, P. G., Roberts, J., and Jones, H. G.: Micrometeorology of temperate and tropical forest, Philosophical Transactions of the Royal Society of London B: Biological Sciences, 324, 299–334, https://doi.org/10.1098/rstb.1989.0050, 1989.

Slik, J. W. F.: El Niño droughts and their effects on tree species composition and diversity in tropical rain forests, Oecologia, 141, 114–120, https://doi.org/10.1007/s00442-004-1635-y, 2004.

Slot, M., Wright, S. J., and Kitajima, K.: Foliar respiration and its temperature sensitivity in trees and lianas: in situ measurements in the upper canopy of a tropical forest, Tree Physiol, 33, 505–515, https://doi.org/10.1093/treephys/tpt026, 2013.

Slot, M., Nardwattanawong, T., Hernández, G. G., Bueno, A., Riederer, M., and Winter, K.: Large differences in leaf cuticle conductance and its temperature response among 24 tropical tree species from across a rainfall gradient, New Phytologist, 232, 1618–1631, https://doi.org/10.1111/nph.17626, 2021.

Smith, B., Prentice, I. C., and Sykes, M. T.: Representation of vegetation dynamics in the modelling of terrestrial ecosystems: comparing two contrasting approaches within European climate space, Global Ecology and Biogeography, 10, 621–637, https://doi.org/10.1046/j.1466-822X.2001.t01-1-00256.x, 2001.

Smith, N. G. and Dukes, J. S.: Plant respiration and photosynthesis in global-scale models: incorporating acclimation to temperature and CO2, Glob Change Biol, 19, 45–63, https://doi.org/10.1111/j.1365-2486.2012.02797.x, 2013.

Smith-Martin, C. M., Xu, X., Medvigy, D., Schnitzer, S. A., and Powers, J. S.: Allometric scaling laws linking biomass and rooting depth vary across ontogeny and functional groups in tropical dry forest lianas and trees, New Phytologist, 226, 714–726, https://doi.org/10.1111/nph.16275, 2020.

Soberón, J.: Grinnellian and Eltonian niches and geographic distributions of species, Ecology Letters, 10, 1115–1123, https://doi.org/10.1111/j.1461-0248.2007.01107.x, 2007.

Sobrado, M. A.: Aspects of tissue water relations and seasonal changes of leaf water potential components of evergreen and deciduous species coexisting in tropical dry forests, Oecologia, 68, 413–416, https://doi.org/10.1007/BF01036748, 1986.

Song, X., Wang, D.-Y., Li, F., and Zeng, X.-D.: Evaluating the performance of CMIP6 Earth system models in simulating global vegetation structure and distribution, Advances in Climate Change Research, 12, 584–595, https://doi.org/10.1016/j.accre.2021.06.008, 2021.

Sousa, T. R., Schietti, J., Ribeiro, I. O., Emílio, T., Fernández, R. H., ter Steege, H., Castilho, C. V., Esquivel-Muelbert, A., Baker, T., Pontes-Lopes, A., Silva, C. V. J., Silveira, J. M., Derroire, G., Castro, W., Mendoza, A. M., Ruschel, A., Prieto, A., Lima, A. J. N., Rudas, A., Araujo-Murakami, A., Gutierrez, A. P., Andrade, A., Roopsind, A., Manzatto, A. G., Di Fiore, A., Torres-Lezama, A., Dourdain, A., Marimon, B., Marimon, B. H., Burban, B., van Ulft, B., Herault, B., Quesada, C., Mendoza, C., Stahl, C., Bonal, D., Galbraith, D., Neill, D., de Oliveira, E. A., Hase, E., Jimenez-Rojas, E., Vilanova, E., Arets, E., Berenguer, E., Alvarez-Davila, E., Honorio Coronado, E. N., Almeida, E., Coelho, F., Valverde, F. C., Elias, F., Brown, F., Bongers, F., Arevalo, F. R., Lopez-Gonzalez, G., van der Heijden, G., Aymard C., G. A., Llampazo, G. F., Pardo, G., Ramírez-Angulo, H., do Amaral, I. L., Vieira, I. C. G., Huamantupa-Chuquimaco, I., Comiskey, J. A., Singh, J., Espejo, J. S., del Aguila-Pasquel, J., Zwerts, J. A., Talbot, J., Terborgh, J., Ferreira, J., Barroso, J. G., Barlow, J., Camargo, J. L., Stropp, J., Peacock, J., Serrano, J., Melgaço, K., Ferreira, L. V., Blanc, L., Poorter, L., Gamarra, L. V., Aragão, L., Arroyo, L., Silveira, M., Peñuela-Mora, M. C., Vargas, M. P. N., Toledo, M., Disney, M., Réjou-Méchain, M., Baisie, M., Kalamandeen, M., Camacho, N. P., Cardozo, N. D., Silva, N., Pitman, N., Higuchi, N., Banki, O., Loayza, P. A., Graça, P. M. L. A., et al.: Water table depth modulates productivity and biomass across Amazonian forests, Global Ecology and Biogeography, 31, 1571–1588, https://doi.org/10.1111/geb.13531, 2022.

Sperry, J. S., Hacke, U. G., Oren, R., and Comstock, J. P.: Water deficits and hydraulic limits to leaf water supply, Plant Cell Environ., 25, 251–263, 2002.

Sperry, J. S., Venturas, M. D., Anderegg, W. R. L., Mencuccini, M., Mackay, D. S., Wang, Y., and Love, D. M.: Predicting stomatal responses to the environment from the optimization of photosynthetic gain and hydraulic cost, Plant, Cell & Environment, 40, 816–830, https://doi.org/10.1111/pce.12852, 2017.

Stahl, C., Herault, B., Rossi, V., Burban, B., Brechet, C., and Bonal, D.: Depth of soil water uptake by tropical rainforest trees during dry periods: does tree dimension matter?, Oecologia, 173, 1191–1201, https://doi.org/10.1007/s00442-013-2724-6, 2013a.

Stahl, C., Burban, B., Wagner, F., Goret, J.-Y., Bompy, F., and Bonal, D.: Influence of seasonal variations in soil water availability on gas exchange of tropical canopy trees, Biotropica, 45, 155–164, https://doi.org/10.1111/j.1744-7429.2012.00902.x, 2013b.

Stephenson, N. L., Das, A. J., Condit, R., Russo, S. E., Baker, P. J., Beckman, N. G., Coomes, D. A., Lines, E. R., Morris, W. K., Rüger, N., Álvarez, E., Blundo, C., Bunyavejchewin, S., Chuyong, G., Davies, S. J., Duque, Á., Ewango, C. N., Flores, O., Franklin, J. F., Grau, H. R., Hao, Z., Harmon, M. E., Hubbell, S. P., Kenfack, D., Lin, Y., Makana, J.-R., Malizia, A., Malizia, L. R., Pabst, R. J., Pongpattananurak, N., Su, S.-H., Sun, I.-F., Tan, S., Thomas, D., van Mantgem, P. J., Wang, X., Wiser, S. K., and Zavala, M. A.: Rate of tree carbon accumulation increases continuously with tree size, Nature, 507, 90–93, https://doi.org/10.1038/nature12914, 2014.

Strigul, N., Pristinski, D., Purves, D., Dushoff, J., and Pacala, S.: Scaling from trees to forests: tractable macroscopic equations for forest dynamics, Ecological Monographs, 78, 523–545, https://doi.org/10.1890/08-0082.1, 2008.

Sun, S., Jung, E.-Y., Gaviria, J., and Engelbrecht, B. M. J.: Drought survival is positively associated with high turgor loss points in temperate perennial grassland species, Functional Ecology, 34, 788–798, https://doi.org/10.1111/1365-2435.13522, 2020.

Swaine, M. D. and Whitmore, T. C.: On the definition of ecological species groups in tropical rain forests, Vegetatio, 75, 81–86, https://doi.org/10.1007/BF00044629, 1988.

Tamme, R., Götzenberger, L., Zobel, M., Bullock, J. M., Hooftman, D. A. P., Kaasik, A., and Pärtel, M.: Predicting species' maximum dispersal distances from simple plant traits, Ecology, 95, 505–513, https://doi.org/10.1890/13-1000.1, 2014.

Thornley, J. H. M. and Cannell, M. G. R.: Modelling the components of plant respiration: representation and realism, Ann Bot, 85, 55–67, https://doi.org/10.1006/anbo.1999.0997, 2000.

Thuiller, W., Albert, C., Araújo, M. B., Berry, P. M., Cabeza, M., Guisan, A., Hickler, T., Midgley, G. F., Paterson, J., Schurr, F. M., Sykes, M. T., and Zimmermann, N. E.: Predicting global change impacts on plant species' distributions: Future challenges, Perspectives in Plant Ecology, Evolution and Systematics, 9, 137–152, https://doi.org/10.1016/j.ppees.2007.09.004, 2008.

Tomasella, J. and Hodnett, M. G.: Estimating soil water retention characteristics from limited data in Brazilian Amazonia., Soil science, 163, 190–202, 1998.

Trueba, S., Pan, R., Scoffoni, C., John, G. P., Davis, S. D., and Sack, L.: Thresholds for leaf damage due to dehydration: declines of hydraulic function, stomatal conductance and cellular integrity precede those for photochemistry, New Phytologist, 223, 134–149, https://doi.org/10.1111/nph.15779, 2019.

Trugman, A. T., Medvigy, D., Mankin, J. S., and Anderegg, W. R. L.: Soil Moisture Stress as a Major Driver of Carbon Cycle Uncertainty, Geophysical Research Letters, 45, 6495–6503, https://doi.org/10.1029/2018GL078131, 2018.

Turner, B. L., Brenes-Arguedas, T., and Condit, R.: Pervasive phosphorus limitation of tree species but not communities in tropical forests, Nature, 555, 367–370, https://doi.org/10.1038/nature25789, 2018.

Tuzet, A., Perrier, A., and Leuning, R.: A coupled model of stomatal conductance, photosynthesis and transpiration, Plant, Cell & Environment, 26, 1097–1116, https://doi.org/10.1046/j.1365-3040.2003.01035.x, 2003.

Tymen, B., Vincent, G., Courtois, E. A., Heurtebize, J., Dauzat, J., Marechaux, I., and Chave, J.: Quantifying micro-environmental variation in tropical rainforest understory at landscape scale by combining airborne LiDAR scanning and a sensor network, Annals of Forest Science, 74, 32, https://doi.org/10.1007/s13595-017-0628-z, 2017.

Urbina, I., Grau, O., Sardans, J., Margalef, O., Peguero, G., Asensio, D., LLusià, J., Ogaya, R., Gargallo-Garriga, A., Van Langenhove, L., Verryckt, L. T., Courtois, E. A., Stahl, C., Soong, J. L., Chave, J., Hérault, B., Janssens, I. A., Sayer, E., and Peñuelas, J.: High foliar K and P resorption efficiencies in old-growth tropical forests growing on nutrient-poor soils, Ecology and Evolution, 11, 8969–8982, https://doi.org/10.1002/ece3.7734, 2021.

Vacchiano, G., Ascoli, D., Berzaghi, F., Lucas-Borja, M. E., Caignard, T., Collalti, A., Mairota, P., Palaghianu, C., Reyer, C. P. O., Sanders, T. G. M., Schermer, E., Wohlgemuth, T., and Hacket-Pain, A.: Reproducing reproduction: How to simulate mast seeding in forest models, Ecological Modelling, 376, 40–53, https://doi.org/10.1016/j.ecolmodel.2018.03.004, 2018.

Van Bodegom, P. M., Douma, J. C., and Verheijen, L. M.: A fully traits-based approach to modeling global vegetation distribution, PNAS, 111, 13733–13738, https://doi.org/10.1073/pnas.1304551110, 2014.

Van Nes, E. H. and Scheffer, M.: A strategy to improve the contribution of complex simulation models to ecological theory, Ecological Modelling, 185, 153–164, https://doi.org/10.1016/j.ecolmodel.2004.12.001, 2005.

Vanclay, J. K.: Aggregating tree species to develop diameter increment equations for tropical rainforests, Forest Ecology and Management, 42, 143–168, https://doi.org/10.1016/0378-1127(91)90022-N, 1991.

Vanclay, J. K.: Modelling forest growth and yield: applications to mixed tropical forests., CAB INternational, Wallingford, 312 pp., 1994.

Vargas Godoy, M. R., Markonis, Y., Hanel, M., Kyselý, J., and Papalexiou, S. M.: The Global Water Cycle Budget: A Chronological Review, Surv Geophys, 42, 1075–1107, https://doi.org/10.1007/s10712-021-09652-6, 2021

Verbeeck, H., Peylin, P., Bacour, C., Bonal, D., Steppe, K., and Ciais, P.: Seasonal patterns of CO2 fluxes in Amazon forests: Fusion of eddy covariance data and the ORCHIDEE model, J. Geophys. Res.-Biogeosci., 116, https://doi.org/10.1029/2010JG001544, 2011.

Verheijen, L. M., Aerts, R., Brovkin, V., Cavender-Bares, J., Cornelissen, J. H. C., Kattge, J., and van Bodegom, P. M.: Inclusion of ecologically based trait variation in plant functional types reduces the projected land carbon sink in an earth system model, Glob Change Biol, 21, 3074–3086, https://doi.org/10.1111/gcb.12871, 2015.

Verhoef, A. and Egea, G.: Modeling plant transpiration under limited soil water: Comparison of different plant and soil hydraulic parameterizations and preliminary implications for their use in land surface models, Agricultural and Forest Meteorology, 191, 22–32, https://doi.org/10.1016/j.agrformet.2014.02.009, 2014.

Vezy, R., Christina, M., Roupsard, O., Nouvellon, Y., Duursma, R., Medlyn, B., Soma, M., Charbonnier, F., Blitz-Frayret, C., Stape, J.-L., Laclau, J.-P., de Melo Virginio Filho, E., Bonnefond, J.-M., Rapidel, B., Do, F. C., Rocheteau, A., Picart, D., Borgonovo, C., Loustau, D., and le Maire, G.: Measuring and modelling energy partitioning in canopies of varying complexity using MAESPA model, Agricultural and Forest Meteorology, 253–254, 203–217, https://doi.org/10.1016/j.agrformet.2018.02.005, 2018.

Villar, R., Held, A. A., and Merino, J.: Dark Leaf Respiration in Light and Darkness of an Evergreen and a Deciduous Plant Species, Plant Physiology, 107, 421–427, https://doi.org/10.1104/pp.107.2.421, 1995.

Visser, M. D., Bruijning, M., Wright, S. J., Muller-Landau, H. C., Jongejans, E., Comita, L. S., and de Kroon, H.: Functional traits as predictors of vital rates across the life cycle of tropical trees, Funct Ecol, 30, 168–180, https://doi.org/10.1111/1365-2435.12621, 2016.

Vleminckx, J., Fortunel, C., Valverde-Barrantes, O., Timothy Paine, C. E., Engel, J., Petronelli, P., Dourdain, A. K., Guevara, J., Béroujon, S., and Baraloto, C.: Resolving whole-plant economics from leaf, stem and root traits of 1467 Amazonian tree species, Oikos, 130, 1193–1208, https://doi.org/10.1111/oik.08284, 2021.

Wagner, F. H., Anderson, L. O., Baker, T. R., Bowman, D. M., Cardoso, F. C., Chidumayo, E. N., Clark, D. A., Drew, D. M., Griffiths, A. D., Maria, V. R., and others: Climate seasonality limits leaf carbon assimilation and wood productivity in tropical forests, Biogeosciences, 13, 2537, 2016.

Walker, A. P., Beckerman, A. P., Gu, L., Kattge, J., Cernusak, L. A., Domingues, T. F., Scales, J. C., Wohlfahrt, G., Wullschleger, S. D., and Woodward, F. I.: The relationship of leaf photosynthetic traits – Vcmax and Jmax – to leaf nitrogen, leaf phosphorus, and specific leaf area: a meta-analysis and modeling study, Ecol Evol, 4, 3218–3235, https://doi.org/10.1002/ece3.1173, 2014.

Wang, Y. P. and Jarvis, P. G.: Description and validation of an array model — MAESTRO, Agricultural and Forest Meteorology, 51, 257–280, https://doi.org/10.1016/0168-1923(90)90112-J, 1990.

Wang, Y.-P. and Leuning, R.: A two-leaf model for canopy conductance, photosynthesis and partitioning of available energy I:, Agricultural and Forest Meteorology, 91, 89–111, https://doi.org/10.1016/S0168-1923(98)00061-6, 1998.

Warneke, C. R., Caughlin, T. T., Damschen, E. I., Haddad, N. M., Levey, D. J., and Brudvig, L. A.: Habitat fragmentation alters the distance of abiotic seed dispersal through edge effects and direction of dispersal, Ecology, 103, e03586, https://doi.org/10.1002/ecy.3586, 2022.

Watt, A. S.: Pattern and Process in the Plant Community, Journal of Ecology, 35, 1–22, https://doi.org/10.2307/2256497, 1947.

Weemstra, M., Mommer, L., Visser, E. J. W., van Ruijven, J., Kuyper, T. W., Mohren, G. M. J., and Sterck, F. J.: Towards a multidimensional root trait framework: a tree root review, New Phytol, 211, 1159–1169, https://doi.org/10.1111/nph.14003, 2016.

Weerasinghe, L. K., Creek, D., Crous, K. Y., Xiang, S., Liddell, M. J., Turnbull, M. H., and Atkin, O. K.: Canopy position affects the relationships between leaf respiration and associated traits in a tropical rainforest in Far North Queensland, Tree Physiol, tpu016, https://doi.org/10.1093/treephys/tpu016, 2014.

Williams, M., Rastetter, E. B., Fernandes, D. N., Goulden, M. L., Wofsy, S. C., Shaver, G. R., Melillo, J. M., Munger, J. W., Fan, S.-M., and Nadelhoffer, K. J.: Modelling the soil-plant-atmosphere continuum in a Quercus–Acer stand at Harvard Forest: the regulation of stomatal conductance by light, nitrogen and soil/plant hydraulic properties, Plant, Cell & Environment, 19, 911–927, https://doi.org/10.1111/j.1365-3040.1996.tb00456.x, 1996.

Williams, M., Law, B. E., Anthoni, P. M., and Unsworth, M. H.: Use of a simulation model and ecosystem flux data to examine carbon–water interactions in ponderosa pine, Tree Physiol, 21, 287–298, https://doi.org/10.1093/treephys/21.5.287, 2001.

Wilson, J. B., Peet, R. K., Dengler, J., and Pärtel, M.: Plant species richness: the world records, Journal of Vegetation Science, 23, 796–802, https://doi.org/10.1111/j.1654-1103.2012.01400.x, 2012.

Wolf, A., Anderegg, W. R. L., and Pacala, S. W.: Optimal stomatal behavior with competition for water and risk of hydraulic impairment, PNAS, 113, E7222–E7230, https://doi.org/10.1073/pnas.1615144113, 2016.

Wolz, K. J., Wertin, T. M., Abordo, M., Wang, D., and Leakey, A. D. B.: Diversity in stomatal function is integral to modelling plant carbon and water fluxes, Nat Ecol Evol, 1, 1292–1298, https://doi.org/10.1038/s41559-017-0238-z, 2017.

Woodruff, D. R. and Meinzer, F. C.: Water stress, shoot growth and storage of non-structural carbohydrates along a tree height gradient in a tall conifer, Plant, Cell & Environment, 34, 1920–1930, https://doi.org/10.1111/j.1365-3040.2011.02388.x, 2011.

Wright, S. J., Kitajima, K., Kraft, N. J. B., Reich, P. B., Wright, I. J., Bunker, D. E., Condit, R., Dalling, J. W., Davies, S. J., Díaz, S., Engelbrecht, B. M. J., Harms, K. E., Hubbell, S. P., Marks, C. O., Ruiz-Jaen, M. C., Salvador, C. M., and Zanne, A. E.: Functional traits and the growth–mortality trade-off in tropical trees, Ecology, 91, 3664–3674, https://doi.org/10.1890/09-2335.1, 2010.

Wu, J., Albert, L. P., Lopes, A. P., Restrepo-Coupe, N., Hayek, M., Wiedemann, K. T., Guan, K., Stark, S. C., Christoffersen, B., Prohaska, N., Tavares, J. V., Marostica, S., Kobayashi, H., Ferreira, M. L., Campos, K. S., Silva, R. da, Brando, P. M., Dye, D. G., Huxman, T. E., Huete, A. R., Nelson, B. W., and Saleska, S. R.: Leaf development and demography explain photosynthetic seasonality in Amazon evergreen forests, Science, 351, 972–976, https://doi.org/10.1126/science.aad5068, 2016.

Wu, J., Serbin, S. P., Xu, X., Albert, L. P., Chen, M., Meng, R., Saleska, S. R., and Rogers, A.: The phenology of leaf quality and its within-canopy variation is essential for accurate modeling of photosynthesis in tropical evergreen forests, Global Change Biology, 23, 4814–4827, https://doi.org/10.1111/gcb.13725, 2017.

Wu, J., Serbin, S. P., Ely, K. S., Wolfe, B. T., Dickman, L. T., Grossiord, C., Michaletz, S. T., Collins, A. D., Detto, M., McDowell, N. G., Wright, S. J., and Rogers, A.: The response of stomatal conductance to seasonal drought in tropical forests, Global Change Biology, 26, 823–839, https://doi.org/10.1111/gcb.14820, 2020.

Xu, X., Medvigy, D., Powers, J. S., Becknell, J. M., and Guan, K.: Diversity in plant hydraulic traits explains seasonal and inter-annual variations of vegetation dynamics in seasonally dry tropical forests, New Phytol, 212, 80–95, https://doi.org/10.1111/nph.14009, 2016.

Yang, X., Wu, J., Chen, X., Ciais, P., Maignan, F., Yuan, W., Piao, S., Yang, S., Gong, F., Su, Y., Dai, Y., Liu, L., Zhang, H., Bonal, D., Liu, H., Chen, G., Lu, H., Wu, S., Fan, L., Gentine, P., and Wright, S. J.: A comprehensive framework for seasonal controls of leaf abscission and productivity in evergreen broadleaved tropical and subtropical forests, The Innovation, 2, 100154, https://doi.org/10.1016/j.xinn.2021.100154, 2021.

Yao, Y., Joetzjer, E., Ciais, P., Viovy, N., Cresto Aleina, F., Chave, J., Sack, L., Bartlett, M., Meir, P., Fisher, R., and Luyssaert, S.: Forest fluxes and mortality response to drought: model description (ORCHIDEE-CAN-NHA r7236) and evaluation at the Caxiuanã drought experiment, Geoscientific Model Development, 15, 7809–7833, https://doi.org/10.5194/gmd-15-7809-2022, 2022.

Yao, Y., Ciais, P., Viovy, N., Joetzjer, E., and Chave, J.: How drought events during the last century have impacted biomass carbon in Amazonian rainforests, Global Change Biology, 29, 747–762, https://doi.org/10.1111/gcb.16504, 2023.

Yao, Y., Ciais, P., Joetzjer, E., Li, W., Zhu, L., Wang, Y., Frankenberg, C., and Viovy, N.: The impacts of elevated CO2 on forest growth, mortality and recovery in the Amazon rainforest, Earth System Dynamics Discussions, 1–23, https://doi.org/10.5194/esd-2024-5, 2024.

Yoda, K., Shinozaki, K., Ogawa, H., Hozumi, K., and Kira, T.: Estimation of the total amount of respiration in woody organs of trees and forest communities., J. Biol. Osaka City Univ, 16, 15–26, 1965.

Yu, W., Albert, G., Rosenbaum, B., Schnabel, F., Bruelheide, H., Connolly, J., Härdtle, W., von Oheimb, G., Trogisch, S., Rüger, N., and Brose, U.: Systematic distributions of interaction strengths across tree interaction networks yield positive diversity–productivity relationships, Ecology Letters, 27, e14338, https://doi.org/10.1111/ele.14338, 2024.

Zaehle, S., Sitch, S., Smith, B., and Hatterman, F.: Effects of parameter uncertainties on the modeling of terrestrial biosphere dynamics, Global Biogeochem. Cycles, 19, GB3020, https://doi.org/10.1029/2004GB002395, 2005.

Zellweger, F., Frenne, P. D., Lenoir, J., Rocchini, D., and Coomes, D.: Advances in Microclimate Ecology Arising from Remote Sensing, Trends in Ecology & Evolution, 34, 327–341, https://doi.org/10.1016/j.tree.2018.12.012, 2019.

Zhou, S., Duursma, R. A., Medlyn, B. E., Kelly, J. W. G., and Prentice, I. C.: How should we model plant responses to drought? An analysis of stomatal and non-stomatal responses to water stress, Agric. For. Meteorol., 182, 204–214, https://doi.org/10.1016/j.agrformet.2013.05.009, 2013.

Zhou, S., Medlyn, B., Sabaté, S., Sperlich, D., Prentice, I. C., and others: Short-term water stress impacts on stomatal, mesophyll and biochemical limitations to photosynthesis differ consistently among tree species from contrasting climates, Tree Physiology, 34, 1035–46, 2014.

Ziegler, C., Coste, S., Stahl, C., Delzon, S., Levionnois, S., Cazal, J., Cochard, H., Esquivel-Muelbert, A., Goret, J.-Y., Heuret, P., Jaouen, G., Santiago, L. S., and Bonal, D.: Large hydraulic safety margins protect Neotropical canopy rainforest tree species against hydraulic failure during drought, Annals of Forest Science, 76, 115, https://doi.org/10.1007/s13595-019-0905-0, 2019.

Appendix A

Table A1. List of symbols and variables.

Symbols	Definition	Units	Nature	Equations
Physical constants				
M_w	Molar mass of water vapor	kg mol^{-1}	Constant	12
R	ideal gas constant	J mol^{-1} K^{-1}	Constant	12-13, 28-31, 46-47
V_w	Partial molal volume of water	m^3 mol^{-1}	Constant	13
κ	von Karman constant	unitless	Constant	8, 15
g	Gravity constant	m s^{-2}	Constant	37
ρ	Density of water	kg m^{-3}	Constant	37
M_a	Molecular mass of air	kg mol^{-1}	Constant	41, 48
C_p	Heat capacity of air	J kg^{-1} K^{-1}	Constant	41, 48
γ	Psychrometric constant	Pa K^{-1}	Constant	41
D_H	Molecular diffusivity to heat	m^2 s^{-1}	Constant	46
σ	Stefan-Boltzmann constant	W m^{-2} K^{-4}	Constant	44, 48
Aboveground environment				
$PPFD_{top}$	Photosynthetic photon flux density at canopy top	μmol photons m^{-2} s^{-1}	Updated at half hourly step, given as input	1
T_{top}	Temperature at canopy top	°C	Updated at half hourly step, given as input	4, 6, 44
VPD_{top}	Vapour pressure deficit at canopy top	kPa	Updated at half hourly step, given as input	5, 7
u_{top}	Wind speed at a reference height above the canopy	m s^{-1}	Updated at half hourly step, given as input	Sections 2.1 and 2.2
T_{night}	Nighttime temperature	°C	Updated daily, given as input	Section 2.2
$PPFD$	Incident photosynthetic photon flux density	μmol photons m^{-2} s^{-1}	Computed every half hour	1, 25
T	Temperature	°C	Computed every half hour	4, 42, 46-48
VPD	Vapour pressure deficit	kPa	Computed every half hour	5
u	Wind speed	m s^{-1}	Computed every half hour	8, 9, 15, 47
c_a	CO_2 concentration	μmol mol^{-1} (ppm)	Constant	Section 2.5
P_{ress}	Atmospheric pressure	Pa	Constant	46-47
$PPFD_{abs}$	Absorbed photosynthetic photon flux density	μmol photons m^{-2} s^{-1}	Computed every half hour	2
T_{mean}	Temperature, averaged per crown layer	°C	Computed every half hour	6
VPD_{mean}	Vapour pressure deficit, averaged per crown layer	kPa	Computed every half hour	7
LAI	Cumulated leaf area per ground area	m^2 m^{-2}	Computed daily for each voxel	1-3, 11, 43
dens	Averaged leaf area density per unit ground area	m^2 m^{-2}	Computed daily, averaged per layer	3, 6-7

k	Effective light extinction coefficient	unitless	Fixed, computed from k_{geom} and $absorptance_{leaves}$	1
k_{geom}	Light extinction coefficient reflecting the geometric arrangement of leaves	unitless	Constant, given as input	1
$absorptance_{leaves}$	Fraction of absorbed light within a single leaf	unitless	Constant, given as input	1
LAI_{sat}	LAI threshold for computing microenvironemntal variation within the canopy	$m^2\ m^{-2}$	Constant	4-7
ΔT	Parameter of the within-canopy variation in temperature	°C	Constant	4, 6
C_{VPD0}	Parameter of the within-canopy variation in vapour pressure deficit	unitless	Constant	5, 7
u*	friction velocity	$m\ s^{-1}$	Constant	
d	zero-plane displacement height	m	Computed from the locally averaged canopy height (H)	8
z_0	aerodynamic roughness	m	Computed from the locally averaged canopy height (H)	8
H	Top canopy height	m	Computed daily	8-9
α	Parameter of wind speed decrease within the canopy	unitless	Constant	9
Water balance				
P	Precipitation	mm	Updated daily, given as input	10
I	Interception	mm	Computed daily	10, 11
Q	Run-off	m^3	Computed daily	10
E	Evaporation from the soil	$kg\ m^{-2}\ s^{-1}$	Computed daily	10, 12
T	Tree transpiration	m^3	Computed daily	10
L	Leakage	m^3	Computed daily	10
K	Parameter for rainfall interception	mm	Constant	11
T_s	Temperature at soil surface	K	Computed daily	12, 13
e_s	Vapor pressure of the soil surface	Pa	Computed daily	12
e_a	Vapor pressure of air above the soil surface	Pa	Computed daily	12
e_{sat}	saturated vapor pressure	Pa	Computed daily	13
r_{soil}	Soil surface resistance	$s\ m^{-1}$	Computed daily	12, 14
r_{aero}	Aerodynamic resistance to heat transfer	$s\ m^{-1}$	Computed daily	12, 15
Z	Reference height for r_{aero} computation	m	Constant	15
Z_m	Momentum soil roughness	m	Constant	15
ψ_l	Soil water potential of layer l	MPa	Computed daily	21
K_l	Soil hydraulic conductivity of layer l	$kg\ m^{-2}\ s^{-1}$	Computed daily	22

$\psi_{soil,top}$	Water potential of the top soil belowground voxel	MPa	Computed daily	13
θ_{top}	Water content of the top soil belowground voxel	m^3	Computed daily	14
$\theta_{fc,top}$	water content at field capacity of the top soil belowground voxel	m^3	Computed daily	14
Species and tree characteristics				
LMA	Leaf mass per area	g m^{-2}	Species-specific means: constant, provided as input; tree-specific values: randomly attributed at tree birth	26, 27, 32, 56
LA	Leaf area	cm^2	Species-specific means: constant, provided as input; tree-specific values: randomly attributed at tree birth	46-47
N	Leaf nitrogen content per dry mass	mg g^{-1}	Species-specific means: constant, provided as input; tree-specific values: randomly attributed at tree birth	26, 27, 32
P	Leaf phosphorous content per dry mass	mg g^{-1}	Species-specific means: constant, provided as input; tree-specific values: randomly attributed at tree birth	26, 27, 32
wsg	Wood specific gravity	g cm^{-3}	Species-specific means: constant, provided as input; tree-specific values: randomly attributed at tree birth	36, 55, 60-61, 66
ψ_{tlp}	Leaf water potential at turgor loss point	MPa	Species-specific means: constant, provided as input; tree-specific values: randomly attributed at tree birth	39-40, 58, 68, section 2.7.1
dbh_{thres}	Threshold diameter at breast height, beyond which growth senescence starts	m	Species-specific means: constant, provided as input; tree-specific values: randomly attributed at tree birth	62, 63

dbh_{max}	Maximal tree diameter at breast height	m	Computed once per tree	Section 2.6.4
h_{lim}	Asymptotic height (parameter of Michaelis-Menten function)	m	Species-specific means: constant, provided as input	16
h_{max}	Maximal tree height	m	Species-specific means: constant, provided as input	67
a_h	Parameter of Michaelis-Menten function	m	Species-specific means: constant, provided as input	16
$f_{reg,s}$	Relative abundance of species s in the external seed rain	unitless	Species-specific, provide as input	64
w_l	Leaf width	m	Computed for each tree	46-47
LL	Leaf lifespan	yr	Computed for each tree	57
$\varepsilon_{i,j}$	Individual effects for trait or variable i and tree j	See traits	Randomly attributed at tree birth	Sections 2.4.1 and 2.4.2
σ_i	standard deviation for intraspecific variability in trait or variable i	See traits	Constant, provided as input	Sections 2.4.1 and 2.4.2
dbh	Tree diameter at breast height	m	Tree variable, updated at each timestep	16, 17, 19, 60-62
h	Tree height	m	Tree variable, updated at each timestep	16, 37, 54-55, 58, 60
cr	Tree crown radius	m	Tree variable, updated at each timestep	17
cd	Tree crown depth	m	Tree variable, updated at each timestep	18, 54
a_{cr}	Coefficients of crown radius allometry	unitless	Species-independent constant, provided as input	17
b_{cr}	Coefficients of crown radius allometry	unitless	Species-independent constant, provided as input	17
a_{cd}	Coefficients of crown depth allometry	m	Species-independent constant, provided as input	18
b_{cd}	Coefficients of crown depth allometry	unitless	Species-independent constant, provided as input	18
shape_crown	Ratio between the radius of the crown at the top of the tree to the radius at the bottom of the crown being a global parameter	unitless	Global parameter, provided as input	Section 2.4.2
f_{gap}	Fraction of gaps (openings) in tree crowns	unitless	Constant, provided as input	Section 2.4.2
RD	Tree root depth	m	Tree variable, updated at each timestep	19
RB_t	Total tree fine root biomass	g	Tree variable, updated at each timestep	20

RB_l	Tree fine root biomass in layer l	g	Tree variable, updated at each timestep	20
ψ_{root}	Soil water potential in the tree root zone	MPa	Tree variable, updated at each timestep	21, 37
$\psi_{R,min}$	Root water potential below which there is no soil water uptake	MPa	Constant	21
G_l	soil-to-root water conductance in layer l	mmol H_20 m^{-2} s^{-1} MPa^{-1}	Variable, computed for each tree and layer at each timestep	21, 22
$L_{a,l}$	Tree total root length per unit area in layer l	m m^{-2}	Variable, computed for each tree and layer at each timestep	22
$L_{v,l}$	Tree total root length per unit soil volume in layer l	m m^{-3}	Variable, computed for each tree and layer at each timestep	23
SRL	Specific root length	m g^{-1}	Constant	22
r_s	Mean fine root radius	m	Constant	22
r_s	half of the mean distance between roots	m	Variable, computed for each tree and layer at each timestep	22, 23
Leaf physiology				
T_l	Leaf temperature	°C	Computed half-hourly for each crown layer	24, 25, 28-31, 33, 46
VPD_s	Vapor pressure deficit at the leaf surface	kPa	Computed half-hourly for each crown layer	35
c_s	CO_2 concentration at the leaf surface	μmol mol^{-1} (ppm or μbar)	Computed half-hourly for each crown layer	34
c_i	CO_2 concentration at carboxylation sites	μmol mol^{-1} (ppm or μbar)	Computed half-hourly for each crown layer	24, 34
A_n	Leaf-level net carbon assimilation rate	µmol CO_2 m^{-2} s^{-1}	Computed half-hourly for each crown layer	24, 52
A_v	Leaf-level net carbon assimilation rate limited by Rubisco activity	µmol CO_2 m^{-2} s^{-1}	Computed half-hourly for each crown layer	24
A_j	Leaf-level net carbon assimilation rate limited by RuBP regeneration	µmol CO_2 m^{-2} s^{-1}	Computed half-hourly for each crown layer	24
R_p	Photorespiration rate	µmol C m^{-2} s^{-1}	Computed half-hourly for each crown layer	24
R_d	Leaf dark respiration rate	µmol C m^{-2} s^{-1}	Computed half-hourly for each crown layer	33
R_{d-M}	Leaf dark respiration rate on a leaf dry mass basis	nmol CO_2 $g^{-1}s^{-1}$	Computed half-hourly for each crown layer	32
V_{cmax}	Maximum rate of carboxylation	µmol CO_2 $m^{-2}s^{-1}$	Computed half-hourly for each crown layer	24, 26, 28
V_{cmax-M}	Maximum rate of carboxylation on a leaf dry mass basis	µmol CO_2 g^{-1} s^{-1}	Computed half-hourly for each crown layer	26
J	Electron transport rate	µmol e^- m^{-2} s^{-1}	Computed half-hourly for each crown layer	24, 25
J_{max}	maximal electron transport capacity	µmol e^- m^{-2} s^{-1}	Computed half-hourly for each crown layer	25, 29

J_{max-M}	maximal electron transport capacity on a leaf dry mass basis	µmol e^- g^{-1} s^{-1}	Computed half-hourly for each crown layer	27
Γ^*	CO_2 compensation point in the absence of dark respiration	μbar	Computed half-hourly for each crown layer	24, 30
K_m	Apparent kinetic constant of the Rubisco	μbar	Computed half-hourly for each crown layer	24, 31
θ	Curvature factor	unitless	Constant	25
α	Apparent quantum yield to electron transport	mol e^- mol *photons*$^{-1}$	Constant	25
LSQ	Effective spectral quality of light	unitless	Constant	25
g_s	stomatal conductance to CO_2	mol CO_2 m^{-2} s^{-1}	Computed half-hourly for each crown layer	34
g_{sw}	stomatal conductance to water vapor	mol H_20 m^{-2} s^{-1}	Computed half-hourly for each crown layer	35
g_0	minimum leaf conductance for water vapor	mol H_20 m^{-2} s^{-1}	Constant, provided by the user	35
g_1	Parameter of the stomatal conductance model	$kPa^{0.5}$	Computed daily for each tree	35, 36
ψ_{pd}	Leaf predawn water potential	MPa	Tree variable, computed daily	24, 25, 28, 29, 36-40
WSF_{ns}	Water stress factor for non-stomatal limitation	unitless	Tree variable, computed daily	28, 29, 40
WSF_s	Water stress factor for stomatal limitation	unitless	Tree variable, computed daily	36, 38-39
a	Parameter of WSF_{ns}	unitless	Constant	40
b	Parameter of WSF_s	unitless	Computed from tree-specific ψ_{tlp}	39, 39
E_l	Leaf-level transpiration rate	mol H_20 m^{-2} s^{-1}	Computed half-hourly for each crown layer	41
λ	Latent heat of water vapor	J mol^{-1}	Computed half-hourly for each crown layer	41, 42
s	slope of the (locally linearized) relationship between saturated vapor pressure and temperature	Pa K^{-1}	Computed half-hourly for each crown layer	41
R_{ni}	isothermal net radiation	J m^{-2} s^{-1}	Computed half-hourly for each crown layer	41, 43
g_H	total leaf conductance to heat	mol m^{-2} s^{-1}	Computed half-hourly for each crown layer	41, 45
g_{bHf}	boundary layer conductance for free convection	mol m^{-2} s^{-1}	Computed half-hourly for each crown layer	45, 46, 50
g_{bHu}	boundary layer for forced convection	mol m^{-2} s^{-1}	Computed half-hourly for each crown layer	45, 47, 50
g_r	radiation conductance	mol m^{-2} s^{-1}	Computed half-hourly for each crown layer	45, 48
g_w	total leaf conductance to water vapor	mol H_20 m^{-2} s^{-1}	Computed half-hourly for each crown layer	41, 49
g_{bw}	boundary layer conductance to water vapor	mol H_20 m^{-2} s^{-1}	Computed half-hourly for each crown layer	49, 50
S_{abs}	Absorbed solar radiation (PAR and NIR)	J m^{-2} s^{-1}	Computed half-hourly for each crown layer	43

$B_{n,0}$	Net longwave radiation at the top of the canopy	J m^{-2} s^{-1}	Computed every half hour	43, 44
k_d	Coefficient of extinction of longwave radiation	Unitless	Constant	43
ε_l	Emissivity of the canopy leaves	Unitless	Constant	44, 48
ε_a	Emissivity of the atmosphere	Unitless	Computed every half hour	44
Tree carbon allocation and demography				
GPP_{ind}	Tree-level gross primary productivity	gC	Computed daily	51
NPP_{ind}	Tree-level net primary productivity	gC	Computed daily	51
NPP_{leaves}	Tree-level net primary productivity allocated to leaf production	gC	Computed daily	56
NPP_{wood}	Tree-level net primary productivity allocated to woody growth	gC	Computed daily	61
AGB	Tree aboveground biomass	kg	Computed daily	59-60
$R_{maintenan}$	Tree-level maintenance respiration	gC	Computed daily	51
R_{stem}	Stem maintenance respiration	μmol C s^{-1}	Computed daily	54
R_{growth}	Tree-level growth respiration	gC	Computed daily	51
LA_t	Tree-level total leaf area	m^2	Updated daily	55
LA_{opt}	Optimal tree leaf area	m^2	Updated daily	Section 2.6.2
LA_l	Leaf area in tree crown layer l	m^2	Updated daily	51, 52-53
LA_{young}	Tree-level young leaf area	m^2	Updated daily	52-53, 56
LA_{mature}	Tree-level mature leaf area	m^2	Updated daily	52-53, 56
LA_{old}	Tree-level old leaf area	m^2	Updated daily	52-53, 56
ϱ	Ratio of young or old leaf assimilation rate over mature leaf assimilation rate	unitless	Constant	52
ϱ'	Ratio of young or old leaf respiration rate over mature leaf respiration rate	unitless	Constant	53
τ_{young}	Leaf residence time in the young age pool	yr	Computed for each tree	56
τ_{mature}	Leaf residence time in the young age pool	yr	Computed for each tree	56
τ_{old}	Leaf residence time in the young age pool	yr	Computed for each tree	56
SA	Tree sapwood area	m^2	Updated daily	54, 55
λ_1	Parameter for sapwood area computation	m^2 cm^{-2}	Constant	55
λ_2	Parameter for sapwood area computation	m cm^{-2}	Constant	55
δ_1	Parameter for sapwood area computation	m^2 cm^{-2}	Constant	55
δ_2	Parameter for sapwood area computation	cm^3 g^{-1}	Constant	55

f_{canopy}	Fraction of NPP_{ind} allocated to tree canopy (including leaves, fruits and twigs)	unitless	Constant, given as input	Sections 2.6.1 and 2.6.2
f_{leaves}	Fraction of NPP_{ind} allocated to leaves	unitless	Constant	Section 2.6.2, 56
f_{fruit}	Fraction of NPP_{ind} allocated to fruits	unitless	Constant	Section 2.6.1
f_{twigs}	Fraction of NPP_{ind} allocated to twigs	unitless	Constant	Section 2.6.1
f_{wood}	Fraction of NPP_{ind} allocated to wood	unitless	Constant, given as input	Section 2.6.2
$\psi_{T,o}$	Water potential threshold for accelerating old leaf shedding	MPa	Computed daily for each tree	58
$a_{T,o}$	Parameter to compute $\psi_{T,o}$ (modulates old leaf drought tolerance)	unitless	Constant, given as input	58
$b_{T,o}$	Parameter to compute $\psi_{T,o}$ (modulates the height dependence of leaf susceptibility to drought)	MPa	Constant, given as input	58
f_o	Factor of the acceleration of old leaf shedding	unitless	Updated daily for each tree	Section 2.6.2
δ_o	Parameter controlling the pace of old leaf shedding acceleration (Δf_0)	unitless	Constant, given as input	
NSC_r	Maximal amount of stored non-structural carbohydrates	gC	Updated daily for each tree	59
ΔV	Increment of stem volume	m^3	Computed daily for each tree	61
$Senesc$	Growth senescence factor	unitless	Computed daily for each tree	61-62
Δdbh	Trunk diameter growth	m	Computed daily for each tree	Section 2.6.4
dbh_{mature}	Diameter threshold beyond which the tree is fertile	m	Computed once for each tree	63
σ_{disp}	Scale parameter of the Rayleigh distribution for seed dispersal	m	Constant	Section 2.7.1
n_s	Number of reproduction opportunities per mature tree	number of seeds	Constant	Section 2.7.1
N_{tot}	Intensity of the external seed rain	number of seeds per hectare	Constant, given as input	64
$n_{ext,s}$	Species-specific number of dispersal events due to the external seed rain	number of seeds	Computed once for each species	64
n_{ha}	Area of the simulated plot	ha	Constant, computed from dimensions given as input	64
LAI_{max}	LAI threshold beyond which the seedling leaf carbon balance is negative	$m^2\ m^{-2}$	Computed once for each tree	Section 2.7.1

d	Tree death rate	events yr^{-1}	Updated daily at tree level	65-66
d_b	Background death rate	events yr^{-1}	Computed once per tree	65
m	reference background mortality rate	events yr^{-1}	Constant, provided as input	66
wsg_{lim}	Parameter of d_b	g cm^{-3}	Constant	66
d_{starv}	Death rate due to carbon starvation	events yr^{-1}	Updated daily at tree level	65
$d_{treefall}$	Death rate due to treefall	events yr^{-1}	Updated daily at tree level	65
Θ	Parameter of treefall probability	m	Computed once per tree	67
$d_{drought}$	Death rate due to drought	events yr^{-1}	Updated daily at tree level	65
v_T	Variance for treefall probability	unitless	Computed once per tree	67
hurt	Parameter of secondary treefall probability	m	Updated daily for each tree	Section 2.7.2
ψ_{lethal}	Water potential threshold for drought-induced mortality	MPa	Computed once per tree	68

Appendix B

Table B1. Representation of stomatal conductance, water stress effect on leaf gas exchange and tree transpiration in several vegetation models. g_0, cuticular or minimal stomatal conductance, i.e. g_s when A -> 0; A, CO_2 assimilation rate; c_s, CO_2 concentration at the leaf surface; D_s, vapour pressure deficit at the leaf surface; h_s, fractional relative humidity at the leaf surface; Γ, CO_2 compensation point; V_{cmax} and J_{max} are the maximum carboxylation rate and electron transport rate. All 0 subscript denotes the values without water stress (except for g_0 by convention). Note stomatal conductance to H_20 is 1.6 times higher than stomatal conductance to CO_2, we here only represent stomatal conductance to H_20.

Vegetation model			Stomatal conductance		Water stress effect on leaf gas exchange		Tree transpiration
Name	**Reference**	**Type**	**Model**	**Reference/type**	**Stomatal limitations**	**Non-stomatal limitations**	
ED2	(Longo et al., 2018; Medvigy et al., 2009)	Cohort-based vegetation model	$g_s = g_0 + \frac{a_1 \times A}{(c_s - \Gamma)(1 + \frac{D_s}{D_0})}$	(Leuning, 1995)/ empirical model	The plant net CO_2 assimilation and evapotranspiration rates (x_{net}) are computed as a linear combination of their rates under open (x_o) and close (x_c) stomata: $x_{net} = f x_o + (1-f)x_c$ with $f = \frac{1}{1+\frac{Demand}{Supply}} = \frac{1}{1+\frac{E_0 \times LA}{K \times W_{avail,tot} \times B_{root}}}$ where E_0 is the evapotranspiration rate under conditions of open stomata times and LA the total plant leaf surface area, and $W_{avail,tot}$ is the amount of water accessible by the vegetation layer, B_{root} the plant root biomass, and K an optimized constant.		Computed with: $E_0 = \varphi_0 \times SLA \times B_{leaf}$ with B_{leaf} the tree leaf biomass and φ_0 its evapotranspiration rate, obtained by solving a set of 6 equations of 6 unknowns (after determining the leaf temperature using a surface energy balance submodel), among which: $\varphi_0 = g_{bw} \times (e_s - e_a)$ $\varphi_0 = g_s \times (e_l - e_s)$
ED2-hydro	(Powell et al., 2018; Xu et al., 2016)	ED2 with a new module of plant hydraulics	Solution of : $\frac{\partial}{\partial g_w}(A_{net} - \lambda g_w D_a) = 0$ with $g_w = \frac{g_s g_b}{g_s + g_b}$ and λ is the Lagrangian multiplier of the optimization problem, representing the marginal water use efficiency (marginal increase in A_{net} per unit change of water loss)	(Vico et al., 2013)/ optimization model, under CO_2 (Rubisco) and light (RuBP regeneration/electron transport) co-limitations	$\lambda = \lambda_0 \times \exp(\beta \times \psi_{pd})$ with λ_0 the value of λ when there is no water stress and β an empirical factor taken from Manzoni *et al.* (2011)	$V_{cmax} = V_{cmax,0} \times \left[1 + \left(\frac{\psi_{leaf}}{\pi_{tlp}}\right)^a\right]^{-1}$ $J_{max} = J_{max,0} \times \left[1 + \left(\frac{\psi_{leaf}}{\pi_{tlp}}\right)^a\right]^{-1}$ where $V_{cmax,0}$ and $J_{max,0}$ denotes the photosynthetic capacities without water stress, and a is a shape factor estimated from Brodribb *et al.* (2003).	Similarly to Medvigy et al. 2009, $E_0 = \frac{g_s g_b}{g_s + g_b} \times D_a \times LA$
TFS	(Fyllas et al., 2014)		$g_s = g_0 + 1.6 \times (1 + \frac{g_1}{\sqrt{D_s}}) \times \frac{A}{c_s}$ g_1 is an empirical coefficient*, associated to the water use efficiency (to the Lagrangian).	(Medlyn et al., 2011)/ optimization, for ele tron-transport limitated photosynthesis (light limitation)	$g_s = g_{s,0} \times \frac{\theta_i - \theta_{wp}}{\theta_{fc} - \theta_{wp}}$ where θ_{wp}, θ_{fc}, θ_{wp} are the actual soil water available for tree i, and the soil water content at field capacity and wilting point respectively.	-	Following MAESTRA (Medlyn et al., 2007), an iterative procedure is used to solve the energy balance of the canopy of each tree, under which the Penman-Monteith equation is used to estimate canopy transpiration.

TFS-Hydro	(Christoffersen et al., 2016)	TFS with a new module of plant hydraulics	"	"	$g_s = g_{s,0} \times \left[1 + \left(\frac{\psi_{leaf}}{\psi_{g_s,50}}\right)^{a_{g_s}}\right]^{-1}$ where $\psi_{g_s,50}$ is the leaf water potential at 50% stomatal closure (assumed a 1:1 relationship between $\psi_{g_s,50}$ and the water potential at 20% loss of xylem hydraulic conductivity ($P_{20,x}$), following results from (Brodribb et al., 2003)), and a_{g_s} is the slope of the curve at $\psi_{leaf} = \psi_{g_s,50}$, computed from $\psi_{g_s,50}$ using the same relationship that relates a_x and $P_{50,x}$.	-	"
Multi-layer CLM4.5	(Bonan et al., 2014)	DGVM	$g_s = g_0 + g_1 \times A \times \frac{h_s}{c_s}$	(Ball et al., 1987; Collatz et al., 1991)/ empirical	$g_0 = g_{0,0} \times \sum_j r_j \frac{\psi_j - \psi_c}{\psi_o - \psi_c}$ where ψ_j is the soil water potential of soil layer j, and ψ_o and ψ_c are the soil water potential at which the stomata are fully open and fully closed respectively, and r_j is the relative root fraction of soil layer j.	$V_{c,max} = V_{c,max,0} \times \sum_j r_j \frac{\psi_j - \psi_c}{\psi_o - \psi_c}$	Iterative procedure
			g_s is iteratively computed such that (1) further opening does not yield a sufficient carbon gain per unit water loss (defined by a stomatal efficiency parameter) or (2) further opening causes leaf water potential to decrease below the minimum sustainable leaf water potential that prevents xylem cavitation	Inspired from the SPA model (Williams et al., 1996)/ optimization within limitations imposed by water use efficiency, plant water storage, and soil-to-leaf water transport	The optimization includes a dependence to ψ_{leaf}, where ψ_{leaf} is computed at each timestep (30-60 min) with Darcy's law (soil-to-leaf pathway, including capacitance).	-	
CLM5	(Kennedy et al., 2019)	Stand-based [illegible]	$g_s = g_0 + 1.6 \times (1 + \frac{g_1}{\sqrt{D_s}}) \times \frac{A}{c_s}$	(Medlyn et al., 2011)/ optimization, under light	-	CML4.5 default: $V_{c,max} = V_{c,max,0} \times \sum_j r_j \frac{\psi_j - \psi_c}{\psi_o - \psi_c}$	An iterative procedure is used to solve the energy balance (determine the leaf temperature and internal CO_2

			g_1, is an empirical coefficient*, associated to the water use efficiency (to the Lagrangian).	limitation (RuBP regeneration)	-	$V_{c,max} = V_{c,max,0} \times 2^{-\left(\frac{\psi_{leaf}}{\psi_{g_s,50}}\right)^{a_{g_s}}}$ where $\psi_{g_s,50}$ is the leaf water potential at 50% loss of stomatal conductance and a_{g_s} is a shape-fitting parameter. The solution for vegetation water potential is the set of values that matches supply with demand, maintaining water balance across each of the vegetation water potential nodes (ψ_{root}, ψ_{stem}, $\psi_{sunlit-leaf}$, $\psi_{shade-leaf}$) based on Darcy's law (without capacitance).	concentration), under which transpiration is computed as $E_0 = \frac{g_s g_b}{g_s + g_b} \times D_a \times LA$.
MAESPA	(Duursma et al., 2012)	Individual- and stand-based model	$g_s = g_0 + 1.6 \times \frac{A}{c_s} \times \frac{1 + e^{s_f \psi_f}}{1 + e^{s_f(\psi_f - \psi_{leaf})}}$ where ψ_{leaf} is computed at each time step using Darcy's law ($E_L = k_L \times (\psi_{soil} - \psi_{leaf})$)	(Tuzet et al., 2003)/ empirical	Already implemented in g_s computation.	-	Following MAESTRA (Medlyn et al., 2007), an iterative procedure is used to solve the energy balance of the canopy of each tree, under which the Penman-Monteith equation is used to estimate canopy transpiration.
CABLE	(De Kauwe et al., 2015a, b)	DGVM (vegetation is represented using a single layer, two-leaf canopy model separated into sunlit and shaded [illegible])	$g_s = g_0 + 1.6 \times (1 + \frac{g_1}{\sqrt{D_s}}) \times \frac{A}{c_s}$	(Medlyn et al., 2011)/ optimization, under light limitation (RuBP regeneration) (was the model of (Leuning, 1995) in previous versions of CABLE (Wang et al., 2011)	Standard version of CABLE (De Kauwe et al., 2015a) : $g_1 = g_{1,0} \times \sum_i r_i \frac{\theta_i - \theta_{wp}}{\theta_{fc} - \theta_{wp}}$ with θ_i the volumetric soil water content and r_i the fraction of root mass in soil layer j, and θ_{wp} the soil wilting point and θ_{fc} its field capacity. New expression for drought sensitivity of gas exchange: $g_1 = g_{1,0} \times \exp(b \times \psi_{pd})$, where b is a fitted (species-specific) parameter representing the sensitivity of g_1 to leaf predawn water potential ψ_{pd} and taken from (Zhou et al., 2013, 2014), while $g_{1,0}$ values are drawn from (Lin et al., 2015).	- $V_{c,max} = V_{c,max,0} \times \frac{1 + e^{s_f \psi_f}}{1 + e^{s_f(\psi_f - \psi_{pd})}}$ where s_f and ψ_f are fitted (species-specific) parameters drawn from (Zhou et al., 2013, 2014).	transpiration from the vegetation to the atmosphere is controlled by several resistances operating in series, both above (aerodynamic) and within the canopy (stomatal and leaf boundary layer), and a longwave radiative balance through radiative conductance on net available energy. These resistances in serial, result in a relatively weak coupling between the canopy surface and the atmosphere.
ORCHIDEE	(Krinner et al., 2005; Naudts et al., 2015)	DGVM	$g_s = mA\frac{h_r}{c_a} + b$	(Ball et al., 1987)	-	In the version of (Krinner et al., 2005): The photosynthetic capacities, Vcmax and Jmax, are multiplied by a water stress factor that is:	

			with m and b derived from laboratory measurements.			$1 \ if \ f_w > f_o$ $1 - \frac{f_w - f_c}{f_o - f_c} \ if \ f_c < f_w < f_o$ $0 \ if \ f_w < f_c$ with f_w the water fraction available for the plant in the root zone, and f_c and f_o the soil water fractions inducing, respectively, closure and maximum opening of stomata.	
					In the CAN version of (Naudts et al., 2015): The model calculates plant water supply according to the implementation of hydraulic architecture by (Hickler et al., 2006), i.e. using Darcy's law and accounting for the hydraulic resistances of fine roots, sapwood and leaves. If the transpiration calculated by the energy budget exceeds the amount of water a plant can transport from the soil to its stomata, transpiration is limited to the plant water supply, and stomatal conductance is then recalculated such that the transpiration equals the amount of water a plant can transport. The energy budget and photosynthesis are then recalculated. This may require up to 10 iterations to converge.	-	

LPJ	(Sitch et al., 2003)	DGVM	The model uses the Farquhar model of photosynthesis as generalized for global modelling purposes by (Collatz et al., 1991). In absence of water stress, canopy conductance is derived from the daytime carbon assimilation rate: $g_c = g_{min} + \frac{1.6\,A}{c_a(1-\lambda)}$	(Collatz et al., 1991)	Under water stress i.e. when $\min\left[1; \frac{E_{supply}}{E_{dema,d}}\right] < 1$, The equations of evapotranspiration rate, assimilation rate and the one related assimilation rate and canopy conductance are solved simultaneously to yield values of canopy conductance consistent with the transpiration rate.	< 1Daily evapotranspiration is calculated for each PFT as the minimum of a plant- and soil-limited supply function (E_{supply}) and the atmospheric demand (E_{demand}). E_{supply} is the product of a plant root-weighted soil moisture availability and a maximum transpiration rate; E_{demand} is calculated following Monteith's empirical relation between evaporation efficiency and surface conductance, that uses gpot, the nonwater-stressed potential canopy conductance calculated by the photosynthesis routine

*although fitted empirically to leaf exchange experimental data (Lin et al., 2015), attempts have been made to relate g1 to functional traits and/or climatological variables (wood density, Lin *et al.*, 2015; leaf $\delta^{13}C$, Franks *et al.*, 2018), based on the premise that water use efficiency should be associated to functional strategies. See also values reported in Domingues *et al.* (2014).

2428 **Table B2. Examples of observational or experimental studies that explored the relative roles of stomatal and non-**
2429 **stomatal limitations of photosynthesis under drought conditions.**

Key message for vegetation models	Reference	Studied system	Main results
Stomatal-limitation only	Santos et al., 2018	57 canopy and understory trees within a central Amazonian forest	Photosynthesis decreased during the extreme dry season, and this was only related to stomatal closure (decline in stomatal conductance) and not to leaf biochemical changes (sustained chlorophyll concentration and fluoresecnce, and nutrient concentration).
	Rowland et al., 2015	Trees in the ThroughFall Exclusion and control plots in Caixuana, Amazonia.	No differences in V_{cmax} and J_{max} between the throughfall exclusion plot and the control plot.
	Trueba et al., 2019	Mature individuals of 10 angiosperms species located on the campus of UCLA and a park in LA	The stomatal and leaf hydraulic systems (50% lost of gs, K_{leaf}) show early functional declines before cell integrity is lost. Substantial damage to the photochemical apparatus (maximum quantum yield of the photosystem) occurs at extreme dehydration, after turgor loss and complete stomatal closure, and seems to be irreversible.
Both stomatal and non-stomatal limitations	Zhou et al., 2013	Meta-analysis of 22 experimental datasets where photosynthesis, stomatal conductance and predawn leaf water potential were measured at increasing water stress, spanning a range of plant functional types	Photosynthesis was found almost universally to decrease more than could be explained by the reduction in g_1 (parameter of the Medlyn model), implying a decline in apparent carboxylation capacity (V_{cmax}).
	Zhou et al., 2014	Two experiments, one in Australia on Eucalyptus, one in Spain on Quercus, on plants grown in glasshouses under control conditions. The non-stomatal response was partitioned into effects on mesophyll conductance (g_m), the maximum Rubisco activity (V_{cmax}) and the maximum electron transport rate (J_{max}).	They found consistency among the drought responses of g_1, g_m, V_{cmax} and J_{max}, suggesting that drought imposes limitations on Rubisco activity and RuBP regeneration capacity concurrently with declines in stomatal and mesophyll conductance. Within each experiment, the more xeric species showed relatively high g_1 under moist conditions, low drought sensitivity of g_1, g_m, V_{cmax} and J_{max}, and more negative values of the critical pre-dawn water potential at which V_{cmax} declines most steeply, compared with the more mesic species. Results showed that the decline in *V*cmax is not explained just by the decline in *g*m, but by the decline in both *g*m and *V*cmax.
	Egea et al., 2011	Outputs from a coupled A-gs model that uses a soil water content-dependent water stress factor were compared to leaf-level values obtained from the literature.	The sensitivity analyses emphasized the necessity to combine both stomatal and non-stomatal limitations of A in coupled A–gs models to accurately capture the observed functional relationships A vs. gs and A/gs vs. gs in response to drought. Accounting for water stress in coupled A–gs models by imposing either stomatal or biochemical limitations of A, as commonly practiced in most ecosystem models, failed to reproduce the observed functional relationship between key leaf gas exchange attributes.
	Drake et al., 2017	Plants in pots of four tree species originating from constrating	as soil water content (θ) was reduced under increasing drought, all species responded by reducing gs, resulting in reduced Ci and Asat. However, Asat was reduced to

		hydrological environment, placed in the field under rainout shelters. Comparison with coupled stomatal conductance-photosynthesis model.	a larger degree than would be predicted only by stomatal reduction of Ci, indicating a coincident reduction in photosynthetic capacity with declining θ. The best model include both stomatal and non-stomatal limitations.

References of Appendix B

Ball, J. T., Woodrow, I. E., and Berry, J. A.: A model predicting stomatal conductance and its contribution to the control of photosynthesis under different environmental conditions, in: Progress in photosynthesis research, edited by: Biggins, J., Springer Netherlands, 221–224, https://doi.org/10.1007/978-94-017-0519-6_48, 1987.

Bonan, G. B., Williams, M., Fisher, R. A., and Oleson, K. W.: Modeling stomatal conductance in the earth system: linking leaf water-use efficiency and water transport along the soil–plant–atmosphere continuum, Geosci. Model Dev., 7, 2193–2222, https://doi.org/10.5194/gmd-7-2193-2014, 2014.

Bondeau, A., Smith, P. C., Zaehle, S., Schaphoff, S., Lucht, W., Cramer, W., Gerten, D., Lotze-Campen, H., Müller, C., Reichstein, M., and Smith, B.: Modelling the role of agriculture for the 20th century global terrestrial carbon balance, Global Change Biology, 13, 679–706, https://doi.org/10.1111/j.1365-2486.2006.01305.x, 2007.

Brodribb, T. J., Holbrook, N. M., Edwards, E. J., and Gutiérrez, M. V.: Relations between stomatal closure, leaf turgor and xylem vulnerability in eight tropical dry forest trees, Plant, Cell & Environment, 26, 443–450, https://doi.org/10.1046/j.1365-3040.2003.00975.x, 2003.

Christoffersen, B. O., Gloor, M., Fauset, S., Fyllas, N. M., Galbraith, D. R., Baker, T. R., Kruijt, B., Rowland, L., Fisher, R. A., Binks, O. J., Sevanto, S., Xu, C., Jansen, S., Choat, B., Mencuccini, M., McDowell, N. G., and Meir, P.: Linking hydraulic traits to tropical forest function in a size-structured and trait-driven model (TFS v.1-Hydro), Geosci. Model Dev., 9, 4227–4255, https://doi.org/10.5194/gmd-9-4227-2016, 2016.

Collatz, G. J., Ball, J. T., Grivet, C., and Berry, J. A.: Physiological and environmental regulation of stomatal conductance, photosynthesis and transpiration: a model that includes a laminar boundary layer, Agricultural and Forest Meteorology, 54, 107–136, https://doi.org/10.1016/0168-1923(91)90002-8, 1991.

De Kauwe, M. G., Kala, J., Lin, Y.-S., Pitman, A. J., Medlyn, B. E., Duursma, R. A., Abramowitz, G., Wang, Y.-P., and Miralles, D. G.: A test of an optimal stomatal conductance scheme within the CABLE land surface model, Geoscientific Model Development, 8, 431–452, https://doi.org/10.5194/gmd-8-431-2015, 2015a.

De Kauwe, M. G., Zhou, S.-X., Medlyn, B. E., Pitman, A. J., Wang, Y.-P., Duursma, R. A., and Prentice, I. C.: Do land surface models need to include differential plant species responses to drought? Examining model predictions across a mesic-xeric gradient in Europe, Biogeosciences, 12, 7503–7518, https://doi.org/10.5194/bg-12-7503-2015, 2015b.

Domingues, T. F., Martinelli, L. A., and Ehleringer, J. R.: Seasonal patterns of leaf-level photosynthetic gas exchange in an eastern Amazonian rain forest, Plant Ecology & Diversity, 7, 189–203, https://doi.org/10.1080/17550874.2012.748849, 2014.

Drake, J. E., Power, S. A., Duursma, R. A., Medlyn, B. E., Aspinwall, M. J., Choat, B., Creek, D., Eamus, D., Maier, C., Pfautsch, S., Smith, R. A., Tjoelker, M. G., and Tissue, D. T.: Stomatal and non-stomatal limitations of photosynthesis for four tree species under drought: A comparison of model formulations, Agricultural and Forest Meteorology, 247, 454–466, https://doi.org/10.1016/j.agrformet.2017.08.026, 2017.

Duursma, R. A., Medlyn, B. E., and others: MAESPA: a model to study interactions between water limitation, environmental drivers and vegetation function at tree and stand levels, with an example application to [CO_2]$\times$ drought interactions, 2012.

Egea, G., Verhoef, A., and Vidale, P. L.: Towards an improved and more flexible representation of water stress in coupled photosynthesis–stomatal conductance models, Agricultural and Forest Meteorology, 151, 1370–1384, https://doi.org/10.1016/j.agrformet.2011.05.019, 2011.

Franks, P. J., Bonan, G. B., Berry, J. A., Lombardozzi, D. L., Holbrook, N. M., Herold, N., and Oleson, K. W.: Comparing optimal and empirical stomatal conductance models for application in Earth system models, Global Change Biology, 24, 5708–5723, https://doi.org/10.1111/gcb.14445, 2018.

Fyllas, N. M., Gloor, E., Mercado, L. M., Sitch, S., Quesada, C. A., Domingues, T. F., Galbraith, D. R., Torre-Lezama, A., Vilanova, E., Ramírez-Angulo, H., Higuchi, N., Neill, D. A., Silveira, M., Ferreira, L., Aymard C., G. A., Malhi, Y., Phillips, O. L., and Lloyd, J.: Analysing Amazonian forest productivity using a new individual and trait-based model (TFS v.1), Geosci. Model Dev., 7, 1251–1269, https://doi.org/10.5194/gmd-7-1251-2014, 2014.

Hickler, T., Prentice, I. C., Smith, B., Sykes, M. T., and Zaehle, S.: Implementing plant hydraulic architecture within the LPJ Dynamic Global Vegetation Model, Global Ecology and Biogeography, 15, 567–577, https://doi.org/10.1111/j.1466-8238.2006.00254.x, 2006.

Kennedy, D., Swenson, S., Oleson, K. W., Lawrence, D. M., Fisher, R., Costa, A. C. L. da, and Gentine, P.: Implementing Plant Hydraulics in the Community Land Model, Version 5, Journal of Advances in Modeling Earth Systems, 11, 485–513, https://doi.org/10.1029/2018MS001500, 2019.

Krinner, G., Viovy, N., de Noblet-Ducoudré, N., Ogée, J., Polcher, J., Friedlingstein, P., Ciais, P., Sitch, S., and Prentice, I. C.: A dynamic global vegetation model for studies of the coupled atmosphere-biosphere system, Global Biogeochem. Cycles, 19, GB1015, https://doi.org/10.1029/2003GB002199, 2005.

Leuning, R.: A critical appraisal of a combined stomatal-photosynthesis model for C3 plants, Plant, Cell & Environment, 18, 339–355, https://doi.org/10.1111/j.1365-3040.1995.tb00370.x, 1995.

Lin, Y.-S., Medlyn, B. E., Duursma, R. A., Prentice, I. C., Wang, H., Baig, S., Eamus, D., de Dios, V. R., Mitchell, P., Ellsworth, D. S., de Beeck, M. O., Wallin, G., Uddling, J., Tarvainen, L., Linderson, M.-L., Cernusak, L. A., Nippert, J. B., Ocheltree, T. W., Tissue, D. T., Martin-StPaul, N. K., Rogers, A., Warren, J. M., De Angelis, P., Hikosaka, K., Han,

Q., Onoda, Y., Gimeno, T. E., Barton, C. V. M., Bennie, J., Bonal, D., Bosc, A., Löw, M., Macinins-Ng, C., Rey, A., Rowland, L., Setterfield, S. A., Tausz-Posch, S., Zaragoza-Castells, J., Broadmeadow, M. S. J., Drake, J. E., Freeman, M., Ghannoum, O., Hutley, L. B., Kelly, J. W., Kikuzawa, K., Kolari, P., Koyama, K., Limousin, J.-M., Meir, P., Lola da Costa, A. C., Mikkelsen, T. N., Salinas, N., Sun, W., and Wingate, L.: Optimal stomatal behaviour around the world, Nature Clim. Change, 5, 459–464, https://doi.org/10.1038/nclimate2550, 2015.

Longo, M., Knox, R. G., Levine, N. M., Alves, L. F., Bonal, D., Camargo, P. B., Fitzjarrald, D. R., Hayek, M. N., Restrepo-Coupe, N., Saleska, S. R., Silva, R. da, Stark, S. C., Tapajós, R. P., Wiedemann, K. T., Zhang, K., Wofsy, S. C., and Moorcroft, P. R.: Ecosystem heterogeneity and diversity mitigate Amazon forest resilience to frequent extreme droughts, New Phytologist, 914–931, https://doi.org/10.1111/nph.15185@10.1111/(ISSN)1469-8137.DroughtImpactsonTropicalForests, 2018.

Manzoni, S., Vico, G., Katul, G., Fay, P. A., Polley, W., Palmroth, S., and Porporato, A.: Optimizing stomatal conductance for maximum carbon gain under water stress: a meta-analysis across plant functional types and climates, Functional Ecology, 25, 456–467, https://doi.org/10.1111/j.1365-2435.2010.01822.x, 2011.

Medlyn, B. E., Pepper, D. A., O'Grady, A. P., and Keith, H.: Linking leaf and tree water use with an individual-tree model, Tree Physiol, 27, 1687–1699, https://doi.org/10.1093/treephys/27.12.1687, 2007.

Medlyn, B. E., Duursma, R. A., Eamus, D., Ellsworth, D. S., Prentice, I. C., Barton, C. V. M., Crous, K. Y., De Angelis, P., Freeman, M., and Wingate, L.: Reconciling the optimal and empirical approaches to modelling stomatal conductance, Global Change Biology, 17, 2134–2144, https://doi.org/10.1111/j.1365-2486.2010.02375.x, 2011.

Medvigy, D., Wofsy, S. C., Munger, J. W., Hollinger, D. Y., and Moorcroft, P. R.: Mechanistic scaling of ecosystem function and dynamics in space and time: Ecosystem Demography model version 2, J. Geophys. Res., 114, G01002, https://doi.org/10.1029/2008JG000812, 2009.

Naudts, K., Ryder, J., McGrath, M. J., Otto, J., Chen, Y., Valade, A., Bellasen, V., Berhongaray, G., Bönisch, G., Campioli, M., Ghattas, J., De Groote, T., Haverd, V., Kattge, J., MacBean, N., Maignan, F., Merilä, P., Penuelas, J., Peylin, P., Pinty, B., Pretzsch, H., Schulze, E. D., Solyga, D., Vuichard, N., Yan, Y., and Luyssaert, S.: A vertically discretised canopy description for ORCHIDEE (SVN r2290) and the modifications to the energy, water and carbon fluxes, Geosci. Model Dev., 8, 2035–2065, https://doi.org/10.5194/gmd-8-2035-2015, 2015.

Powell, T. L., Koven, C. D., Johnson, D. J., Faybishenko, B., Fisher, R. A., Knox, R. G., McDowell, N. G., Condit, R., Hubbell, S. P., Wright, S. J., Chambers, J. Q., and Kueppers, L. M.: Variation in hydroclimate sustains tropical forest biomass and promotes functional diversity, New Phytologist, 219, 932–946, https://doi.org/10.1111/nph.15271, 2018.

Rowland, L., Lobo-do-Vale, R. L., Christoffersen, B. O., Melém, E. A., Kruijt, B., Vasconcelos, S. S., Domingues, T., Binks, O. J., Oliveira, A. A. R., Metcalfe, D., da Costa, A. C. L., Mencuccini, M., and Meir, P.: After more than a decade of soil moisture deficit, tropical rainforest trees maintain photosynthetic capacity, despite increased leaf respiration, Glob Change Biol, 21, 4662–4672, https://doi.org/10.1111/gcb.13035, 2015.

Sakschewski, B., von Bloh, W., Boit, A., Rammig, A., Kattge, J., Poorter, L., Peñuelas, J., and Thonicke, K.: Leaf and stem economics spectra drive diversity of functional plant traits in a dynamic global vegetation model, Glob Change Biol, n/a-n/a, https://doi.org/10.1111/gcb.12870, 2015.

Sakschewski, B., von Bloh, W., Boit, A., Poorter, L., Peña-Claros, M., Heinke, J., Joshi, J., and Thonicke, K.: Resilience of Amazon forests emerges from plant trait diversity, Nature Climate Change, 6, 1032–1036, https://doi.org/10.1038/nclimate3109, 2016.

Santos, V. A. H. F. dos, Ferreira, M. J., Rodrigues, J. V. F. C., Garcia, M. N., Ceron, J. V. B., Nelson, B. W., and Saleska, S. R.: Causes of reduced leaf-level photosynthesis during strong El Niño drought in a Central Amazon forest, Global Change Biology, 24, 4266–4279, https://doi.org/10.1111/gcb.14293, 2018.

Sitch, S., Smith, B., Prentice, I. C., Arneth, A., Bondeau, A., Cramer, W., Kaplan, J. O., Levis, S., Lucht, W., Sykes, M. T., Thonicke, K., and Venevsky, S.: Evaluation of ecosystem dynamics, plant geography and terrestrial carbon cycling in the LPJ dynamic global vegetation model, Glob. Change Biol., 9, 161–185, https://doi.org/10.1046/j.1365-2486.2003.00569.x, 2003.

Smith, B., Prentice, I. C., and Sykes, M. T.: Representation of vegetation dynamics in the modelling of terrestrial ecosystems: comparing two contrasting approaches within European climate space, Global Ecology and Biogeography, 10, 621–637, https://doi.org/10.1046/j.1466-822X.2001.t01-1-00256.x, 2001.

Trueba, S., Pan, R., Scoffoni, C., John, G. P., Davis, S. D., and Sack, L.: Thresholds for leaf damage due to dehydration: declines of hydraulic function, stomatal conductance and cellular integrity precede those for photochemistry, New Phytologist, 223, 134–149, https://doi.org/10.1111/nph.15779, 2019.

Tuzet, A., Perrier, A., and Leuning, R.: A coupled model of stomatal conductance, photosynthesis and transpiration, Plant, Cell & Environment, 26, 1097–1116, https://doi.org/10.1046/j.1365-3040.2003.01035.x, 2003.

Vico, G., Manzoni, S., Palmroth, S., Weih, M., and Katul, G.: A perspective on optimal leaf stomatal conductance under CO2 and light co-limitations, Agricultural and Forest Meteorology, 182–183, 191–199, https://doi.org/10.1016/j.agrformet.2013.07.005, 2013.

Wang, Y. P., Kowalczyk, E., Leuning, R., Abramowitz, G., Raupach, M. R., Pak, B., Gorsel, E. van, and Luhar, A.: Diagnosing errors in a land surface model (CABLE) in the time and frequency domains, Journal of Geophysical Research: Biogeosciences, 116, https://doi.org/10.1029/2010JG001385, 2011.

Williams, M., Rastetter, E. B., Fernandes, D. N., Goulden, M. L., Wofsy, S. C., Shaver, G. R., Melillo, J. M., Munger, J. W., Fan, S.-M., and Nadelhoffer, K. J.: Modelling the soil-plant-atmosphere continuum in a Quercus–Acer stand at Harvard Forest: the regulation of stomatal conductance by light, nitrogen and soil/plant hydraulic properties, Plant, Cell & Environment, 19, 911–927, https://doi.org/10.1111/j.1365-3040.1996.tb00456.x, 1996.

Xu, X., Medvigy, D., Powers, J. S., Becknell, J. M., and Guan, K.: Diversity in plant hydraulic traits explains seasonal and inter-annual variations of vegetation dynamics in seasonally dry tropical forests, New Phytol, 212, 80–95, https://doi.org/10.1111/nph.14009, 2016.

Zhou, S., Duursma, R. A., Medlyn, B. E., Kelly, J. W. G., and Prentice, I. C.: How should we model plant responses to drought? An analysis of stomatal and non-stomatal responses to water stress, Agric. For. Meteorol., 182, 204–214, https://doi.org/10.1016/j.agrformet.2013.05.009, 2013.

Zhou, S., Medlyn, B., Sabaté, S., Sperlich, D., Prentice, I. C., and others: Short-term water stress impacts on stomatal, mesophyll and biochemical limitations to photosynthesis differ consistently among tree species from contrasting climates, Tree Physiology, 34, 1035–46, 2014.